MULTI-PHASE TRANSPORT OF TOLUENE IN UNSATURATED SOIL UNDER TRANSIENT FLOW CONDITIONS

By

JOHN LINDEN ROLL

Bachelor of Science
University of Illinois
Urbana, Illinois
1971

Master of Science
University of Illinois
Urbana, Illinois
1973

Submitted to the Faculty of the
Graduate College of the
Oklahoma State University
in partial fulfillment of
the requirements for
the Degree of
DOCTOR OF PHILOSOPHY
May, 1996

MULTI-PHASE TRANSPORT OF TOLUENE IN UNSATURATED SOIL UNDER TRANSIENT FLOW CONDITIONS

Thesis Approved:

Thesis Advisor

Dean of the Graduate College

ACKNOWLEDGMENTS

The decision to return to school after seventeen years of professional experience was a leap of faith. I placed my trust in fate and did something that didn't necessarily make sense at that point in my career. My doctorate studies have been challenging, but they were made easier through the support of many people, the department, and the USDA National Needs Fellowship. Without this support, it is unlikely that I would have completed my studies.

The most important person in this endeavor has been my wife, Sarah. She has provided financial support and has kept me on line when I became discouraged. Our daughters, Betsy, Maggie and Katy, have provided their own measure of support by being understanding and thriving in Stillwater. It helped immensely to see the family do well in their own activities. I dedicate this work to Sarah and the girls for their contribution to my efforts.

My advisor, Dr. Glenn Brown, has been a friend and mentor throughout my studies. He has helped me through many trying times and I especially want to say, "thanks Glenn". The members of my committee, Dr. Basta, Dr. Elliott, and Dr. Smolen have provided valuable inputs to my research and their assistance is greatly appreciated. Dr. Kranzler, Dr. Elliott and Dr. Stone deserve special thanks for their ability to listen and provide guidance. I want to express my thanks to Dr. Barfield and the rest of the faculty,

staff and graduate students of Biosystems and Agricultural Engineering for their friendship and encouragement during my studies.

Several people helped me build equipment and analyze samples. Wayne Kiner and the lab staff were very helpful in building several different soil columns until we got it right. Tom Underwood drilled additional holes in the microsyringe needles which enabled collection of 20 microliter soil air samples during the column tests. Jose Murillo, Weiping Hsiao, Ming Yu, Jian Yue, Barry Allred and Jack Gazin have my thanks for their help collecting and analyzing various samples.

Funding was provided by the U.S. Department of Agriculture through a National Needs Fellowship in Water Science, the Oklahoma Agricultural Experiment Station and the U.S. Geological Survey through federal Grant No. 14-08-0001-G2089. Their funding made this research possible and I thank them for their assistance.

TABLE OF CONTENTS

Chapter **Page**

Chapter **Page**

Chapter **Page**

LIST OF TABLES

LIST OF FIGURES

Figure **Page**

NOMENCLATURE

Item	Definition
AEC	Anion exchange capacity
ASTM	American Standard for Testing of Materials
BET	Brunauer, Emmett and Teller equation
BTX	Benzene, toluene and xylenes
CEC	Cation exchange capacity
DC	Direct current
DNAPL	Denser than water non-aqueous phase liquid
EPA or USEPA	Environmental Protection Agency
EPICS	Equilibrium partitioning in a closed system
FID	Flame ionization detector
GC	Gas chromatograph
LAS	Linear alkylbenzene sulfonate
LPE	Local phase equilibrium
LNAPL	Lighter than water non-aqueous phase liquid
M	Molarity
N	Normality
NAPL	Non-aqueous phase liquid
PTFE	Teflon polytetrafluoroethylene
RVE	Representative volume element
SOM	Soil organic matter
TCE	Trichloroethene
TDS	Total dissolved solids
UV	Ultraviolet
VOC	Volatile organic chemical

LIST OF SYMBOLS

Variable	Definition	Dimensions
A	cross-sectional area of the column	L^2
C_{ij}	concentration of component i in phase j	ML^{-3}
C_{sm}	concentration of the solute in the adsorbed phase	MM^{-1}
C^*_{sm}	concentration of the solute in the adsorbed phase at equilibrium	MM^{-1}
C_{sl}	concentration of the solute in the liquid phase	ML^{-3}
C_{sg}	concentration of the solute in the liquid phase	ML^{-3}
C_{wl}	concentration of water in liquid phase	ML^{-3}
C_{wg}	concentration of water in the gas phase	ML^{-3}
C_{ag}	concentration of air in the gas phase	ML^{-3}
C_T	total mass of solute/unit volume of porous media	ML^{-3}
$C_{sg}(x,t)$	solute gas phase concentration boundary conditions	------
$C_{sg}(\lambda)$	transformed gas phase solute boundary conditions	------
C_i	gas phase solute inlet concentration at $t = 0$	ML^{-3}
C_0	gas phase solute inlet concentration at $t > 0$	ML^{-3}
D_{wl}	dispersion-diffusion coefficient for water in the liquid phase	L^2T^{-1}
D_{sl}	dispersion-diffusion coefficient for solute in the liquid phase	L^2T^{-1}
D_{wg}	diffusion coefficient for water in the gas phase	L^2T^{-1}
D_{ag}	diffusion coefficient for air in the gas phase	L^2T^{-1}
D_{sg}	diffusion coefficient for solute in the gas phase	L^2T^{-1}
$D_{s(air)}$	molecular diffusion rate of pure solute gas phase in air	L^2T^{-1}
Dm	mean sample difference	------
D_i	difference between the paired values	------

Variable	Definition	Dimensions
f_{oc}	fraction of organic carbon	MM^{-1}
F_{ij}	mass flux of component *i* in phase *j*	$ML^{-2}T^{-1}$
F_{wl}	flux of water in the liquid phase	$ML^{-2}T^{-1}$
F_{sl}	flux of solute in liquid phase	$ML^{-2}T^{-1}$
F_{wg}	flux of water in the gas phase	$ML^{-2}T^{-1}$
F_{ag}	flux of air in the gas phase	$ML^{-2}T^{-1}$
F_{sg}	flux of solute in the gas phase	$ML^{-2}T^{-1}$
F_{sm}	flux of solute in the adsorbed phase	$ML^{-2}T^{-1}$
i	component	------
I	cumulative infiltration	L
j	component phase	------
J_{sg}	flux of solute in the gas phase	$ML^{-2}T^{-1}$
k	component phase	------
ki	constant of integration	------
K	Freundlich adsorption coefficient	L^3M^{-1}
K_d	linear adsorption coefficient for partitioning from liquid to solid	L^3M^{-1}
K_H	Henry coefficient	------
K_{oc}	organic carbon partition coefficient	L^3M^{-1}
K_{ow}	octonal-water partitioning coefficient	------
M	soil mass in the vial	M
M_{sl}^{m}	net phase transfer non-equilibrium term of the solute from the liquid to the adsorbed phase	$ML^{-3}T^{-1}$
M_T	total toluene mass	M
n	number of different phases	------
n	number of paired comparisons	------
P	normalized net phase transfer term	ML^{-3}
q_g	specific discharge of the gas phase	LT^{-1}
q_l	specific discharge of the liquid phase	LT^{-1}
q_{wl}	specific discharge of water in the liquid phase	LT^{-1}

Variable	Definition	Dimensions
q_{sl}	specific discharge of the solute in liquid phase	LT^{-1}
q_{wg}	specific discharge of the water in the gas phase	LT^{-1}
q_{ag}	specific discharge of the air in the gas phase	LT^{-1}
q_{sg}	specific discharge of solute in the gas phase	LT^{-1}
r_i	liquid infiltration rate	LT^{-1}
R_{sl}	retardation factor for solute in liquid phase	------
R_{sg}	retardation factor for solute in gas phase	------
R_{sm}	retardation factor for solute in adsorbed phase	ML^{-3}
S	soil sorptivity	$LT^{-0.5}$
SDm	standard deviation of Dm	------
t	Student t distribution value	------
t	time	T
T_{ij}^{k}	mass transfer of component i from phase j to k	$ML^{-3}T^{-1}$
T^{g}_{sl}	transfer of solute from liquid to gas phase	$ML^{-3}T^{-1}$
T^{l}_{sg}	transfer of solute from gas to liquid phase	$ML^{-3}T^{-1}$
T^{m}_{sl}	transfer of solute from liquid to solid phase	$ML^{-3}T^{-1}$
$T_{sl}^{m^*}$	solute transfer of liquid to solid phase at equilibrium	$ML^{-3}T^{-1}$
T^{l}_{sm}	transfer of solute from solid to liquid phase	$ML^{-3}T^{-1}$
T^{m}_{sg}	transfer of solute from gas to solid phase	$ML^{-3}T^{-1}$
T^{g}_{wl}	transfer of water from liquid to gas phase	$ML^{-3}T^{-1}$
T^{l}_{wg}	transfer of water from gas to liquid phase	$ML^{-3}T^{-1}$
T^{m}_{wg}	transfer of water from gas to solid phase	$ML^{-3}T^{-1}$
T^{m}_{wl}	transfer of water from liquid to solid phase	$ML^{-3}T^{-1}$
T^{l}_{wm}	transfer of water from solid to liquid phase	$ML^{-3}T^{-1}$
V	total volume injected	L^3
V_g	gas phasevolume	L^3
V_l	liquid phase volume	L^3
W_{ij}	source-sink term for component i in phase j	$ML^{-3}T^{-1}$

Variable	Definition	Dimensions
X	total mass of toluene adsorbed by the soil	M
x,y,z	Cartesian coordinates for 3-d distance	L
α	the significance level	------
Δ	disequilibrium term for the variance of the solid phase adsorption from equilibrium	MM^{-1}
ε	volumetric air content	L^3L^{-3}
ϕ	porosity	L^3L^{-3}
γ	activity coefficient	------
λ	Boltzman variable	$LT^{-0.5}$
θ_{ij}	volumetric content of component i in phase j	L^3L^{-3}
θ	volumetric water content	L^3L^{-3}
θ_i	initial moisture content at $t = 0$	L^3L^{-3}
θ_0	constant inlet moisture content for $t > 0$	L^3L^{-3}
$\theta(x,t)$	moisture content boundary conditions	------
$\theta(\lambda)$	transformed moisture boundary conditions	------
θ_{1i}	moisture value from test no. 1 at a given lambda value	L^3L^{-3}
θ_{2i}	moisture value from test no. 2 at a given lambda value	L^3L^{-3}
ρ_b	soil dry bulk density	ML^{-3}
ρ_g	gas phase density	ML^{-3}
ξ_g	tortuosity factor for gas phase solute	LL^{-1}

CHAPTER 1

INTRODUCTION

Statement of the Problem

Volatile petroleum products, liquid solvents and pesticides are organic chemicals beneficial to society, but these chemicals may create environmental concerns when spilled, leaked or improperly disposed. Drinking water standards for volatile organic compounds are usually low, so even a small spill can potentially contaminate a significant amount of ground water. Time consuming and expensive field sampling is normally required to determine the extent of contamination (Baker, 1989), and even when the extent is known, cleanup is difficult. Remediation efforts at contaminated sites have met with varying levels of success (Mercer and Cohen, 1990) because contaminant fate is affected by many factors which are themselves difficult to quantify. Additional information about interactions of volatile organic chemicals with the soil and ground water matrix is needed to assist development of remediation plans with a high probability for success.

Organic chemicals are extensively used, so the potential for additional contamination is high. Moreau (1985) estimated that in excess of 200 billion gallons of petroleum products are used yearly in the United States. Most petroleum products are stored in underground tanks, and the Environmental Protection Agency (EPA) has

estimated that over 300,000 underground gasoline tanks may be leaking into ground water (Devitt et al., 1987). Agricultural operations consume significant amounts of petroleum products, and organic pesticides are commonly used to control weeds, insects and fungi. In their study, Rao et al. (1985) compiled ground water data from several states and found that twenty-one of the forty-one most commonly identified (regardless of concentration) toxic chemicals in ground water were pesticides.

The transport mechanisms for volatile organic solutes in unsaturated soil are difficult to study because of the multiphase nature of the chemicals, heterogeneity of the soils, transient ground water flow characteristics and numerous possible reactions occurring within the unsaturated zone. Figure 1-1 shows potential fates for a volatile

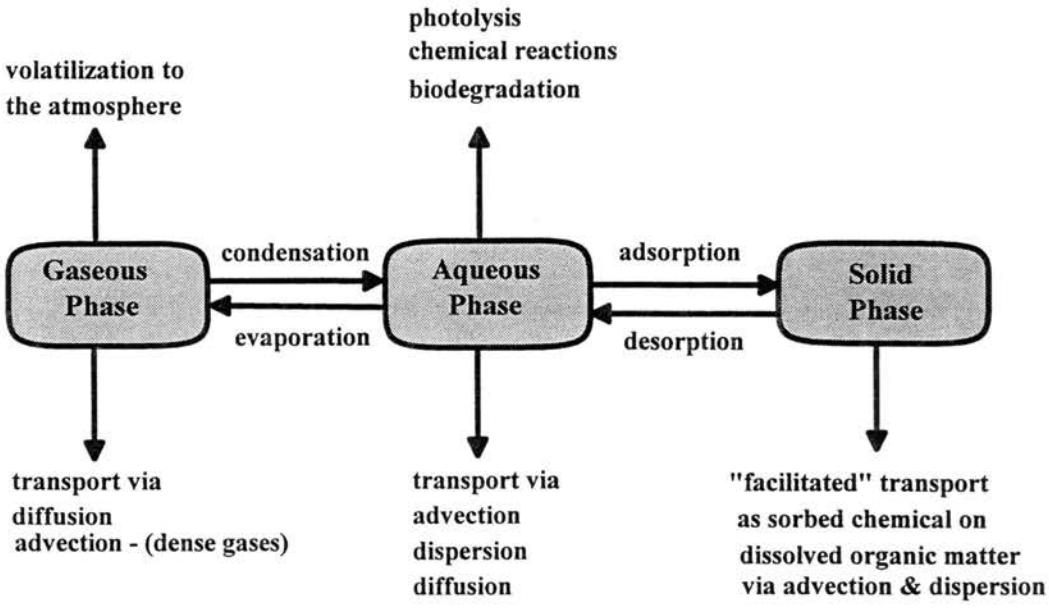

Figure 1-1. Possible volatile organic solute fates in unsaturated soil.

organic solute present in unsaturated soil at low concentrations (no pure phase). At low

concentrations, the solute is found as gaseous, aqueous and solid (adsorbed) phases in the unsaturated soil; with the mass in each phase determined by chemical characteristics, ground water chemistry and soil properties.

Since field data are usually limited and data collection is expensive, remediation plans are often developed using a suitable contaminant transport model. It is assumed that local equilibrium among phases is present. Complicating the development of a remediation plan is the fact that contamination by organic chemicals almost always begins in the unsaturated soil zone, where ground water flow is transient and a non-linear function of the moisture content. The presence of the air phase in unsaturated soil means that a volatile contaminant can vaporize to the soil air and transport as a gas. Multiphase transport of volatile organic chemicals in unsaturated soil is more difficult to investigate than contaminant transport under saturated conditions. As a result, unsaturated conditions have been studied less.

Value of Study

This study investigated the movement of toluene in unsaturated soil during transient flow conditions. Toluene is used for two reasons. First, toluene is a major component of gasoline (Verschueren, 1990) at 5-15% by weight and is commonly found at gasoline-contaminated sites. Second and more importantly, toluene is a good tracer compound for multiphase studies because of its properties. Toluene is slightly soluble in water, adsorbs on the soil organic matter and volatilizes to the soil air with measurable quantities of each phase in the soil matrix at the same time.

Much current research is directed towards understanding and predicting multiphase movement of volatile chemicals in the soil and ground water matrix (Gierke et al., 1992). Desktop computers have made it easier for researchers to develop complex models to predict multiphase mass transport of chemicals. However, many model parameters are subject to simplifications, so how well a model predicts the field conditions is often dependent on the user's skill. Biodegradation, adsorption and chemical reactions moderate the amount of chemical available for mass transport, and these relationships are often included as sink terms in the more complex transport models. Equilibrium values of phase partitioning coefficients are used in models because they are easily determined in the laboratory. Coefficients for transient conditions are difficult to determine. A user must have confidence in the simplifications and assumptions used in any contaminant transport model, especially when the model output is used to help plan an expensive remediation operation.

Remediating a contaminated site using vapor extraction creates transient gas flow conditions and transient conditions exist at the advecting front of a contaminant plume, so equilibrium may be an inaccurate assumption in both cases. Predicting how the vapor phase transports away from the aqueous contaminant plume and quantifying vapor removal is valuable to remediation plan development. This experiment utilized horizontal soil column tests to measure toluene gas phase movement and total compound transport under transient conditions. The measured results were compared to values predicted by local phase equilibrium (LPE) theory to provide insight in the use of equilibrium coefficients for parameter estimation in ground water models.

Objectives

The overall objective was to test the validity of LPE assumptions near the advecting front of a toluene plume during unsaturated transient flow. The specific objectives of the research were to: (1) determine all properties of the experimental soil which affect toluene's equilibrium phase partitioning relationships, (2) develop methods to sample and analyze toluene gas phase during transient soil column experiments, (3) measure total toluene (all phases) concentration advancement by destructively sampling along the column length immediately upon test completion, (4) at each sampling position compare the measured toluene gas phase concentration to the gas concentration calculated from theory (assuming equilibrium) at the same sampling position and (5) if LPE conditions are not present, then determine and quantify the form of the non-equilibrium term.

CHAPTER 2

REVIEW OF THE LITERATURE

Introduction

Volatile organic chemicals (VOCs), such as toluene, in the soil and ground water are complex chemicals in a biochemical and physical chemical environment. During ground water movement toluene is subject to mass transport, chemical mass transfers and biologically mediated mass transfers. Toluene is a hydrophobic (water hating) liquid, and similar to many VOCs, it is multiphase in behavior with limited water solubility. At low concentrations in unsaturated soil it partitions among the liquid, adsorbed and gas phases. At higher concentrations, when the maximum adsorptive capacity and solubility limit are exceeded, the toluene is also found as a separate non-aqueous phase liquid (NAPL). Most contaminated sites involve multiple chemicals with resultant interactions among those chemicals and their surroundings. This makes it difficult to interpret field data for cause and effect. As a result, much information on volatile transport is from single-contaminant laboratory experiments rather than field studies (Khondaker et al., 1990; Jury and Flühler, 1992).

Volatile transport has been studied in part by many different disciplines: soil chemistry, soil physics, hydrogeology, petroleum engineering, environmental engineering, microbiology and mathematics. Therefore information is scattered and frequently

discipline-specific. In order to conduct this research it was necessary to review a wide variety of literature. This chapter would be lengthy if I commented on all the literature reviewed. The scope is therefore limited to the more important literature. Factors affecting transport, partitioning models, diffusion models, transport models and laboratory soil column experiments are covered in this review.

Factors Affecting Transport

Transport is affected by the soil's physical and chemical properties, toluene's chemical and physical properties, toluene concentration, the ground water chemistry, the ground water flow condition and such external influences as barometric pressure and temperature. Reaction rates for toluene in the soil and ground water matrix are slower than solution chemistry reaction rates due largely to less rapid mixing and lower temperature. Biodegradation and volatilization are significant toluene-loss mechanisms which must be controlled in laboratory experiments as they are difficult to quantify.

Contaminant Properties

Contaminant chemical and physical properties determine whether a VOC's reactions with its surroundings are reversible or irreversible (National Research Council, 1990). In reversible reactions, such as adsorption then desorption, a contaminant's chemical structure is unaltered when it changes phase. In an irreversible reaction, for example biodegradation, toluene's chemical structure is permanently altered. Contaminants are often grouped based on common properties. The USEPA groups its 129 priority pollutants according to similar analytic techniques, while Domenico and

Schwartz (1992) categorize contaminants in a more general way according to reaction type and mode of occurrence (ie. radioactive, inorganic, organic, and biological). Toluene is a gasoline component and a common organic ground water contaminant according to Domenico and Schwartz (1992). It is slightly soluble in water and frequently present in the soil simultaneously in multiple phases. At low concentrations toluene partitions among the dissolved, gaseous (vapor), and adsorbed phases until equilibrium among the phases is reached. Adsorption temporarily removes toluene from the ground water, thereby "retarding" the chemical from transporting until it desorbs from the soil when less contaminated water flows past the soil particle. Organic contaminants adsorb to soil organic matter primarily through van der Waals-London interactions, hydrophobic bonding and hydrogen bonding (Stumm, 1992, and Hamaker; Thompson, 1972).

Density and viscosity of organic liquids influence how they transport in the soil and ground water matrix. Under certain conditions organic liquids transport as pure compound (Mercer and Cohen, 1990). Nonaqueous phase liquids (DNAPLs) denser than water, such as trichloroethene (TCE), tend to sink through the soil profile where they accumulate along the bottom of the aquifer. Lighter than water nonaqueous compounds (LNAPLs) such as toluene, tend to float on the surface of the ground water table and diffuse into the ground water below as well as the porous media above. DNAPLs may require more effort to remediate than a LNAPL contaminant since they penetrate the aquifer completely thereby affecting a larger volume of soil and ground water. Important chemical and physical properties for toluene are listed in Table 2-1.

TABLE 2-1

Physical and Chemical Properties of Toluene

Property	Value	Reference
Chemical structure	methylbenzene	Verschueren, 1990
Polarity	nonpolar	Verschueren, 1990
Molecular weight	92.15 g mol^{-1}	Verschueren, 1990
Specific gravity	0.867 g cm^{-3} @ 20 °C	Verschueren, 1990
Boiling point	110.6 °C	Verschueren, 1990
Vapor pressure (sat'd)	10 mm Hg @ 6.4 °C 22 mm Hg @ 20 °C	Verschueren, 1990
Vapor conc. (sat'd)	110 mg L^{-1} @ 20 °C	Verschueren, 1990
Solubility	470 mg L^{-1} @ 16 °C 515 mg L^{-1} @ 20 °C	Verschueren, 1990
Henry's law constant	0.261 0.270	Garbarini and Lion, 1985 Ong et al., 1992
Diffusion coefficient in pure air	6570 cm^2 d^{-1}	Ong et al., 1992
Diffusion coefficient in pure water	0.084 cm^2 d^{-1}	Ong et al., 1992
Surface tension	28.5 dynes cm^{-1} @ 20 °C	Mercer and Cohen, 1990

Organic contaminants are degraded by chemical or biological methods, and the degradability is related to their chemical and physical properties (Kobayashi and Rittmann, 1982; National Research Council, 1990). Depending on its structure, a contaminant is irreversibly transformed in the soil by several mechanisms: precipitation,

hydrolysis, photolysis or redox reactions. Toluene is subject to chemical photolysis and hydrolysis in the soil (National Research Council, 1990). Biodegradation of organic chemicals by microorganisms is an important method of transforming the chemical into a form non-toxic to the environment. The diverse population of microorganisms found in the soil can degrade most organic compounds, if the proper conditions are present (McCarty et al., 1981). However, some chemicals are difficult to degrade due to complex structure, presence of toxic components, concentration less than a threshold value or recalcitrance to degradation because of halogens present in the structure (Kobayashi and Rittmann, 1982). The main mechanisms for toluene biodegradation are cleavage of the ring under aerobic conditions to form bicarboxylic acid (Robinson, et al., 1990; Fetter, 1993), and cleavage of the ring under anaerobic conditions in the presence of nitrate to form carboxylic acid (Fetter, 1993; Barbaro et al., 1992).

Soil Matrix Properties

The chemical and physical properties of the soil particles and ground water are significant to toluene's fate (Hillel, 1980). Reactions occur on the soil surface, so finer textured soils with higher percentages of clay and silt are more reactive. Soil organic matter (SOM) is an important soil component with specific surface areas similar to clay particles. In mineral soils the SOM is normally a small percentage of the total soil content, but its impact on soil properties is significant because it coats the soil mineral particles creating a larger surface area for reactions. The SOM is made up of decaying vegetative matter, animal matter and humus. The humus is decomposed matter with many organic polymers and functional groups (Jury et al., 1991). The organic polymers

are especially important to toluene adsorption. The fraction of organic carbon (f_{oc}) present in the soil is often used as a measure of the organic chemical sorption capacity of a soil (Karickhoff et al., 1979).

Soil texture, SOM, and soil forming processes determine a soil's bulk density (ML^{-3}), porosity (L^3L^{-3}) and permeability (LT^{-1}). Bulk density measures soil compaction with typical surface soil densities varying from 1.2 to 1.8 g cm^{-3} with corresponding porosity of 0.55 to 0.32 cm^3 cm^{-3}. Fine textured soils high in clay have high porosity, but since the pore size is small, the permeability is low and ground water movement is slow. Sandy soils are lower in porosity, but the pores are larger and permeability is several orders of magnitude higher than in clay soils.

Ground water movement depends on whether the soil is saturated or unsaturated and the potential gradient of the soil water. Dissolved toluene transports with the ground water and it adsorbs on the soil organic matter during transport. Toluene vaporizes to the soil air in unsaturated conditions. In the gas phase it transports independently from the water through gas diffusion due to concentration gradients, or gas phase advection due to vapor density gradients. Toluene will adsorb until the soil's maximum capacity is filled or local phase equilibrium reached, whichever occurs first.

In unsaturated conditions both dissolved and gas phase toluene are present. An extremely dry soil with relative humidity corresponding to less than eight monolayer coverage of the particles by water molecules adsorbs more contaminant from the gas phase than the same soil adsorbs from liquid phase at higher relative humidity (Lion et al., 1990). Thus a very dry soil can act as a sink for toluene vapor. At moisture levels

above eight monolayers of water coverage, the toluene adsorption is controlled by the liquid phase.

Other chemical and physical reactions affect volatile organic contaminants. Reducing or oxidizing agents may react with a contaminant resulting in permanent removal. The ionic strength of the soil solution affects the phase equilibrium status within the soil, thereby changing the ratio among phases for a multiphase chemical. The presence of excess sodium in the soil matrix may cause dispersion of the clay particles which clog the soil pores and significantly decrease soil permeability. Dissolved gases in soil water decrease the surface tension of ground water, and this lessens the capillary rise of water.

External Influences on Transport

Besides the contaminant and the soil matrix properties, some external conditions affect transport. Precipitation or irrigation provides the driving force for ground water movement, so it stands to reason that water addition to the soil matrix directly affects the contaminant movement through the profile. Ambient air temperature influences the soil temperature which in turn controls the rate of reaction and microbial activity in the soil. Most biological activity in a soil is located near the surface, where most of the nutrients, favorable temperature, water, oxygen and other growth factors are present.

Wind speed, barometric pressure, vegetation, and surface condition influence the movement of a volatile chemical through the soil surface. Windy conditions remove the contaminant next to the surface more effectively by causing a larger concentration gradient and more rapid transport through the surface. Barometric pressure affects vapor

pressure and the volatility of organic chemicals. Surface vegetation affects the thickness of the boundary layer adjacent to the soil surface. With thick vegetative cover, surface winds are not able to remove contaminants near the surface as effectively, which lowers transfer rates. Surface disturbances such as tillage do two things; first, they remove the vegetative cover increasing the transfer rate, and second, they redistribute the contaminate in the tilled layer changing the concentration gradient, thereby increasing the chemical mass transfer.

Partitioning Models

Equilibrium among phases is the preferred chemical state of a natural system. When that system is disturbed, it reacts by shifting its equilibrium position to counteract the effect of a disturbance (LeChâtelier's Principle). Contaminant phase distribution in the soil matrix responds to concentration, temperature or pressure gradients by shifting its equilibrium position among the phases. How quickly local equilibrium among phases establishes is important to contaminant transport. Equilibrium partitioning coefficients are usually determined by 24 hour isothermal batch tests using the soil and chemical of interest. Because flow in the soil matrix is relatively slow (measured in cm per day), equilibrium partitioning is normally assumed when apportioning the chemical among the various phases in transport models.

Early research focused on pesticide partitioning between liquid to solid phase (Jury et al., 1983; Voice and Weber, 1983; Weber et al., 1983; Jury et al., 1984a, b and c; Rao et al., 1985) because of concern about pesticide movement. While partitioning

theory is the same for pesticides and VOCs, their properties are different. Most pesticides are relatively non-volatile and strongly adsorbed when compared to VOCs. Volatile chemicals such as toluene are slightly soluble, volatile and adsorb readily. Such multi-phase behavior makes applying partitioning theory more challenging.

Complicating partitioning even more is the fact that most contaminated sites involve a mixture of chemicals. This results in interactions, cosolvent effects and a more complicated behavior than predicted by theory (Mercer and Cohen, 1990; Park and Eichholz, 1990; Cline et al., 1991; Rao et al., 1991; Walton et al., 1992). Park and Eichholz (1990) stressed knowing the actual soil moisture conditions when developing a migration model for mixed waste near the surface. Cline et al. (1991) related partitioning in a complex mixture (gasoline) to Raoult's Law using fuel component partitioning in water. Rao et al. (1991) and Walton et al. (1992) suggest that partitioning in mixtures is reliably predicted using K_{ow} values. Each approach worked well for the situation evaluated, but the variability among media and chemicals makes it challenging to determine which approach is the best.

Analysis of partitioning and transport is challenging, even when the complication of a mixture of chemicals is simplified to a single chemical. Single contaminant experiments have dominated the research on partitioning and transport. The effect of adsorption at various soil moisture levels was studied (Chiou and Shoup, 1985; Crittenden et al., 1989; Lion et al., 1990; Shimizu et al., 1992) and each investigator found that K_d was a function of moisture content to a certain level where liquid phase adsorption dominates. This agrees with laboratory results by Yu (1995) in her

dissertation research. Shoemaker et al. (1990) found that adsorption on relatively dry porous media can be more than two orders of magnitude greater than adsorption controlled by the liquid phase. They developed an analytic model of this two-phase adsorption and a sensitivity analysis suggests that the chemical and physical processes interact significantly.

Ahlert and Uchrin (1990) showed that benzene and toluene undergo a very rapid adsorption to organic matter and with time a secondary uptake as the compounds apparently diffuses into the soil pores. Jury et al. (1990) developed a screening model based on partitioning theory to estimate relative volatility of different compounds through a soil layer. This approach provided only relative information to compare different compounds and is not useful to predict movement. Cohen et al. (1990) developed a more complex screening model to explore steady-state partitioning of a volatile chemical under different situations and parameters. While this is a more robust model it is still a screening model and gives results within a factor of 2-4.

.

Diffusive Models

Another approach to modeling volatile contaminant location within a system is application of diffusion theory. This is often done to existing partitioning models in an attempt to model systems not well described by partitioning alone. Diffusive models account for spreading of the chemical and usually assume Fickian diffusion with concentration gradients, temperature gradients and sometimes mobile or non-mobile pore water. They enhance equilibrium partitioning models and are used to explain the

movement and spreading of the chemical within the porous media. However, equilibrium partitioning is still at the heart of a diffusive model.

Fick's Law is valid for the case of a dilute compound diffusing into a bulk phase, and for most vapor transport situations in unsaturated soil this is a good description. There have been many models developed for vapor phase transport without advective gas flux using Fick's Law (Jury et al., 1983; Abriola and Pinder, 1985 a and b; Baehr and Corapcioglu, 1987; Baehr, 1987; Thortenson and Pollock, 1989; Cho and Jaffe, 1990; Amali and Rolston, 1992). This appears to be a valid approach when the contaminant is dilute and falls within the linear adsorption range. It also works best when there is not any organic liquid phase of a contaminant with a high vapor pressure present. In this situation the organic vapor would likely create a density gradient which could result in advective transport. Another situation where Fick's Law estimates exhibit discrepancies is when a mixture of organic vapors occurs. A multicomponent effect typically appears when the total mole fraction of the organics is 0.05 or higher. Fick's Law then underestimates diffusion of a single species (Amali and Rolston, 1992).

Fickian diffusion is not the only process affecting gas movement (Cho and Jaffe, 1990). As stated above, density gradients can cause gas advection. Changes in air volume due to temperature fluctuations and barometric pressure can cause gas advection. Displacement of air by liquid infiltration also can cause bulk movement of air and vapors. Baehr and Bruell (1990) suggest using the more general Stefan-Maxwell Equations in models when the contaminant vapor is a significant portion of the vapor phase. Data from their column experiments suggests that tortuosity is overestimated by Fick's Law

even though Fick's Law provides a good fit to the data. In general, Fick's Law adequately describes vapor diffusion for most situations, including those for the column experiments in this research.

Moisture content in the soil has a significant influence on vapor transport by reducing the effective diffusion rate when moisture increases slightly or by increasing the effective diffusion rate when moisture decreases. At moisture conditions favorable to vapor transport, diffusion spreads the contaminant to surrounding uncontaminated soil where it dissolves and adsorbs (Mendoza and McAlary, 1990). Some models predict diffusion under varied moisture content to assist in planning vapor extraction operations (Gierke et al., 1992; Ong et al., 1992). These models account for increased vapor adsorption and the resulting nonequilibrium as the profile becomes drier. This implies that there is an optimum moisture level where vapor extraction is most efficient.

Predictive Transport Models

Partitioning and diffusion are combined with an advection/dispersion model to make a predictive transport model covering all processes. It is difficult and expensive to sample ground water, and predictive transport models can use a limited number of field samples to locate the contaminant source and project how the contaminant will move in the future. Every predictive model includes a ground water flow model, since the bulk of the contaminant mass moves by advection and dispersion. LPE assumptions and diffusive theory are at the heart of most models. The challenge is making the model reflect the heterogeneity of an actual system.

Approaches to addressing uncertainty in transport have resulted in the development of many different models for contaminant transport. In order to apply a particular model with confidence, the theory and assumptions behind it must be understood. A model used for steady saturated flow of a non-volatile contaminant is not the best choice for unsaturated flow of a volatile compound. Steady conditions differ significantly from unsteady conditions. The processes occurring at the invading front of a contaminated plume moving into uncontaminated soil determine how the chemical spreads.

Jury et al. (1983, 1984a, b and c) wrote a series of papers on a screening model they developed for trace organics in soil. The model evaluated soil applied chemicals, assumed equilibrium among phases, first order degradation of the chemical and volatilization to the atmosphere at the surface. Either steady state upward or downward flow of water was assumed in order to calculate the chemical distribution and volatilization flux. Using the model, relative comparisons of different chemicals can be made for volatility, advective transport, diffusion and persistence. The model is unable to predict what happens under the transient conditions found when a contaminant is just beginning to invade clean soil.

Multiphase approaches to modeling of volatile organic contaminants were developed by several researchers (Abriola and Pinder, 1985 a and b; Corapcioglu and Baehr, 1987; Baehr and Corapcioglu, 1987). Abriola's and Pinder's model can evaluate the transport of a volatile chemical as dissolved phase in the ground water, gas phase and as a nonaqueous liquid phase (NAPL). The model uses LPE assumptions and

conservation of mass principles to develop a system of non-linear, partial differential equations to solve for capillary pressure between the organic and water phase and the water and gas phase. Their model also uses the mass fraction in the water, gas and organic liquid phase. While their model attempts to describe complex multiphase movement of organic chemicals, it does not include adsorption and biodegradation. These two processes have a significant effect on transport within a soil.

Baehr's and Corapcioglu's model is similar to Abriola's and Pinder's but it includes adsorption of the chemical to the soil organic matter, incorporates a sink term to represent degradation and can also evaluate transport outside of the organic liquid plume. Mass balance and LPE assumptions are also at the heart of the model. Their model is general and requires considerable data input, so it is best applied to special situations that are part of a larger problem.

More recent models have attempted to include nonequilibrium due to various processes in their equations. Brusseau et al. (1989) developed a model that evaluated transport and sorption-caused nonequilibrium and then checked the results against equilibrium calculations. Their model attempted to represent the physiochemical processes between transport and adsorption in saturated conditions. Their results suggest that multiple processes may be contributing to nonequilibrium. Sleep and Sykes (1989) developed another model to evaluate liquid phase advection and gas phase advection due to a density gradient. The model included gas phase volatilization and gas-liquid partitioning but not adsorption. The model is limited in its application to relatively specific conditions.

Brusseau (1991, 1992b) developed a model to predict gas advection in a structured soil where rate-limiting adsorption is present. The model considers transport only by gas phase advection and gas phase dispersion. The liquid phase is considered immobile in a condition which is similar to vacuum extraction remediation procedures. The model accurately predicts some situations using limited data. Benson et al. (1993) also developed a model to simulate vapor extraction remediation processes. This model considered variable permeability and heterogeneity, but not rate-limited adsorption. As with the other models mentioned, it worked well for some situations and poorly for others. Recognizing the strengths and limitations of a model is critical to its successful application.

Laboratory Soil Column Experiments

Because real sites are heterogeneous, they are difficult to study. Thus, the importance of numeric models developed from theory becomes clearer. Laboratory column experiments are often used to evaluate numeric models for their predictive ability. Column experiments have contributed significantly to the art and science of predicting contaminant transport, but they also have limitations. Many laboratory column experiments use vertical columns with steady flow in either saturated or unsaturated moisture conditions. Steady conditions are not similar to the dynamic conditions found at the leading edge of the contaminant plume in an unsaturated soil. Column experiments are flexible and allow quicker testing of more soils than could be done in the field. Often the test soil has been comprised of glass beads, sands or soils with limited adsorption in

order to study dispersion and liquid advection without the complicating effect of adsorption/desorption.

Unsaturated column tests are conducted under steady-state conditions with non-adsorbing soils in most studies. Some transient flow tests have been conducted on volatile compound gas transport for use in designing vapor extraction projects. Soil column experiments are numerous and only limited by the ability of the researcher to match the boundary conditions and physiochemical principles involved. Examples of tests similar to this study, using transient, unsaturated column experiments with a volatile multiphase chemical, under wetting conditions in a soil with significant adsorption capacity, were not located during the literature review.

Many recent column tests have focused on petroleum products and other immiscible contaminants in an effort to understand more completely how they transport. This information is used to assist remediation planning. Zalidis et al. (1991) used steady state unsaturated vertical column tests to evaluate the potential of immobile residual benzene, toluene, and xylenes (BTX) to contaminate infiltrating water. The tests used a sandy loam soil with an organic carbon fraction of 0.004. Their tests did not address the basic theory of the multiphase system but were more along the line of a screening test to assess bulk potential for remediation at a particular condition. Reible et al. (1990) did a column study on infiltration of a NAPL into a vertical sand column at field capacity moisture levels to model what happens when a spill infiltrates into the soil under gravity and capillary forces. This was a relatively simple modeling approach to predict

movement by a liquid phase NAPL through the soil. The research did not analyze other phase transport by the contaminants.

MacIntyre et al. (1991) did a study comparing adsorption coefficient estimation by batch, box and column procedures on low organic carbon aquifer material. In the low organic carbon soil they found that there was no significant difference in the adsorption coefficient among the methods. This provides confidence in using batch-test determined adsorption coefficients, but their study did not include soils with higher adsorption capacity. Li and Voudrias (1992) used vertical columns of dry sand and dry soil to compare unsteady state vapor transport from classes of mixed organic chemicals. They also tested a wet soil with a relatively low bulk density of 1.03 g cm^{-3} and a moisture content of 0.267 cm^3 cm^{-3} . Their experiments agreed well with Fick's Law of Diffusion for the dry columns, where adsorption was controlled by the vapor phase, but the results did not fit well in the wet soil. This study only concerned itself with breakthrough of the vapor phase and its retardation.

Gierke et al. (1990) developed a model to evaluate several different processes in unsaturated soil and used column tests for validation. Their model included dispersion and advection in both the air and water phases, mass transfer from both the air and water phase assuming LPE, adsorption, diffusion of the organic into immobile water and mass transfer between mobile and immobile water. The model did not address the vapor diffusion processes directly. The laboratory columns were conducted under steady flow and constant moisture conditions using TCE and a bromide tracer for breakthrough tests in an Ottawa sand and a verilite soil type material. Both of these materials are not highly

similar to common soils, so their results may be difficult to extrapolate. The columns used relatively high pore water velocities and under this condition vapor diffusion was not an important transport mechanism.

Unsaturated horizontal column experiments similar to those used in this research are not as common. They have been used most for water diffusivity experiments because of the ability to transform the flow from time and space dependence to the single Boltzman variable. Brown and Allred (1992) and Allred (1995) have used horizontal tests to determine diffusivity and study surfactant movement in soil and its subsequent effect on diffusivity and unsaturated hydraulic conductivity. Their studies considered adsorption or immobilization of the surfactant and biodegradation. The surfactants are nonvolatile and considerably different in properties than a VOC, so procedures and methods that worked well with surfactants were unsuccessful with a volatile such as toluene. This study developed procedures and methods that were consistent with the horizontal column theory and boundary constraints in order to collect multiphase transport data.

CHAPTER 3

TRANSPORT PROCESS AND THEORY

This theoretical analysis of volatile organic compound (VOC) transport is limited to unsaturated conditions similar to those used in the horizontal soil column experiments. Specifically, the analysis evaluates isothermal, one dimensional, horizontal, unsaturated transport of a VOC. The soil column experiments had constant dry bulk density, an initial volumetric moisture content around 8% and uncontaminated soil and water within the column. Dilute toluene solution was injected into the soil column using a syringe pump to maintain the Bruce/Klute unsaturated boundary conditions (Brown and Allred, 1992) of constant moisture potential and constant solute concentration potential at the column inlet.

Unsaturated Contaminant Transport Relationships

During unsaturated flow the transport relationships are more complex because a volatile contaminant, such as toluene, can be transported in the gas phase as well as the liquid phase. The general continuity equation for volatile solute transport in unsaturated porous media is

$$\frac{\partial}{\partial t}(\theta_{ij} C_{ij}) = -\nabla F_{ij} - W_{ij} + \sum_{i=1}^{n} T_{ij}^{k} \quad , \qquad \textbf{(3-1)}$$

where i is the component (contaminant, water, air or solid), j the component's phase, θ_{ij} the volumetric content (L^3L^{-3}) of component i in phase j, C_{ij} the concentration (ML^{-3}) of component i in phase j, F_{ij} the mass flux ($ML^{-2}T^{-1}$) of component i in phase j, W_{ij} the source-sink term ($ML^{-3}T^{-1}$) for component i in phase j, T_{ij}^{k} the mass transfer ($ML^{-3}T^{-1}$) of component i from phase j to phase k and n the number of different phases present. In the column experiments W_{ij} is zero because there are no sources or sinks.

Porosity (ϕ) is the volume of soil voids represented by

$$\phi = \theta + \varepsilon \quad , \tag{3-2}$$

where θ is the volumetric water content (L^3L^{-3}), and ε the volumetric air content (L^3L^{-3}) of the porous media. Toluene is slightly soluble in water and at dilute concentrations is found in the soil in the gas, liquid and adsorbed phases. Expanding the left side of Equation 3-1 for toluene's three phases gives

$$\frac{\partial}{\partial t}(\theta_{ij}C_{ij}) = \frac{\partial}{\partial t}(\rho_b C_{sm} + \theta C_{sl} + \varepsilon C_{sg}) \ . \tag{3-3}$$

Since no sources or sinks are present, it follows that

$$\rho_b C_{sm} + \theta C_{sl} + \varepsilon C_{sg} = C_T \ , \tag{3-4}$$

where C_{sm}, C_{sl}, and C_{sg} are the concentrations respectively of the solute in the adsorbed phase (MM^{-1}), liquid phase (ML^{-3}), and gas phase (ML^{-3}), ρ_b the soil dry bulk density (ML^{-3}) and C_T the total mass (ML^{-3}) of solute per unit volume of the porous media.

Expanding the mass flux and mass transfer terms on the right side of Equation 3-1 completes the mass balance for all components. The column experiments investigated unsaturated flow rates with liquid phase advection of the solute, and solute spreading due to liquid dispersion and molecular diffusion. In one dimension the liquid flux terms are

$$F_{wl} = q_{wl}C_{wl} - D_{wl}\frac{\partial C_{wl}}{\partial x} \tag{3-5}$$

and

$$F_{sl} = q_{sl}C_{sl} - D_{sl}\frac{\partial C_{sl}}{\partial x} \quad , \tag{3-6}$$

where F_{wl} is the flux of water in the liquid phase, q_{wl} the specific discharge (LT^{-1}) of the water in the liquid phase, C_{wl} the concentration of water in liquid phase, D_{wl} the dispersion-diffusion (L^2T^{-1}) coefficient for water in the liquid phase, F_{sl} the flux of solute in liquid phase, q_{sl} the specific discharge of the solute in liquid phase, C_{sl} the concentration of solute in liquid phase and D_{sl} the dispersion-diffusion coefficient for solute in the liquid phase.

Gas phase flux of the components is subject to advection and spreading due to molecular diffusion alone. Expanding the gas phase flux terms gives

$$F_{wg} = q_{wg}C_{wg} - D_{wg}\frac{\partial C_{wg}}{\partial x} \quad , \tag{3-7}$$

$$F_{ag} = q_{ag}C_{ag} - D_{ag}\frac{\partial C_{ag}}{\partial x} \quad , \tag{3-8}$$

and

$$F_{sg} = q_{sg}C_{sg} - D_{sg}\frac{\partial C_{sg}}{\partial x} \quad , \tag{3-9}$$

where F_{wg} is the flux of water in the gas phase, q_{wg} the specific discharge of the water in the gas phase, C_{wg} the concentration of water in the gas phase, D_{wg} the diffusion coefficient for water in the gas phase, F_{ag} the flux of air in the gas phase, q_{ag} the specific discharge of the air in the gas phase, C_{ag} the concentration of air in the gas phase, D_{ag} the diffusion coefficient of air in the gas phase, F_{sg} the flux of solute in the gas phase, q_{sg} the specific discharge of solute in the gas phase, C_{sg} the concentration of solute in the gas phase and D_{sg} the diffusion coefficient for the solute in the gas phase.

The final flux term is solid phase diffusion or movement of the adsorbed solute along the surface of the solid particles. While there is some evidence according to

Hamaker (1972) that adsorbed solutes migrate along the particle surface, the rate is negligible compared to the other flux terms. Then solute solid phase flux is

$$F_{sm} = 0 \quad . \tag{3-10}$$

Next, the applicable mass transfer terms are determined to complete the mass balance. While air and solid phase components do not exhibit mass transfer, the solute and water phases undergo mass transfers which affect contaminant transport. Net mass transfer terms for the solute include: T^{g}_{sl} the transfer of solute from liquid to the gas phase by vaporization, T^{l}_{sg} the transfer of solute from gas to liquid phase by condensation, T^{m}_{sl} the transfer of solute from liquid to solid phase by adsorption on the porous media solids, T^{l}_{sm} the transfer of solute from solid to liquid phase by desorption and T^{m}_{sg} the transfer of solute from gas to solid phase by adsorption. The transfer of the solute directly from gas phase to adsorbed solid phase occurs only in extremely dry (less than 8% moisture) soil, so T^{m}_{sg} is not applicable to this analysis.

Net mass transfer terms for water are: T^{g}_{wl} the transfer of water from liquid to gas phase by evaporation, T^{l}_{wg} the transfer of water from gas to liquid phase by condensation, T^{m}_{wg} the transfer of water from gas (water vapor) to solid phase by adsorption, T^{m}_{wl} the transfer of water from liquid to solid phase by adsorption on the solid media and T^{l}_{wm} the transfer of water from solid phase to liquid phase by desorption. Desorption and adsorption of water on the solid phase are equal, and are opposite under the experimental conditions, so these terms cancel each other. Adsorption of water vapor directly to the soil surface occurs only under extremely dry conditions (Lion et al., 1990) and is not applicable to the column experiments or this analysis.

It should be noted that for the net mass transfer terms: T^{g}_{sl} equals the negative of T^{l}_{sg}, and T^{m}_{sl} equals the negative of T^{l}_{sm}. Summing the applicable mass flux and phase transfer terms gives

$$\frac{\partial}{\partial t}(\rho_b C_{sm} + \theta C_{sl} + \varepsilon C_{sg}) = -\frac{\partial}{\partial x}(q_{wl}C_{wl} + q_{sl}C_{sl} + q_{wg}C_{wg} + q_{ag}C_{ag} + q_{sg}C_{sg})$$

$$+D_{wl}\frac{\partial^2 C_{wl}}{\partial x^2} + D_{sl}\frac{\partial^2 C_{sl}}{\partial x^2} + D_{wg}\frac{\partial^2 C_{wg}}{\partial x^2} + D_{ag}\frac{\partial^2 C_{ag}}{\partial x^2} + D_{sg}\frac{\partial^2 C_{sg}}{\partial x^2},$$

$$+ T^{g}_{sl} + T^{g}_{wl} + T^{l}_{wg} + T^{l}_{sg} + T^{l}_{sm} + T^{l}_{wm} + T^{m}_{sl} + T^{m}_{sg} + T^{m}_{wg} + T^{m}_{wl} \quad , \quad \textbf{(3-11)}$$

which is further simplified by considering partitioning, phase continuity of each component and local phase equilibrium (LPE) conditions.

Partitioning

Partitioning is the mass transfer of a component from one phase to another, and it is critical to contaminant transport. Applicable phase partitioning coefficients for the solute in the column experiments are Henry's coefficient, K_H (dimensionless), for partitioning between the gas and liquid phase, and the linear adsorption coefficient, K_d (L^3M^{-1}), for partitioning between liquid and adsorbed (solid) phase. According to Henry's Law, the vapor pressure of a volatile solute in dilute aqueous solution varies linearly with its concentration. Under isothermal and equilibrium conditions it is related to the gas and liquid concentration by

$$C_{sg} = K_H C_{sl} \quad . \qquad \textbf{(3-12)}$$

Soil adsorption under isothermal and equilibrium conditions is modeled by several different empirical isotherms. Each assumes that: the system is at equilibrium without kinetic effects, adsorption is reversible without hysteresis and equilibrium is

unaffected by the presence of other ions or solutes. Two adsorption isotherms used to describe similar column experiments are the Freundlich model and the linear model. The Freundlich is

$$C_{sm} = KC_{sl}^{n} \quad , \quad with \quad (n \leq 1) \ , \tag{3-13}$$

and the linear is

$$C_{sm} = K_d C_{sl} \ . \tag{3-14}$$

The linear model is just the special case of the Freundlich isotherm where $n = 1$. Karickhoff et al. (1979) found that adsorption of hydrophobic organic compounds to soil was linear up to approximately 50% of their water solubility. Toluene solubility is around $5x10^{-3}$ M and the 50% guideline for the linear model is approximately 230 mg L^{-1} toluene. This is markedly above the approximately 75 mg L^{-1} toluene concentration levels used in the column experiments, so the linear model is used in the analysis.

At equilibrium the liquid phase of the solute is related to solute concentration in both the adsorbed and gas phases. The total solute concentration of Equation 3-4 is related to each individual phase by

$$C_T = C_{sm}[\rho_b + \frac{\theta}{K_d} + \varepsilon\frac{K_H}{K_d}] \ ,$$

$$C_T = C_{sl}[\rho_b K_d + \theta + \varepsilon K_H]$$

and

$$C_T = C_{sg}[\rho_b \frac{K_d}{K_H} + \frac{\theta}{K_H} + \varepsilon] \ . \tag{3-15}$$

The lumped terms in the brackets are called retardation (R) factors, and each R-factor is a function of θ when the soil density is constant. Total concentration in each phase is related to the retardation factors by

$$C_T = C_{sm}R_{sm} = C_{sl}R_{sl} = C_{sg}R_{sg} \ , \tag{3-16}$$

where both R_{sl} and R_{sg} are dimensionless, and R_{sm} has dimensions of ML^{-3}.

Phase Continuity

Gas Phase

The solute liquid concentration is dilute, which means that the gas phase concentration is low. A density gradient is not present to cause gas phase advection, and the component gas flows are related by

$$q_{wg} = q_{ag} = q_{sg} = q_g \quad . \tag{3-17}$$

Summing the gas phase continuity for Equation 3-11 yields

$$\frac{\partial \varepsilon (C_{sg}+C_{wg}+C_{ag})}{\partial t} = -\frac{\partial q_g (C_{sg}+C_{wg}+C_{ag})}{\partial x} + \frac{\partial}{\partial x}(D_{sg}\frac{\partial C_{sg}}{\partial x} + D_{wg}\frac{\partial C_{wg}}{\partial x} + D_{ag}\frac{\partial Cag}{\partial x}) + T_{sl}^{g} + T_{wl}^{g} \quad , \tag{3-18}$$

where the sum of the three gas phase concentration terms equals the gas phase density (ρ_g). The column tests are isothermal with an initial moisture content above 8%, so relative humidity is 100% throughout the column. At the experimental conditions, the concentration of the water in the gas phase is constant at approximately 20 mg L^{-1}, and the solute gas phase concentration varies from zero to above 3 mg L^{-1}. Both values are negligible compared to the concentration of the air in the gas phase (C_{ag}) at approximately 1200 mg L^{-1}. Since C_{ag} and C_{wg} are constant, their partial differentials, with respect to distance, in the diffusion term of Equation 3-23 are zero. The gas phase continuity equation reduces to

$$\frac{\partial \varepsilon \rho_g}{\partial t} = -\frac{\partial q_g \rho_g}{\partial x} + D_{sg}\frac{\partial^2 C_{sg}}{\partial x^2} + T_{sl}^{g} + T_{wl}^{g} \quad . \tag{3-19}$$

Solute gaseous diffusion (D_{sg}) in soil is a function of tortuosity, the molecular diffusion rate for the solute in air and the soil air porosity (Jury et al., 1991). Diffusion flux for a gas phase solute is

$$J_{sg} = -\xi_g D_{s(air)}\frac{\partial C_{sg}}{\partial x} = -D_{sg}\frac{\partial C_{sg}}{\partial x} \quad , \tag{3-20}$$

where J_{sg} is the flux ($ML^{-2}T^{-1}$), ξ_g is the tortuosity factor (LL^{-1}) and $D_{s(air)}$ is the molecular diffusion rate of pure solute gas phase in air.

The solute diffusion coefficient for the gas phase equals

$$D_{sg} = \xi_g D_{s(air)} \quad , \tag{3-21}$$

and in 1961 Millington and Quirk (Jury et al., 1991) developed a theoretical model for tortuosity. Their soil tortuosity model uniformly agrees with soil data over a wide range of moisture levels, and it is related to the total and gas phase porosities by

$$\xi_g = \frac{\varepsilon^{\frac{10}{3}}}{\phi^2} \quad , \tag{3-22}$$

where ϕ is total soil porosity and ε is the air filled porosity. Since tortuosity is a function of θ, it should be inside the differential. Substituting into Equation 3-19 for D_{sg} gives

$$\frac{\partial \varepsilon (C_{sg}+C_{ag}+C_{wg})}{\partial t} = -\frac{\partial q_g (C_{sg}+C_{ag}+C_{wg})}{\partial x} + D_{s(air)} \frac{\partial^2 (\frac{\varepsilon^{\frac{10}{3}}}{\phi^2} C_{sg})}{\partial x^2} + T_{sl}^g + T_{wl}^g \; . \tag{3-23}$$

At low pressure gradients and solute concentrations C_{ag} and C_{wg} may be assumed constant, so their partial differentials with respect to time and distance equal zero. Applying the simplifications for gas phase continuity yields

$$\frac{\partial \varepsilon C_{sg}}{\partial t} = -\frac{\partial q_g C_{sg}}{\partial x} + D_{s(air)} \frac{\partial^2 (\frac{\varepsilon^{\frac{10}{3}}}{\phi^2} C_{sg})}{\partial x^2} + T_{sl}^g + T_{wl}^g \; . \tag{3-24}$$

Liquid Phase

The liquid phase continuity equation is

$$\frac{\partial \theta (C_{sl}+C_{wl})}{\partial t} = -\frac{\partial}{\partial x}(q_{wl} C_{wl} + q_{sl} C_{sl})$$

$$+ D_{wl} \frac{\partial^2 C_{wl}}{\partial x^2} + D_{sl} \frac{\partial^2 C_{sl}}{\partial x^2} + T_{wg}^l + T_{sg}^l + T_{sm}^l + T_{wm}^l \; . \tag{3-25}$$

With dilute solute concentrations, the water in the liquid phase (C_{wl}) is constant during the experiment so its partial, with respect to time or distance, is zero. The solute transports with the water flow, so the solute and liquid phase flow rates are equal and

$$q_{sl} = q_{wl} = q_l \; , \tag{3-26}$$

where q_l is the liquid flow rate. The liquid phase continuity is

$$\frac{\partial \theta C_{sl}}{\partial t} = -\frac{\partial q_l C_{sl}}{\partial x} + D_{sl}\frac{\partial^2 C_{sl}}{\partial x^2} + T^l_{wg} + T^l_{sg} + T^l_{sm} + T^l_{wm}. \quad \textbf{(3-27)}$$

Solid Phase

The solid phase exhibits negligible flux, so adsorbed solute and water on the solid phase only change due to mass transfer. The solid phase mass continuity is

$$\frac{\partial}{\partial t}(\rho_b C_{sm} + \rho_b C_{wm}) = T^m_{sl} + T^m_{sg} + T^m_{wg} + T^m_{wl} \ . \quad \textbf{(3-28)}$$

The soil dry bulk density (ρ_b) is constant and the moisture levels of the isothermal experiments are at a level where the soil is always surrounded by a water film. This means that the net transfer of water adsorbing or desorbing is zero, and T^m_{wl} cancels out T^l_{wm}. Since the soil particles are surrounded by water, the gas phase cannot adsorb directly to the solid phase and T^m_{sg} and T^m_{wg} are zero. These simplifications reduce the solid phase continuity to

$$(\rho_b)\frac{\partial C_{sm}}{\partial t} = T^m_{sl} \ . \quad \textbf{(3-29)}$$

Summation of Gas, Liquid, and Solid Phase Continuity

The net mass transfer terms are equal but opposite in effect and cancel each other. Summing the gas, liquid, and solid phase continuity relationships gives

$$\frac{\partial}{\partial t}(\varepsilon C_{sg} + \theta C_{sl} + \rho_b C_{sm}) = -\frac{\partial}{\partial x}(q_g C_{sg}) - \frac{\partial}{\partial x}(q_l C_{sl}) + D_{g(air)}\frac{\partial^2 (\frac{\varepsilon^{\frac{10}{3}}}{\phi^2} C_{sg})}{\partial x^2} + D_{sl}\frac{\partial^2 C_{sl}}{\partial x^2} \ . \quad \textbf{(3-30)}$$

Since the experiments are unsaturated, the advective velocity of the liquid phase is low, making it reasonable to ignore liquid dispersion. The molecular diffusion coefficient, $D_{g(air)}$, of toluene gas in air is approximately 6600 $cm^2\ d^{-1}$, while the molecular diffusion coefficient, D_{sl}, for dissolved toluene in water is approximately 0.08 $cm^2\ d^{-1}$ (Ong et al., 1992). Therefore the liquid diffusion coefficient is smaller than the gaseous diffusion coefficient by a factor of six and its effect on transport is considered negligible.

The soil column is gas tight with air discharge at the column outlet by bubbling through a methanol trap to capture any chemical leaving. The gas discharge is located just below the surface of the methanol, therefore outlet pressure is approximately atmospheric. The experiments are isothermal with constant gas density Under these conditions the air movement within the column is due to water displacement. Assuming that water and gas are incompressible fluids, a relationship between q_g and q_l is evaluated in order to simplify Equation 3-30.

The horizontal column experiments have constant potential at the inlet, therefore total fluid flow throughout the column is constant. This relationship implies that

$$\frac{\partial}{\partial x}(q_l + q_g) = 0 \text{ or } \frac{\partial q_g}{\partial x} = -\frac{\partial q_l}{\partial x} \quad . \tag{3-31}$$

Integrating Equation 3-31 over the interval from $x = [0, x]$ yields

$$q_g(x) - q_g(0) = -(q_l(x) - q_l(0)) + ki \quad , \tag{3-32}$$

where ki is the constant of integration. Considering the boundary conditions for q_l and q_g at the inlet gives

$$ki = q_l(0) = r_i \quad , \tag{3-33}$$

where r_i is the liquid infiltration rate (LT^{-1}) at the inlet. Then gas flow is

$$q_g = r_i - q_l \quad , \tag{3-34}$$

and Equation 3-30 becomes

$$\frac{\partial}{\partial t}(\varepsilon C_{sg} + \theta C_{sl} + \rho_b C_{sm}) = -\frac{\partial (r_i - q_l) C_{sg}}{\partial x} - \frac{\partial q_l (C_{sl})}{\partial x} + D_{g(air)} \frac{\partial^2 (\frac{\varepsilon^{\frac{10}{3}}}{\phi^2} C_{sg})}{\partial x^2} . \tag{3-35}$$

.

Local Phase Equilibrium Establishment

The column experiments assess the validity of LPE establishment near a contaminated wetting front as it advects through uncontaminated soil and water. Contaminant transport models typically use LPE assumptions because equilibrium

coefficients are easily determined as compared to kinetic phase coefficients. Normally LPE assumptions give acceptable predictions of field data for steady state flow conditions, but this may not hold under transient flow conditions. The boundary conditions, LPE assumptions and transport relationships assisted in determining equilibrium or lack of the same during the column experiments.

Equilibrium Functional Relationship

Assuming local phase equilibrium allows the use of phase partitioning constants K_H and K_d in Equations 3-12 and 3-14 respectively. The governing equations for solute gas phase or solute liquid phase are

$$\frac{\partial}{\partial t}[C_{sg}(\rho_b \frac{K_d}{K_H} + \frac{\theta}{K_H} + \varepsilon)] = -\frac{\partial(r_i - q_l)C_{sg}}{\partial x} - (\frac{1}{K_H})\frac{\partial(q_l C_{sg})}{\partial x} + D_{g(air)}\frac{\partial^2(\frac{\varepsilon^{\frac{10}{3}}}{\phi^2}C_{sg})}{\partial x^2}, \qquad \textbf{(3-36)}$$

and

$$\frac{\partial}{\partial t}[C_{sl}(\rho_b K_d + \theta + \varepsilon K_H)] = -(K_H)\frac{\partial(r_i - q_l)C_{sl}}{\partial x} - \frac{\partial(q_l C_{sl})}{\partial x} + (K_H)D_{g(air)}\frac{\partial^2(\frac{\varepsilon^{\frac{10}{3}}}{\phi^2}C_{sl})}{\partial x^2}. \qquad \textbf{(3-37)}$$

The column experiments are conducted under isothermal conditions at a constant dry bulk density, so porosity and the molecular diffusion rate are constant. Assuming the presence of equilibrium infers that the linear adsorption coefficient and the Henry coefficient are also constant.

Deviation from Local Phase Equilibrium Establishment

If phase equilibrium is not present, the relationships are more complicated and additional assumptions are required to determine the transport equations.

Adsorption Functional Relationship

The experiments have a relatively large liquid surface area within the column. Thus it is reasonable to assume that phase transfers from gas to liquid and back are instantaneous and in equilibrium. This implies that the Henry coefficient is met and that any non-equilibrium is probably due to adsorption related mass transfers. At the wetting front the mobile phases, C_{sg} and C_{sl}, in Equation 3-35 are assumed to be in equilibrium. Therefore, since C_{sm} is non-mobile, it is considered the source of non-equilibrium during transport.

Equation 3-35 is evaluated for the mobile phases by dropping C_{sm} from the left side of the equation. Next a non-equilibrium phase transfer term, M_{sl}^{m}, is defined to replace the influence of C_{sm} on equilibrium conditions in Equation 3-35. The mass transfer rate term, T_{sl}^{m}, and the non-equilibrium phase transfer term, M_{sl}^{m}, are related by

$$M_{sl}^{m} = T_{sl}^{m*} - T_{sl}^{m} \quad , \tag{3-38}$$

where M_{sl}^{m} is the phase transfer non-equilibrium ($ML^{-3}T^{-1}$), T_{sl}^{m*} the phase transfer rate from liquid to solid ($ML^{-3}T^{-1}$) at equilibrium and T_{sl}^{m} the actual phase transfer rate term ($ML^{-3}T^{-1}$). During mass transfer from liquid to the adsorbed phase, the value of T_{sl}^{m} is always less than or equal to the equilibrium value, T_{sl}^{m*}. At equilibrium they are equal and M_{sl}^{m} equals zero.

The mass transfer non-equilibrium term is added to the right side of the equation to reflect the influence of C_{sm} on equilibrium conditions. With this substitution the adsorption functional relationship becomes

$$\frac{\partial}{\partial t}(\theta C_{sl} + \varepsilon C_{sg}) = -\frac{\partial (r_i - q_l) C_{sg}}{\partial x} - \frac{\partial q_f(C_{sl})}{\partial x} + D_{g(air)} \frac{\partial^2 (\frac{\varepsilon^{\frac{10}{3}}}{\phi^2} C_{sg})}{\partial x^2} + M_{sl}^{m} \quad , \tag{3-39}$$

and expressed in the solute gas phase concentration the relationship is

$$\frac{\partial}{\partial t}[C_{sg}(\frac{\theta}{K_H}+\varepsilon)] = -\frac{\partial(r_i-q_l)C_{sg}}{\partial x} - (\frac{1}{K_H})\frac{\partial q_l C_{sg}}{\partial x} + D_{g(air)}\frac{\partial^2(\frac{\varepsilon^{\frac{10}{3}}}{\phi^2}C_{sg})}{\partial x^2} + M_{sl}^m \quad . \qquad \textbf{(3-40)}$$

The solute liquid phase concentration relationship is similar. However, since only the gas phase was measured with time during the column experiments, the remainder of Chapter 3 discusses just gas phase equations.

Disequilibrium Functional Relationship

An additional way to view the non-equilibrium relationship is to consider it as a variance from the equilibrium adsorption concentration. This may be due to resistance of the solid surface to adsorption, slow adsorption due to diffusion into the solid pores or another rate limiting process. During the adsorption process, the adsorbed solute is always less than or equal to the equilibrium value as represented by

$$C_{sm} \leq C_{sm}^* \quad , \qquad \textbf{(3-41)}$$

where C^*_{sm} is the concentration of adsorbed solute at equilibrium. Next Δ (delta) is defined as a disequilibrium term with units of MM^{-1}. Delta represents the variance from the equilibrium value by C_{sm} and is defined as

$$\Delta = C_{sm}^* - C_{sm} \quad . \qquad \textbf{(3-42)}$$

When equilibrium is present, Δ is zero and C_{sm} equals C^*_{sm}. Substituting into Equation 3-35 for C_{sm} gives a disequilibrium functional relationship. This relationship is expressed in the solute gas phase concentration as

$$-\rho_b\frac{\partial\Delta}{\partial t} + \frac{\partial}{\partial t}[C_{sg}(\rho_b\frac{K_d}{K_H}+\frac{\theta}{K_H}+\varepsilon)] = -\frac{\partial(r_i-q_l)C_{sg}}{\partial x} - (\frac{1}{K_H})\frac{\partial q_l C_{sg}}{\partial x} + D_{g(air)}\frac{\partial^2(\frac{\varepsilon^{\frac{10}{3}}}{\phi^2}C_{sg})}{\partial x^2} \quad . \qquad \textbf{(3-43)}$$

Boundary Conditions

The equations in the previous sections are functions of time and distance, which makes them difficult to evaluate. In order to simplify these equations, the contaminant

concentration and moisture boundary conditions are specified and then a transformation turns them into single variable functions. The experiments used a horizontal soil column with the soil uniformly packed at a constant initial moisture content. In order to maintain the Bruce/Klutt unsaturated boundary conditions, the column was of sufficient length to be considered semi-infinite. A computer controlled syringe pump maintained unsaturated transient flow conditions with constant moisture potential and constant solute concentration at the inlet. The moisture content boundary conditions, $\theta(x,t)$, are

$$\theta(x,0) = \theta_i \quad ,$$

$$\theta(0,t) = \theta_0 \quad ,$$

and

$$\theta(\infty,t) = \theta_i \quad . \tag{3-44}$$

In the boundary conditions, x represents distance along the column, t the time since the start of injection, θ_i the initial moisture content, and θ_0 the constant inlet moisture content for time greater than zero.

Similarly the solute gas phase concentration boundary conditions, $C_{sg}(x,t)$, are

$$C_{sg}(x,0) = C_i \quad ,$$

$$C_{sg}(0,t) = C_0 \quad ,$$

and

$$C_{sg}(\infty,t) = C_i \quad , \tag{3-45}$$

where C_i is the gas phase solute concentration throughout the column at $t = 0$ and C_0 is the gas phase solute concentration at the inlet at $t > 0$. C_i is zero in these experiments and analysis.

The boundary conditions for moisture content and gas phase solute concentration are functions of both time and distance, and the Boltzman variable defined as

$$\lambda = \frac{x}{\sqrt{t}} \quad , \tag{3-46}$$

converts the boundary conditions to single value functions. The transformed moisture boundary conditions, $\theta(\lambda)$, are

$$\theta(0) = \theta_0 \quad ,$$

and

$$\theta(\infty) = \theta_i \quad . \tag{3-47}$$

The transformed gas phase solute boundary conditions, $C_{sg}(\lambda)$, are

$$C_{sg}(0) = C_0 \quad ,$$

and

$$C_{sg}(\infty) = C_i \quad . \tag{3-48}$$

Boltzman Transformation

The Boltzman transformation converts the governing equations into single value functions, and the partial derivatives become ordinary differentials under the transformed boundary conditions. Differentiating the Boltzman variable with respect to time and distance gives

$$\partial x = t^{\frac{1}{2}} \partial\lambda \quad , \tag{3-49}$$

and

$$\partial t = -(\frac{2t^{\frac{3}{2}}}{x})\partial\lambda \quad . \tag{3-50}$$

Substituting these into Equation 3-36 for the partial differential of time and distance yields

$$-(\frac{x}{2t^{1.5}})\frac{\partial}{\partial\lambda}[C_{sg}(\rho_b \frac{K_d}{K_H} + \frac{\theta}{K_H} + \varepsilon)] = (\frac{1}{t^{0.5}})[-\frac{\partial(r_i - q_l)C_{sg}}{\partial\lambda} - (\frac{1}{K_H})\frac{\partial q_l C_{sg}}{\partial\lambda}] + \frac{1}{t} D_{g(air)} \frac{\partial^2 (\frac{\varepsilon^{\frac{10}{3}}}{\phi^2} C_{sg})}{\partial\lambda^2} \quad . \tag{3-51}$$

Multiplying the equation on both sides by t, and substituting in on the left side for the Boltzman variable gives

$$-(\frac{\lambda}{2})\frac{\partial}{\partial\lambda}[C_{sg}(\rho_b \frac{K_d}{K_H} + \frac{\theta}{K_H} + \varepsilon)] = (t^{0.5})[-\frac{\partial(r_i - q_l)C_{sg}}{\partial\lambda} - (\frac{1}{K_H})\frac{\partial q_l C_{sg}}{\partial\lambda}] + D_{g(air)} \frac{\partial^2 (\frac{\varepsilon^{\frac{10}{3}}}{\phi^2} C_{sg})}{\partial\lambda^2} \quad . \tag{3-52}$$

The square root of time still remains in Equation 3-52 and this requires replacement. Time is removed by considering the boundary conditions of the experiment. The experimental boundary conditions include constant initial soil moisture content and constant final moisture content. In horizontal infiltration these experimental conditions are described by the Philip infiltration rate model (Jury et al., 1991). The infiltration rate (r_i) is

$$r_i = \tfrac{1}{2} S t^{-0.5} \quad , \tag{3-53}$$

where S represents the soil sorptivity in units of $LT^{-0.5}$. The soil sorptivity is

$$S = \int_{\theta_i}^{\theta_0} \lambda d\theta = I t^{-.05} \quad , \tag{3-54}$$

where I equals the cumulative infiltration (L) into the horizontal column. Sorptivity is a function of an individual soil and its dry bulk density, and sorptivity is constant under isothermal conditions at constant density. Moisture potential at the inlet is constant in the experiments, which means that the infiltration rate (r_i) must equal q_l. Substituting in for q_l and t in Equation 3-52 yields the ordinary differential equation with respect to the Boltzman variable given by

$$-(\tfrac{\lambda}{2})\tfrac{d}{d\lambda}\left[C_{sg}(\rho_b \tfrac{K_d}{K_H} + \tfrac{\theta}{K_H} + \varepsilon)\right] = -(\tfrac{S}{2})(\tfrac{1}{K_H})\tfrac{d}{d\lambda} C_{sg} + D_{g(air)} \frac{d^2(\frac{\varepsilon^{\frac{10}{3}}}{\phi^2} C_{sg})}{d\lambda^2} \quad . \tag{3-55}$$

The development of the adsorption functional relationship and disequilibrium functional relationship mirror that of the equilibrium functional relationship in Equation 3-55, with the exception of the non-equilibrium phase transfer term, M_{sl}^m. The adsorption functional relationship is

$$-(\tfrac{\lambda}{2})\tfrac{d}{d\lambda}\left[C_{sg}(\tfrac{\theta}{K_H} + \varepsilon)\right] = -(\tfrac{S}{2})(\tfrac{1}{K_H})\frac{dC_{sg}}{d\lambda} + D_{g(air)} \frac{d^2(\frac{\varepsilon^{\frac{10}{3}}}{\phi^2} C_{sg})}{d\lambda^2} + t M_{sl}^m \quad , \tag{3-56}$$

where the phase transfer term is multiplied by time. Rearranging Equation 3-56 gives

$$-(\tfrac{\lambda}{2})\tfrac{d}{d\lambda}[C_{sg}(\tfrac{\theta}{K_H}+\varepsilon)]+(\tfrac{S}{2})(\tfrac{1}{K_H})\tfrac{dC_{sg}}{d\lambda}-D_{g(air)}\frac{d^2(\frac{\varepsilon^{\frac{10}{3}}}{\phi^2}C_{sg})}{d\lambda^2}=tM_{sl}^m\ , \qquad \textbf{(3-57)}$$

where all the values on the left-hand side are known and only the phase transfer term on the right-hand side is unknown. The left-hand side is only a function of θ which implies that the right-hand is also only a function of θ. Then the non-equilibrium phase transfer term on the right-hand side is equated to a normalized net phase transfer term given as

$$\frac{P_{sl}^m(\theta)}{t}=M_{sl}^m \quad \text{or} \quad P=tM_{sl}^m\ , \qquad \textbf{(3-58)}$$

where P has units of ML^{-3}. Then the transformed adsorption functional relationship is

$$P=-(\tfrac{\lambda}{2})\tfrac{d}{d\lambda}[C_{sg}(\tfrac{\theta}{K_H}+\varepsilon)]+(\tfrac{S}{2})(\tfrac{1}{K_H})\tfrac{dC_{sg}}{d\lambda}-D_{g(air)}\frac{d^2(\frac{\varepsilon^{\frac{10}{3}}}{\phi^2}C_{sg})}{d\lambda^2}\ , \qquad \textbf{(3-59)}$$

and the transformed disequilibrium functional relationship is

$$\rho_b(\tfrac{\lambda}{2})\tfrac{d}{d\lambda}\Delta=(\tfrac{\lambda}{2})\tfrac{d}{d\lambda}[C_{sg}(\rho_b\tfrac{K_d}{K_H}+\tfrac{\theta}{K_H}+\varepsilon)]-(\tfrac{S}{2})(\tfrac{1}{K_H})\tfrac{dC_{sg}}{d\lambda}+D_{g(air)}\frac{d^2(\frac{\varepsilon^{\frac{10}{3}}}{\phi^2}C_{sg})}{d\lambda^2}\ . \qquad \textbf{(3-60)}$$

Data Evaluation

The gas phase analyses of the column experiments are evaluated using the Boltzman space equations. The relevant equations for the solute gas phase are:

1. Equilibrium functional relationship - equilibrium among phases

$$-(\tfrac{\lambda}{2})\tfrac{d}{d\lambda}[C_{sg}(\rho_b\tfrac{K_d}{K_H}+\tfrac{\theta}{K_H}+\varepsilon)]+(\tfrac{S}{2})(\tfrac{1}{K_H})\tfrac{dC_{sg}}{d\lambda}-D_{g(air)}\frac{d^2(\frac{\varepsilon^{\frac{10}{3}}}{\phi^2}C_{sg})}{d\lambda^2}=0\ ; \qquad \textbf{(3-61)}$$

2. Adsorption functional relationship - liquid to solid net phase transfer non-equilibrium

$$P=-(\tfrac{\lambda}{2})\tfrac{d}{d\lambda}[C_{sg}(\tfrac{\theta}{K_H}+\varepsilon)]+(\tfrac{S}{2})(\tfrac{1}{K_H})\tfrac{dC_{sg}}{d\lambda}-D_{g(air)}\frac{d^2(\frac{\varepsilon^{\frac{10}{3}}}{\phi^2}C_{sg})}{d\lambda^2}\ ; \qquad \textbf{(3-62)}$$

3. Disequilibrium functional relationship - variance of solid phase adsorption from equilibrium

$$\rho_b(\tfrac{\lambda}{2})\tfrac{d}{d\lambda}\Delta=(\tfrac{\lambda}{2})\tfrac{d}{d\lambda}[C_{sg}(\rho_b\tfrac{K_d}{K_H}+\tfrac{\theta}{K_H}+\varepsilon)]-(\tfrac{S}{2})(\tfrac{1}{K_H})\tfrac{dC_{sg}}{d\lambda}+D_{g(air)}\frac{d^2(\frac{\varepsilon^{\frac{10}{3}}}{\phi^2}C_{sg})}{d\lambda^2}\ . \qquad \textbf{(3-63)}$$

Next adding the disequilibrium functional relationship and the adsorption functional relationship gives the following relationship between Δ and P, where

$$P + \rho_b(\frac{\lambda}{2})\frac{d}{d\lambda}\Delta = (\frac{\lambda}{2})\frac{d}{d\lambda}[C_{sg}(\rho_b\frac{K_d}{K_H})] \quad , \qquad \textbf{(3-64)}$$

and rearranging Equation 3-64 yields

$$\frac{d}{d\lambda}(\Delta) = (\frac{K_d}{K_H})\frac{d}{d\lambda}[C_{sg}] - (\frac{2}{\lambda\rho_b})P \quad . \qquad \textbf{(3-65)}$$

Determination of Δ and P

The values of ρ_b, K_d, K_H, ϕ, S, and $D_{g(air)}$ are constants which are either experimentally measured or calculated based on the soil type and experimental conditions. Values of C_{sg}, θ, ε, Δ, and P are variable and functions of λ. In this analysis θ versus λ is determined from the measured water content profile for an experiment and ε is determined by subtracting θ from ϕ. Values of C_{sg} were measured periodically during the experiment and an equation was fitted to the C_{sg} versus λ data using linear regression.

The fitted equation for C_{sg} is used to determine Δ and P. The values of P are determined directly from Equation 3-62 using the fitted values for C_{sg} and its differentials. Values for Δ are calculated using either a central difference numeric method or by integrating Equation 3-65 to determine an analytic solution. The central difference numeric method uses the boundary condition where $\Delta(\lambda=0) = 0$ in order to calculate values for delta. The analytic solution of Equation 3-65 is

$$\Delta(\lambda) = [\frac{K_d}{K_H} + \frac{1}{\rho_b}(\frac{\theta}{K_H} + \phi - \theta)](C_{sg} - C_0) + [const][\log(\lambda) - \frac{b}{\lambda}](C_{sg}) + ki \, , \qquad \textbf{(3-66)}$$

where the fitted values for the experimentally measured gas phase data have the form

$$C_{sg} = a(10^{b\lambda}) \quad , \qquad \textbf{(3-67)}$$

and a and b are constants determined by linear regression. The constant term ([*const*]) in Equation 3-66 is

$$[const] = [\frac{b}{\rho_b(1-b^2)}][(2b)D_{g(air)}(\frac{(\phi-\theta)^{3.33}}{\phi^2}) - \frac{S}{K_H}] \quad . \qquad \textbf{(3-68)}$$

The value *ki* in Equation 3-66 is the constant of integration, and it is determined using the boundary condition $\Delta(\lambda = \infty) = 0$. In this study delta is determined for lambda values close to zero (0.0001) to λ =0.2 which is the approximate extent of movement for measurable toluene gas phase during the experiments. The integration procedure for Δ is covered in more detail in Appendix A.

CHAPTER 4

METHODS AND PROCEDURES

Introduction

Prior to conducting the column tests, preliminary work was necessary to quantify soil and solution properties affecting toluene partitioning between phases. Laboratory analyses of the Teller loam soil determined its properties. Twenty-four hour isothermal batch tests determined toluene's Henry coefficient and linear adsorption coefficient for partitioning between liquid to gas phase and liquid to adsorbed phase respectively. The partitioning coefficients were used with the measured gas concentration to calculate whether local phase equilibrium (LPE) was established during a column test. The ability to sample and analyze toluene gas phase within the soil column during transport was critical to evaluating equilibrium status.

Throughout the study careful sample handling and test preparations were required to prevent toluene loss prior to analysis. During testing of the methods and procedures several possible toluene loss mechanisms were identified, and techniques were developed to prevent sample loss. Procedures to collect gas phase samples during a column test had to meet the following criteria: periodically sample the soil air inside the column, be sensitive enough to analyze low toluene gas concentrations in the air and collect small air sample volumes. Collecting small air samples was important to prevent significant

shifting of phase equilibrium conditions within the column by removing too much soil air. Upon test conclusion, the column was destructively sampled to analyze for soil moisture content and total toluene content throughout. Sampling procedures that minimized exposure time to the atmosphere were developed to prevent toluene and moisture loss during destructive sampling. Mass balances of both moisture and toluene were critical to experimental validity, and necessary when comparing different time duration column tests.

Soil Collection and Handling

The ground water laboratory in the Biosystems and Agricultural Engineering Department uses Oklahoma soils in many of its studies. Teller loam (Udic Argiustolls) is used because its properties are similar to other good agricultural cropland soils in Oklahoma. The Teller soil is moderately permeable with a sandy loam texture and has an organic carbon content of 0.7% to 0.9% by weight. More importantly, the previous agricultural practices at the soil collection site are known, and the collected soil was not exposed to organic chemicals or pesticides which could interfere with experiments involving other organic chemicals.

Most studies on transport of volatile compounds use soils low in organic carbon content, such as a clean sand, to eliminate the effect of adsorption on contaminant movement. While a low organic carbon content is representative of many sandy aquifers, it is not necessarily true for soils in the upper portion of the unsaturated zone. Organic carbon content tends to be highest near the surface and decreases rapidly with soil depth.

This research desired to study multiphase transport including adsorption, in the unsaturated zone so the Teller loam soil with its higher organic carbon content was the best choice of the soils available for use in the ground water laboratory.

The Teller loam soil was collected adjacent to a garden plot at Oklahoma State University's Perkins Research Station. The garden plot is located in the NW ¼, of Section 36, R.2E., T.18N., in Payne County, Oklahoma. The use history of the collection site is known, and according to the Perkins Research Station staff chemicals or pesticides have not been applied on the site. The soil surface was first cleared of vegetation and undecomposed debris. Approximately 25 cm (shovel blade depth) of soil was collected including the A1 and some of the A2 soil horizons. Roots and other foreign materials were removed after collection. After air drying the soil was broken up using a hammer mill grinder in OSU's Agronomic Services Laboratory to less than 2 mm particle size. During grinding, care was taken to assure that the soil was homogeneous and well mixed. After grinding, the soil was stored in covered steel barrels at its air dry moisture content of approximately 2% to 4% by weight.

Soil Property Analysis

Physical and chemical properties of Teller loam soil which affect toluene transport were determined prior to conducting the column experiments. Soil pH was analyzed in both a 1:1 and 2:1 mixture of soil:distilled water according to procedures outlined by McLean (1982). The results are reported as pH_W or soil pH in water with the mixture ratio listed. Soil particle size analysis was determined by the hydrometer method outlined

in ASTM Method D 422-63. A pycnometer was used to determine soil particle density according to procedures outlined in ASTM Method D 854-58. The cation exchange capacity (CEC) of Teller loam was determined using the ammonium acetate method described by G.W. Thomas (1982).

Specific surface area of the Teller loam was determined by exposing the soil to different relative humidity levels using various salt solutions. Then the Brunauer, Emmett, and Teller (BET) equation for water vapor adsorption as described by Brunauer et al. (1938) was used to calculate the soil's specific surface area. Capillary moisture relationships for Teller loam's drying cycle were determined according to procedures outlined in ASTM Method D 2325-68. The capillary moisture relationship was determined using porous plates and pressure containers for soil bulk densities corresponding to 1.4, 1.5, and 1.6 g cm^{-3}. The soil water diffusivity and sorptivity of the Teller loam soil were previously determined by Brown and Allred (1992) in their syringe pump performance in unsaturated horizontal column experiments. This research study utilized Brown's and Allred's diffusivity and sorptivity results for unsaturated Teller loam soil.

Soil Water Solution Preparation

Laboratory experiments involving contaminant transport require either ground water collected from the study site or a test fluid which simulates natural ground water chemistry. Using deionized or distilled water to simulate a natural ground water is not recommended since these waters can cause changes in soil structure which affect the soil

permeability (Klute and Dirksen, 1986). If the experiments concern a specific site, it is best to collect uncontaminated ground water from the site area and utilize it as the test fluid. Because many experiments do not involve a specific site, an artificial ground water prepared in the laboratory under controlled conditions is considered best.

One artificial ground water fluid commonly used by the soil science profession is the 0.01 N (0.005 M) $CaSO_4$ solution recommended by Klute and Dirksen (1986). Some test fluids use a sodium sulfate solution instead of calcium sulfate. Sodium may cause dispersion of clays in a fine textured soil, which could affect permeability by clogging the soil pores. Since the calcium sulfate solution has performed well in other flow experiments in the lab, it was chosen for this research. The 0.01 N calcium sulfate solution is prepared by diluting one part saturated calcium sulfate solution with two parts deionized water. Both saturated and 0.01 N calcium sulfate solutions are stock solutions kept at room temperature in capped bottles in the ground water laboratory.

Toluene Stock Solution Preparation

Saturated toluene solution is prepared by adding reagent grade toluene to 0.01 N calcium sulfate solution until a layer of toluene floats on top of the water. The saturated toluene solution is stored at room temperature (23 ± 2 °C) under an exhaust hood in a two liter clear glass aspirator-type bottle. The bottle has a teflon covered stopper and bottom spigot with a teflon stopcock. A foil bag covers the bottle to limit light entry and prevent photolysis of the toluene. A magnetic stirrer slowly rotates the solution to keep the saturated toluene solution in equilibrium with the floating toluene. This process yields a

solution with a relatively constant toluene concentration of around 525 mg L^{-1}. Saturated solution is withdrawn as needed through the bottom spigot to make dilutions for standards, injection solution, or soil wetting solution. Dilute solutions of toluene were not kept as stock because the concentration will vary whenever the liquid or gas volume changes. This is due to partitioning and re-establishment of equilibrium between the liquid and gas phases.

Toluene Biodegradation

Another concern when studying organic contaminants in the soil and ground water is biodegradation of the organic by soil microorganisms. Biodegradation of the toluene is a fate which must be quantified or eliminated, and screening tests conducted at the beginning of the study determined toluene's degradability by the indigenous soil microorganisms. The biodegradability tests were conducted using the equilibrium partitioning in closed systems (EPICS) method described by Garbarini and Lion (1985).

The screening tests added 20 mL of 0.01 N calcium sulfate solution spiked with toluene to 40 mL EPA vials each with equal masses of air dried Teller loam soil. This gave each vial the same toluene mass, soil mass, liquid volume, and gas volume. After the vials were capped with a silicon rubber and PTFE teflon dual-faced septum, they incubated at room temperature (23 ± 2 °C) with occasional shaking to mix the contents. Triplicate vials of the toluene and Teller soil were analyzed periodically over time for gas phase toluene concentration. Since each vial was prepared similarly, a decrease in toluene gas phase concentration was attributed to biodegradation. The screening tests

indicated that under batch test conditions where the toluene solution was added to the air-dried soil, the microorganisms did not significantly degrade the toluene during the first 36 hours. Therefore, a bacterial inhibitor was considered unnecessary for 24-hour batch tests or column tests lasting 24 hours or less.

This observation proved false for the column tests. The toluene mass recovery in the first few column tests was low. Initially it appeared that leaks and incomplete extraction of total toluene were the cause of the low recovery values. However, after the leaks were sealed and the extraction method improved, recovery was still below 50%. The possibility of biodegradation during the column tests was then re-investigated.

The packed soil columns were handled differently than the degradation screening tests because the column tests required a starting soil moisture level. Soil used in the column tests was wetted with 0.01 N calcium sulfate solution (without toluene present) and held overnight. The column was then packed with the wetted soil and allowed to sit overnight for moisture equilibration prior to starting the column test. This meant that the Teller loam was wetted for 36-48 hours prior to injecting the toluene solution. The original screening test had not investigated this situation.

Another biodegradation batch screening test was conducted where the Teller loam soil was wetted 36 hours prior to adding toluene. Head space analysis was conducted on the samples and the results indicated that soil which was wetted for 36 hours prior to chemical introduction exhibited significant toluene degradation in just a few hours. A microbial inhibitor was needed for the column tests. Klute and Dirksen (1986) suggested three different inhibitors that could be added to the artificial ground water including:

phenol (0.1%), mercuric chloride (20-500 mg L^{-1}), or thymol (0.16-0.27 g L^{-1}). Brusseau (1992a) added 0.02% sodium azide to the 0.01 N calcium sulfate solution in his experiments, and this successfully inhibited microbial activity.

The phenol and thymol additions might cause interference with toluene GC analysis, so their use was rejected. Mercuric chloride addition was rejected because it created a soil which might be considered a hazardous material. The biodegradation problem was solved by first drying the soil at 105 °C prior to wetting. Then sodium azide was added to the 0.01 N calcium sulfate wetting and injection solutions to control biodegradation during a column test. The percentage of sodium azide was reduced to 0.01% from the 0.02% solution used by Brusseau (1992a) to prevent possible sodium dispersive effects on the Teller loam soil texture. The heat drying and 0.01% sodium azide solution combination inhibited bacterial activity and mass recovery of toluene in the final four column tests ranged from 71% to 94%.

Analytic Methods for Toluene

In this research, toluene was measured in the gas phase, liquid phase (to verify standard solution concentrations), and the total concentration (including gas, liquid, and adsorbed). The gas phase analytic techniques had to be sensitive since small gas sample volumes were collected to prevent the act of sampling from shifting equilibrium conditions. Rapid gas phase analysis was desirable in order to have results available while the column test was ongoing. The analytic method also needed to be insensitive to interference from naturally occurring soil organic compounds. Toluene is subject to rapid

volatilization losses when exposed to the atmosphere, so a procedure minimizing open exposure to the atmosphere was necessary.

A Hewlett Packard 5890 Series II gas chromatograph (GC) and a Hitachi U-1100 spectrophotometer were utilized for toluene analysis during the research. The GC is equipped with a flame ionization detector (FID), direct injector, megabore (0.530 mm) capillary column, and a microcomputer with HP Chemstation™ software to interface with the GC. The spectrophotometer operates in either UV or visible light wave lengths using a four cell sample vial holder or an automatic sample sipper.

Swisher (1970) describes a technique for analyzing surfactants for the presence of a benzene ring using UV wavelengths and a spectrophotometer. Benzene rings exhibit UV spectral peaks at 190 nM, 223 nM, and 260 nM, and the transmission of light at these wavelengths is related to the concentration of the benzene ring structure. Toluene is methyl benzene, and the use of spectrophotometric analysis was evaluated for this research. The laboratory spectrophotometer was not equipped to analyze wavelengths below 200 nM, so trials were run at 223 and 260 nM wavelengths for toluene dissolved in 0.01 N calcium sulfate, methylene chloride, and methanol. Calibration standards for the toluene in calcium sulfate solution were made by dissolving linear alkylbenzene sulfonate (LAS) surfactant in the calcium sulfate solution. The standards for toluene in the organic solvents methylene chloride and methanol were made by diluting a stock solution of toluene in methylene chloride or methanol.

The UV analysis was sensitive for toluene to about ± 1 mg L^{-1} at 260 nM and slightly better at 223 nM. This applied only to clean samples. The samples exposed to

soil gave erratic results due to interference from soil organics which discolored the water, methanol or methylene chloride. The spectrophotometric procedure was used on toluene dissolved in water or solvent to verify the saturated toluene solution and injection solution concentrations. GC analysis exhibited few interferences and was more sensitive than spectrophotometric analysis of toluene.

The EPA has published methods for analyzing multiple volatile organics, including toluene, using purge-and-trap methods. The EPA method would have required purchasing purge-and-trap equipment, additional capillary columns, and long run times on the GC, all of which were unnecessary to get the desired results. This study utilized only toluene and interfering compounds were absent. Knowledge of gas chromatography theory and toluene's chemical properties helped in determining the combination of inlet conditions, column selection, temperature program, and detector used in this research.

The GC analysis of air samples is straight forward and can be completed within minutes using isothermal oven conditions. In addition to toluene in air samples, toluene dissolved in an organic solvent after extraction from the Teller loam soil was measured by the GC. Analysis of an analyte dissolved in a liquid solvent is more involved than a gas sample because of the presence of the solvent. The injected liquid must be flash vaporized, and an oven temperature program developed to separate the toluene, solvent and other compound peaks. The GC analytic programs listed in Table 4-1 were developed through experimentation and modification of published procedures. The toluene in air analysis modified a program used by Lion et al. (1990) for toluene

headspace analysis. Methods suggested in Hewlett Packard's analytic column and supplies catalog reference section for toluene in a solvent were modified for this study.

TABLE 4-1

Gas Chromatographic Conditions

	ANALYSIS PROGRAM FOR TOLUENE IN AIR
Column:	J & W Scientific DB™-1
	Dimethylpolysiloxane
	(30 M x 0.53 mm x 1.5 μM)
Carrier:	Helium at 5 mL min^{-1}
Make-up:	Nitrogen at 20 mL min^{-1}
Oven:	150 °C (5.0 min) for batch tests
	150 °C (360 - 610 min) for column tests
Injection:	Direct 10 μL of air, 150 °C
Detector:	FID, 225 °C
	ANALYSIS PROGRAM FOR TOLUENE IN SOLVENT
Column:	J & W Scientific DB™-1
	Dimethylpolysiloxane
	(30 M x 0.53 mm x 1.5 μM)
Carrier:	Helium at 5 mL min^{-1}
Make-up:	Nitrogen at 20 mL min^{-1}
Oven:	40 °C - 80 °C (4 °C min^{-1})
	80 °C - 135 °C (10 °C min^{-1})
	135 °C (0.5 min)
Injection:	Direct 0.75 μL of liquid, 150 °C
Detector:	FID, 225 °C

Analysis of Toluene in Air

The GC procedure listed in Table 4-1 for toluene in air was used for batch equilibrium samples and air samples from the column. Batch equilibrium samples were analyzed by sequentially collecting and injecting three individual gas samples into the GC from the same vial during a single five minute GC run. The results of the three peaks were compared and averaged when in agreement. Figure 4-1 shows a chromatogram for

toluene in a standard sample where three samples of the headspace air were analyzed sequentially from the same vial. The procedure was modified when analyzing samples of air taken from the soil column during the transient flow experiments by extending the GC isothermal run time to longer periods lasting from 360 minutes to 610 minutes. During a column test, a single gas sample was taken periodically from a sample site along the column and immediately injected to the GC for analysis. The time of sampling, sample location, and GC run time at injection were recorded to allow correlation of the GC chromatogram results with each individual sample injection. Figure 4-2 shows a 360 minute chromatogram from column test number 10. Figure 4-3 shows an enlarged portion of the chromatogram in Figure 4-2. The analysis was sensitive to a toluene gas concentration of 10 to 20 $\mu g\ L^{-1}$ with few interference problems.

A Hamilton 25 mL gas tight syringe (Model 1702RN) with 22s gauge removable needles was used to collect and inject gas samples into the GC. After each use the syringe was cleaned immediately by flushing with methanol three to four times. Then the syringe was dried by insertion into a Hamilton syringe cleaner which had needle heating to 250 °C and vacuum extraction of the vapors. Methanol was chosen as the preferable cleaning solvent because its gas chromatographic peak occurs about one-half minute prior to toluene's peak. The retention times were consistent with enough separation so that there was no interference with the toluene peak if trace amounts of methanol were present after syringe cleaning. The cleaning procedure required at least five minutes of drying time in the heated syringe cleaner to adequately evaporate the methanol cleaning solvent.

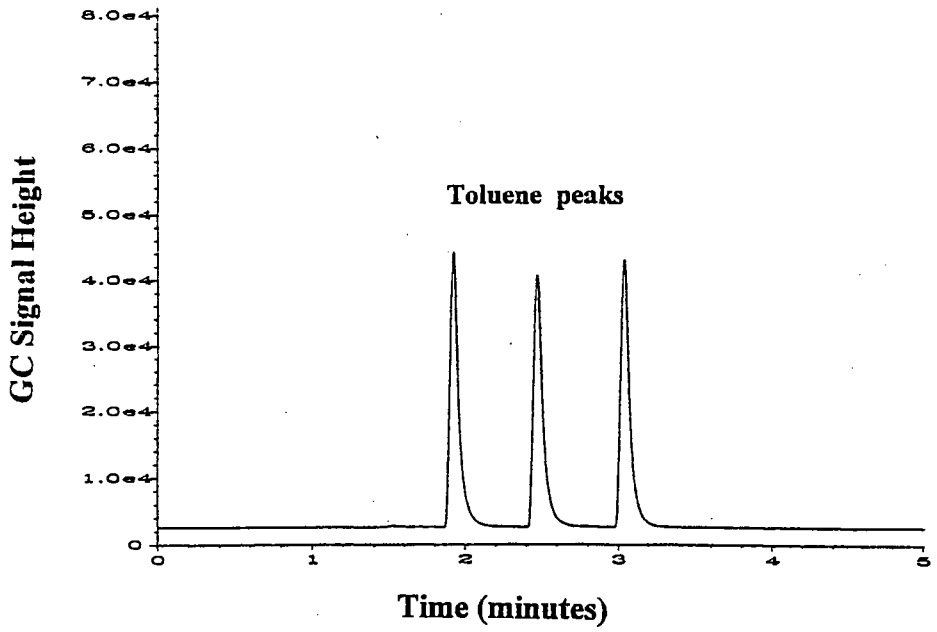

Figure 4-1. Chromatogram of toluene gas phase in air (from calibration standard used in column test no. 11).

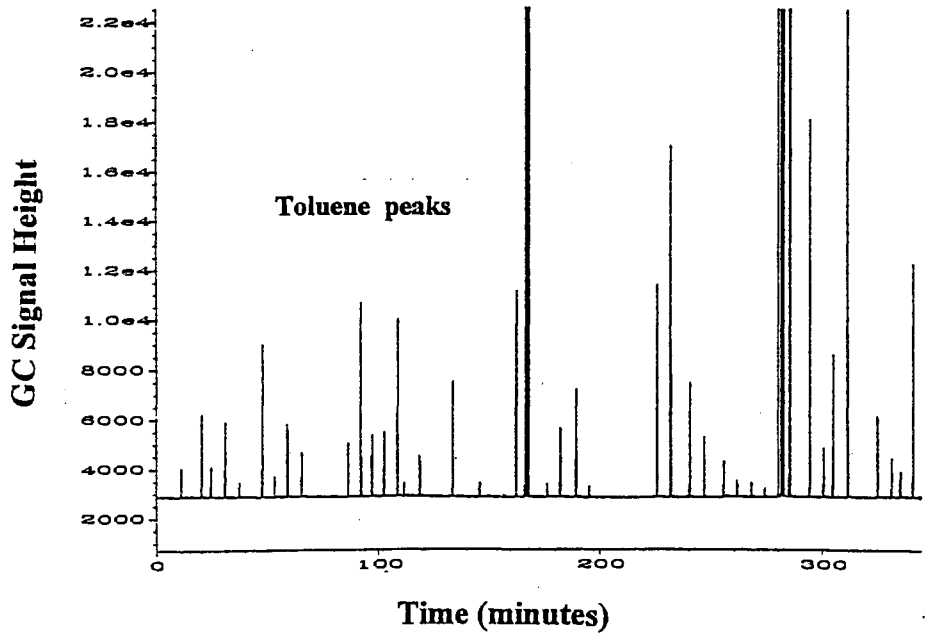

Figure 4-2. Chromatogram of toluene gas phase in soil air (from column test no 11).

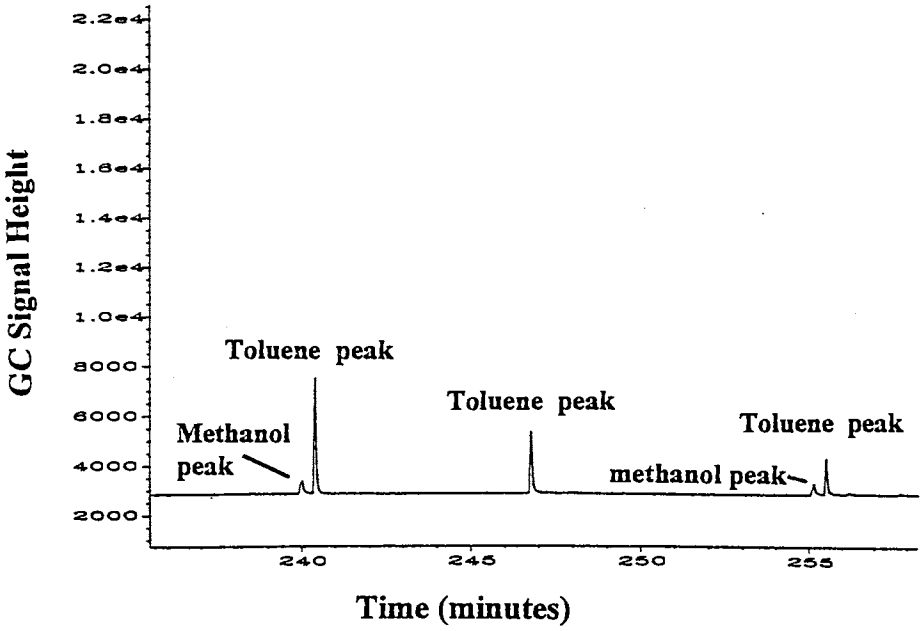

Figure 4-3. Enlargement of the time scale for a portion of the chromatogram shown in Figure 4-2.

Analysis of Toluene in an Organic Solvent

The GC procedure for toluene in solvent listed in Table 4-1 was used throughout the study. Three different capillary columns were tested before choosing a non-polar 30 meter column with a 1.5 μM thick coating of dimethylpolysiloxane. This column is well suited for analysis of other non-polar compounds besides toluene. Polar solvents such as methanol and water are incompatible with the column, so they were not tested for use as extracting fluids for the toluene. Even trace amounts of water injected into the capillary column created a very noisy chromatographic baseline, so care was taken throughout the study to prevent water injection into the column.

Hexane and methylene chloride were tested as extractants for toluene adsorbed on the soil and toluene dissolved in aqueous solution. Both solvents worked well as extractants for toluene in aqueous solution and were comparable as extractants for

adsorbed toluene. Hexane was chosen as the extractant of choice because it was more convenient to sample since it floats on water. The chromatographic separation for toluene in hexane was slightly better than toluene in methylene chloride. The GC temperature program was developed to give good separation between the large hexane solvent peak and the toluene analyte peak, and to complete the analysis quickly. The flow rates, temperature ramps and injection volumes were tested until the desired result was obtained. Samples were collected from the solvent with a Hamilton CR-700 constant rate syringe with a pipette needle point. The syringe's micrometer setting device allowed accurate deliveries of less than one μL samples. After each sample the syringe was flushed several times with whichever solvent the toluene was dissolved. The cleaning solvent was evaporated from the needle and barrel using the heated syringe cleaner used for the gas sample syringes. Figure 4-4 shows a typical chromatogram for toluene dissolved in hexane.

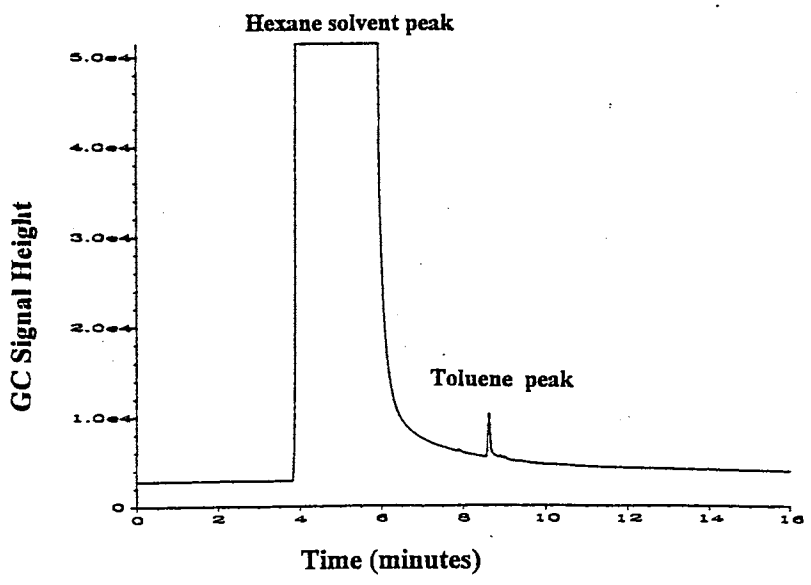

Figure 4-4. Chromatogram of extracted toluene in hexane solvent (from column test no. 9).

Extraction of Toluene from the Teller Loam Soil

Procedures to extract toluene from the Teller soil were developed in conjunction with the GC program for analysis of toluene in solvent. The extraction method for toluene required high recovery, limited volatile losses and ease of use. Extraction in a single step was desired since multiple extraction might dissolve unwanted constituents which would require extensive cleanup before analysis. Several extraction techniques were reviewed for their compatibility with the objectives.

Two methods suggested by Eagle et al. (1991) are shaking the soil sample with either a cold extractant or a heated solvent. One problem with a heated solvent procedure such as Soxhlet extraction is dissolution of additional constituents which might interfere with toluene analysis. Robinson et al. (1990) extracted absorbed toluene for soil biodegradation studies using vortex mixing, extraction of toluene using water and finally extraction with methylene chloride. Robinson et al. (1990) samples used zero headspace above the soil and water to eliminate the gas phase. Their procedure required separate GC analysis of the toluene in both water and methylene chloride. First the toluene concentration was measured in the water and then the sample was centrifuged and the water decanted. Methylene chloride was added to extract adsorbed toluene from the soil particles. Robinson et al. (1990) achieved 83 ± 4.0% toluene recovery with their procedure.

Miller and Staes (1992) utilized hexane and orbital shaking to extract toluene during sorption equilibrium and rate experiments on aquifer material. Recovery efficiency was not reported for their tests. Miller et al. (1992) tumbled a sandy aquifer

material with the cosolvents, acetone and hexane, to recover four non-ionic organic solutes, including toluene. Triple extraction of the aquifer material was used by Miller et al. (1992), but recovery efficiency was not reported.

Extraction in a single step using a small amount of cold solvent was desired for this study, and three methods to extract toluene from the Teller loam soil were evaluated: 1) shaking the soil and extractant together, 2) shaking the soil and extractant with a sodium hexametaphosphate dispersant, and 3) tumbling the soil and extractant with the dispersant. Spiked soil for the method evaluation was prepared by adding 62 mL of 0.01 N $CaSO_4$ solution containing 64 mg L^{-1} toluene to 464 g of Teller loam soil in a capped bottle packed to zero headspace. The toluene solution addition yielded a soil moisture content of between 20-30% on a volume basis to simulate the anticipated moisture content of the unsaturated samples collected during a column test. The capped bottle was equilibrated in a water bath (25 °C ± 0.5 °C) overnight prior to sample removal.

Samples were collected from the bottle using the procedures planned for the column experiments. A brass tube was pushed into the packed soil to collect small core samples (2-4 grams) from the spiked soil. Immediately after soil collection a glass rod pushed the core sample into a 15 mL glass centrifuge tube containing the extracting solvent with or without dispersant. The centrifuge tube was capped immediately with a dual faced silicon rubber and PTFE septum to seal the tube. A hole in the cap allowed the constant rate syringe to puncture the septum and remove a sample of the extractant without opening the tube. The rapid sample collection, sealed centrifuge tube and sampling through a septum minimized volatile losses to the atmosphere. Septum

replacement on the centrifuge tubes occurred immediately after sampling to prevent loss of solvent and analyte through the puncture hole. The samples were then stored at 4 °C in case additional analyses were required.

Method 1 involved toluene extraction from the soil using continuous shaking in a water bath with either 4 mL of methylene chloride or hexane without dispersant. The samples were shaken in a constant temperature water bath overnight with removal three times for vigorous shaking to thoroughly mix the soil and extractant. To improve solvent and soil particle contact, 0.065 M sodium hexametaphosphate solution dispersing agent (ASTM D422-63) was added to the centrifuge tubes for Methods 2 and 3. Extraction from the spiked soil sample used 10 mL of dispersant and 2-3 mL of solvent for Methods 2 and 3. Addition of the dispersant and the extractant to the tubes occurred before introducing the soil. In Method 2 the samples were shaken overnight in a water bath and removed for shaking three times similar to Method 1. The hexane floated on top of the dispersant while the methylene chloride formed a layer between the settled solids and water in the centrifuge tubes. The floating hexane layer sampled easily after centrifuging, but the methylene chloride samples required inverting to prevent the syringe needle from passing through the water layer to sample the extractant.

In Methods 1 and 2 the soil particles tended to settle out during shaking with only finer particles remaining in suspension. A rotating tumbler was made for Method 3 to keep the solids, dispersant, and extractant in continuous contact. The tumbler used a variable speed DC motor turning a 38 cm diameter plate at 12 rpm. The samples were

clipped to the plate and rotated overnight. After tumbling the samples were centrifuged and analyzed by the same analytic procedure as the samples from Methods 1 and 2.

In Method 1 the Teller loam soil agglomerated into small soil balls surrounded by a layer of methylene chloride. Much of the Teller loam soil adhered to the sidewalls and bottom of the tube in the hexane extracted samples. Recovery results were low for both hexane and methylene chloride indicating poor soil contact with the extractant. Samples with the sodium hexametaphosphate solution dispersed well in Methods 1 and 2. Shaken samples in Method 2 had heavier soil particles settling out with only soil fines still in suspension in the dispersant. In Method 3 the tumbler continuously mixed the soil, extractant and dispersant which allowed more thorough contact and gave better mass transfer of toluene to the extractant. Table 4-2 lists the results for methylene chloride and hexane for all methods.

Method 1 had a mean toluene recovery for shaken samples of 64% for methylene chloride and 84% for hexane. Method 2 had a mean toluene recovery for samples shaken with dispersant of 84% for methylene chloride and 75% for hexane. Method 3 had a mean toluene recovery for samples tumbled with dispersant of 94% for methylene chloride and 94% for hexane. Method 3 gave the best results with recoveries for a single extraction greater than 90% for both hexane and methylene chloride. Hexane had a coefficient of variation of 9% and methylene chloride had a coefficient of variation of 11%. The recovery ranges were 83-106% for hexane and 81-104% for methylene chloride. The results for hexane and methylene chloride tumbled with dispersant were equivalent and either extractant is suitable for toluene extraction. Hexane was considered

the extractant of choice because it had clearer GC separation for toluene. Since it floats on the dispersant it is easier to sample.

TABLE 4-2

Toluene Recovery in Teller Loam Soil Using Single Extraction with Either Hexane or Methylene Chloride by Shaking or Tumbling with and without Sodium Hexametaphosphate Dispersant

Parameter	Extractant: Hexane	Extractant: Methylene chloride
All Methods		
Soil sample size		
Range	1.22-2.92 g	1.57-4.06 g
Extractant volume		
Range	1.84-4.08 mL	1.88-4.53 mL
Method 1 - Shaken without dispersant		
Toluene recovery		
n†	3	3
Mean	84%	64%
C_v‡	4%	5%
Range	81-87%	61-68%
Method 2 - Shaken with dispersant		
Toluene recovery		
n	4	3
Mean	75%	84%
C_v	6%	4%
Range	71-82%	80-87%
Method 3 - Tumbled with dispersant		
Toluene recovery		
n	10	10
Mean	94%	94%
C_v	11%	9%
Range	83-106%	81-104%

† Number of samples
‡ Coefficient of variation

Gas and Liquid Sampling Syringe Problems

During the development of the GC analytic procedures, problems with the gas and liquid injection syringes were observed and remedies to the problems developed. The initial column tests used a sampling apparatus to take several soil air samples from the column at the same time. After sampling, the syringe needles were pushed into rubber stoppers to seal the end. The samples were then analyzed sequentially within the next hour. The toluene gas analysis results were erratic, and tests of the syringes showed that the syringes were not sufficiently gas tight to hold the sample. The 25 mL gas tight syringes only retained the toluene in a sample for a maximum of 5-10 minutes before significant loss occurred. Sampling methods for the column tests were changed to insure that any gas sample taken was analyzed within five minutes.

Two Hamilton constant rate syringes were used for liquid solvent samples, and it was discovered that one of the two syringes was not calibrated accurately at the factory. It was recalibrated using procedures suggested in the care and use instructions that came with the syringe. The constant rate syringe was filled and evacuated three to four times with solvent to assure a representative sample. Ten to twenty μL of solvent was removed from the sample, and the syringe was inverted to remove any air bubbles. Liquid volume was reduced to the 0.75 μL delivery volume. Few problems occurred with the constant rate syringes. Occasionally the pipette needle point would plug by coring the septum during sampling from the EPA vial, so the needle point was observed prior to injecting into the GC to make sure it was clear.

Adsorption of Toluene by Materials and Experimental Apparatus

Other problems observed during the development stage involved adsorption of toluene by various materials. Using headspace techniques, materials to be in contact with the soil and toluene were tested for adsorption. Samples of the material were exposed to toluene and then placed in a clean EPA vial at room temperature. The gas phase toluene was measured in the headspace and then the vials were heated to about 60 °C. Any increase in gas phase toluene measured at the higher temperature was attributed to toluene adsorption by the material. Materials showing significant toluene increases at the higher temperature were unacceptable for use in direct contact with soil or water containing toluene. Red rubber gasket material, rubber stoppers, teflon thread sealing tape, red rubber syringe needle sleeves and plugs, and hard plastics all adsorbed toluene significantly. Viton gasket material, the teflon surface of the PTFE septa, brass, aluminum foil, and aluminum foil from a weighing tin did not adsorb toluene.

Preparation of Toluene Standards

External toluene standards were freshly prepared to calibrate the GC each time samples were analyzed. The toluene standards were made at concentration levels within the linear response range and also at concentrations close to the expected sample levels. The standards were analyzed periodically throughout the measurement of the unknown samples as a check to assure that the GC responded linearly during the run. A calibration curve was determined using linear regression. The external standards worked well, so internal standards were not used. Several methods were tested to prepare and store the

toluene standards. In a fashion similar to the analytic methods for toluene, the best method was learned through experimentation. Gas phase standards were prepared by three different methods during the study with the third method considered the best. Toluene in hexane standards were prepared the same way throughout the study.

All vials and bottles used for the gas samples had their volume individually determined by filling to zero headspace and weighing the distilled water it held. Prior to each use, the bottles, vials, and septa were cleaned thoroughly with soap solution, rinsed with deionized water, rinsed with methanol, and finally oven dried. After cooling in a desiccator, the bottles and vials were stored with cap and septum in place until needed.

Gas phase standards were normally made up the day before analysis, and no more than two days before use. The gas standards were kept in a shaking water bath at 25 °C until analyzed. Early in the study it was discovered that the dual faced PTFE septums leaked after puncturing with the syringe needle. The septums are considered self-sealing by the EPA for semi-volatile compounds in water, but this was not true for the more volatile toluene. It was observed that the gas standards showed decreasing toluene concentration after the septum was punctured. This was observed by Robinson et al. (1990) in their work. Robinson et al. (1990) also found that rapidly replacing the punctured septum of an unknown or standard yielded losses of less than 1%, if the cap was removed for less than 30 seconds. Samples that might require additional analysis had the septa replaced after puncture to prevent further loss.

The first method to prepare the gas phase standards used a spike solution prepared by dissolving toluene in methanol. Varied microliter volumes of the spike solution were

added to different 40 mL EPA vials each containing 20 mL of 0.01 N calcium sulfate solution to prepare the standards. Henry's coefficient and partitioning relationships were used to determine the toluene concentration in the headspace air volume above the solution. The toluene in methanol spike solution was easy to handle because the toluene did not volatilize significantly from the methanol solvent during the standard preparation. This method did, however, introduce a methanol cosolvent in the water solution which might affect the partitioning relationships and give results inconsistent with toluene in water. The method was therefore abandoned.

The second method utilized dilutions of the stock saturated toluene solution kept in the lab. Several 40 mL EPA vials were filled with varying amounts of 0.01 N calcium sulfate solution. Each vial then had saturated toluene solution added until each had a total of 20 mL of liquid. The saturated solution concentration was determined and then the Henry's coefficient and partitioning relationships were used to determine the gas phase concentration in the standards. Since the addition of saturated solution exposed each vial briefly to the atmosphere during the filling operation, this introduced uncertainty related to toluene volatilization losses to the atmosphere. The method was inconsistent when making gas phase standards close to or below one mg L^{-1}, so it was abandoned.

The third method of preparing gas phase standards gave the best results. Pure toluene was added to the calcium sulfate solution in the EPA vials using calibrated constant delivery rate microsyringes. The mass of toluene added to a vial was calculated by the microliter volume delivered divided by the specific gravity of toluene. The toluene standards were prepared by rapidly injecting toluene into a vial with cap and septum

offset just enough to allow the syringe needle into the bottle. Immediately after injection, the cap was tightened securely. To make gas concentrations below one mg L^{-1} of toluene, larger 500 mL volume vials were used to keep the added toluene within the most accurate delivery range of the 20 μL constant rate syringe. This method gave the most consistent results and took away the uncertainty of losses due to volatilization during standard preparation.

Standards for toluene in hexane were prepared from dilutions of a stock solution of toluene in hexane. The stock solution was prepared by adding 150 μL of reagent grade toluene to a weighed volume of approximately 20 mL of pure hexane. The stock solution was refrigerated at 4 °C and the standards were made from dilutions of the stock solution with hexane. It was found that hexane significantly escaped from the EPA vials at room temperature but not when refrigerated. The toluene in hexane liquid standards were always refrigerated until use. The septum was immediately replaced after puncturing and the standard placed in the refrigerator. Toluene in hexane standards were made up a day or two before using, and had a shelf life of a week when stored in the refrigerator.

Equilibrium Partitioning Coefficients

The equilibrium partitioning coefficients for toluene were determined using 24-hour isothermal batch experiments. Both the Henry's coefficient and the activity coefficient were determined by equilibrium partitioning in closed systems (EPICS) headspace techniques according to procedures used by Garbarini and Lion (1985), and Lion et al. (1990). The linear adsorption coefficient for the Teller loam soil was

determined using the 24-hour batch test procedures outlined in ASTM SD 4646-87, and Roy et al. (1987). The batch test samples determined gas phase toluene from the headspace air, and then using local phase equilibrium (LPE) assumption the mass of toluene in the dissolved and adsorbed phases were calculated. Gas phase analysis was used whenever possible in this research because of its rapid analytic time and its lack of interference from soil particle effects or toluene adsorbed on dissolved soil organic matter.

The Henry's and activity coefficient samples were placed in a shaking water bath at 25 °C during their 24 hour incubation period. Initially the linear adsorption samples were incubated in the shaking water bath and taken out and shaken thoroughly three or four different times during the 24 hours. A variable speed rotating tumbler built for the soil extraction analyses was used for the batch tests. The adsorption samples were incubated at room temperature (23 ± 2 °C) on the tumbler, rotating just rapidly enough (12 rpm) to keep the soil solids from settling out in the vials. An hour prior to analysis the tumbled samples were placed in the shaking water bath to allow the gas and liquid phase toluene to equilibrate.

Samples to determine the Henry's coefficient were prepared using pairs of 40 mL EPA vials where both had the same toluene mass but different volumes of 0.01 N calcium sulfate solution. The EPA vials varied slightly from 40 mL, so each was accurately measured to allow normalization to a 40 mL standard volume. The EPICS procedure assumes LPE conditions, so all samples are prepared within the linear partitioning range for toluene. The mass of solute in a vial with just water and air is described by

$$M_T = C_{sg}V_g + C_{sl}V_l \ , \qquad \textbf{(4-1)}$$

where M_T is the total toluene mass, C_{sg} the concentration of solute in the gas phase, V_g the volume for the gas phase, C_{sl} the concentration of solute in the liquid phase and V_l the liquid volume. The gas phase concentration is related to liquid phase concentration as

$$C_{sg} = K_H C_{sl} , \tag{4-2}$$

where K_H is Henry's coefficient. Two vials (1 and 2) with the same mass of toluene and different liquid and gas volumes are related by

$$C_{sg1} V_{g1} + \frac{C_{sg1}}{K_H} V_{l1} = C_{sg2} V_{g2} + \frac{C_{sg2}}{K_H} V_{l2} , \tag{4-3}$$

then K_H is related to the gas phase concentrations in the two vials as

$$K_H = \frac{V_{l2} - (\frac{C_{g1}}{C_{g2}}) V_{l1}}{(\frac{C_{g1}}{C_{g2}}) V_{g1} - V_{g2}} . \tag{4-4}$$

Gas chromatographic response is proportional to concentration, so the ratio of the GC responses can be used. Determining the actual toluene concentration is unnecessary.

The 0.01 N calcium sulfate was tested for the compound activity coefficient (γ) of the ionic solution using a procedure similar to that for the Henry's coefficient. Two 40 mL EPA vials were used with the same toluene mass, liquid volume and gas volume in each vial. One vial was pure distilled water and the other vial contained the 0.01 N calcium sulfate solution. If the toluene behaves nonideally in the 0.01 N calcium sulfate solution, its gas and liquid phases are related to activity coefficient as

$$C_{sg} = \gamma K_H C_{sl} . \tag{4-5}$$

Assuming that the calcium sulfate solution is in vial 2 and the distilled water is in vial 1, the activity coefficient is determined by equating the masses

$$C_{sg1} V_g + (\frac{C_{sg1}}{K_H}) V_l = C_{sg2} V_g + (\frac{C_{sg2}}{\gamma K_H}) V_l . \tag{4-6}$$

Next solving for the activity coefficient of the 0.01 N calcium sulfate yields

$$\gamma = \frac{(\frac{V_l}{K_H})}{(\frac{C_{sg1}}{C_{sg2}})(V_g + \frac{V_l}{K_H}) - V_g} . \tag{4-7}$$

When both the activity and Henry's coefficients have been independently determined, the EPICS procedure is extended to adsorption and used to determine the linear partitioning coefficient (K_d) for a solute and soil. The partitioning coefficient determination uses triplicate samples with the same soil mass in each of the three vials and a blank vial without soil for each set of triplicates. Teller loam soil mass additions of 10, 12, 14, 16, 18 or 20 grams were added to the EPA vials to make six different sets of triplicates. Each sample and each blank had 20 mL of 0.01 N calcium sulfate solution added, and all were spiked with the same mass of pure toluene. The toluene was injected into each vial by the same method used in making the gas phase standards. The samples with soil were placed on the tumbler at room temperature for 24 hours and the blanks were placed in the shaking water bath at 25 °C. One hour prior to analyzing, the samples with soil were placed in the shaking water bath to allow the gas and liquid phases to equilibrate.

For the partitioning coefficient headspace procedure to be valid, the differences in toluene gas phase concentration between the blanks and the samples with soil are attributed to adsorption by the soil organic matter. The blanks for all six sets of triplicates are averaged and this value is compared against the averaged value of each set of triplicate soil samples. Total mass of toluene is the same in each blank and sample, so using Equations 4-1 and 4-5 they are equated to the liquid concentration by

$$C_{sl1}(\gamma K_H V_{g1} + V_l) + X = C_{sl2}(\gamma K_H V_{g2} + V_l)\,, \qquad \textbf{(4-8)}$$

where sample 1 has soil, sample 2 is the blank and X is the total mass of toluene adsorbed by the soil. If one has a linear isotherm then

$$\frac{X}{M} = K_d C_{sl1}\,, \qquad \textbf{(4-9)}$$

where M is the soil mass in the vial. Solving for C_{sg1} yields

$$C_{sg1} = \gamma K_H C_{sl1} \text{ and } C_{sg2} = \gamma K_H C_{sl2} \ . \quad \textbf{(4-10)}$$

The mass of soil varies with this technique so it is necessary to account for the volume displaced by the soil and normalize the sample gas concentration to the same volume of gas in the blanks. The normalized results have $V_{g1} = V_{g2} = V_g$ and

$$C_{sg1(normalized)} = C_{sg1(observed)}\left(\frac{(V_l+\gamma K_H V_{g1})_{actual}}{(V_l+\gamma K_H V_{g2})_{blanks}}\right) \ . \quad \textbf{(4-11)}$$

Combining Equations 4-8, 4-9, 4-10, and 4-11 produces

$$\frac{C_{sg2(blanks)}}{C_{sg1(normalized)}} = K_d\left(\frac{M}{\gamma K_H V_g + V_l}\right) + 1 \ . \quad \textbf{(4-12)}$$

Plotting the results of the different soil masses for Equation 4-15 gives a straight line in the linear adsorption range, and K_d is the slope of the regression line plotted through the sample sets of triplicate results. Good results in the linear range give a regression analysis with the R-squared value close to 1.0 and a y-intercept close to 1.0.

Description of the Soil Column

The research used a horizontal soil column and relied on a computer controlled syringe pump to maintain the desired unsaturated moisture content at the column inlet. Gas samples were collected from the soil air throughout each test and soil matrix samples were collected immediately upon test conclusion. Toluene losses had to be controlled, so the soil column needed to be gas tight, non-adsorptive and easy to sample in order to minimize losses to the atmosphere during sampling. Collection of water from the unsaturated soil in the column was desired, but a satisfactory method to sample the soil water without shifting phase equilibrium within the unsaturated soil was not discovered. Removing water from the unsaturated soil required vacuum extraction methods which

shifted the equilibrium among the phases. As a result, the research only measured the gas phase during the column test and total toluene within the soil matrix immediately upon test conclusion. The measured total and gas phase toluene along with the partitioning relationships allowed calculation of the toluene in the adsorbed and liquid phases.

Four different soil column types were tested with the first three being rejected as unsatisfactory. The first column used 0.5, 1 or 2 cm wide teflon rings (3.5 cm inner diameter) taped together to form the column. This column is flexible since it can be made in any length required, and it has been used successfully in the lab with conservative contaminants. Upon test completion the taped rings are cut apart, and all of the soil in each ring is analyzed for contaminant concentration. With volatile contaminants such as toluene, collecting soil samples by cutting the rings apart exposed the soil to significant toluene losses through volatilization from the multiple ring column.

The second column tested was a teflon ground water sampling bailer (3.8 cm inner diameter) modified for use as a soil column. Column 2 was a single piece with 12.7 mm diameter holes drilled along the top for soil sampling, and 6.3 mm diameter holes drilled (90° from the top holes) along the side for removing gas samples. The soil sampling holes were covered with teflon tape or aluminum foil, and the gas sampling ports sealed with red rubber needle plugs. Sampling equipment was designed and built to simultaneously collect soil samples and gas samples from all holes upon test conclusion. This column was not gas tight, and the soil sampling equipment required too much force to operate easily by hand. In addition, placing the soil samples in EPA vials for toluene extraction allowed too much exposure time and toluene volatilized to the atmosphere.

The gas sampling equipment worked but had two problems. The sampling procedure gave only a single sample at each location for the column experiment, and if a syringe failed to collect a gas sample for any reason there was no opportunity to collect another sample. The 25 μL syringes were gas tight for only a few minutes and toluene loss occurred from the syringes while the samples were waiting to be analyzed on the GC.

The third column was made from 4 cm inner diameter brass pipe threaded on each end for inlet and outlet connectors. The column had a row of bushings soldered to the top of the pipe for soil sampling. The bushings were plugged with a 19.0 mm diameter brass bolt and teflon o-ring, and the bolt was removed using a power socket driver prior to collecting a soil sample with a 9.5 diameter brass tube. The gas sampling ports were 1/8 inch copper tubing connectors soldered along the side of the column (90° from the bushings). The gas ports were covered with a PTFE dual faced septum to seal the syringe needle and held in place by a tubing cap with a hole drilled for the needle. Column tightness was checked at a pressure of 25 cm of water and some of the column solder joints leaked. The leaks were sealed with epoxy glue but tended to leak after use. In addition, the bolts had about 2.5 cm of threads and removal for sampling was slow. This column did not fit the requirements, so the design was simplified to eliminate solder joints and one of the two sets of holes in the column.

The fourth soil column was easy to sample, gas tight and non-adsorbing. This column also used 4.0 cm inner diameter (4.8 cm outer diameter) brass pipe cut to a length of 60.0 cm and threaded on each end for inlet and outlet connectors. The brass column had fourteen 11.1 mm diameter holes drilled on center every four centimeters starting 4.0

cm from the column end. The inlet fittings added 1.3 cm to the overall length of the packed soil, so this meant that the holes were located at 5.3, 9.3, 13.3, 17.3, 21.3, 25.3, 29.3, 33.3, 37.3, 41.3, 45.3, 49.3, 53.3 and 57.3 centimeters from the inlet. In addition to these holes, two additional holes were drilled at 3.5 and 7.3 centimeters to give more samples close to the inlet. All holes were covered with individual viton gaskets which were kept in place using a 15.9 mm wide stainless steel hose clamp centered over each hole. Each hose clamp had a 3.2 mm diameter hole drilled through it which was then lined up with the center of the hole in the column. The gas sampling syringe needles were pushed through the viton gasket into the soil column through the 3.2 mm diameter hole in the hose clamp band. Figures 4-5 and 4-6 show the soil column with the gas sampling syringes in place.

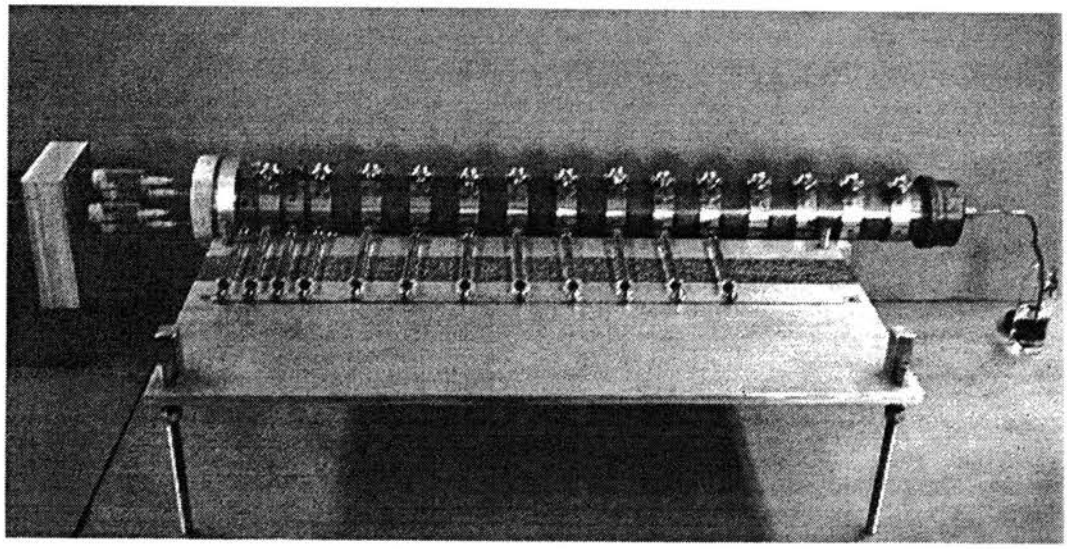

Figure 4-5. Photo of the column with gas sampling syringes.

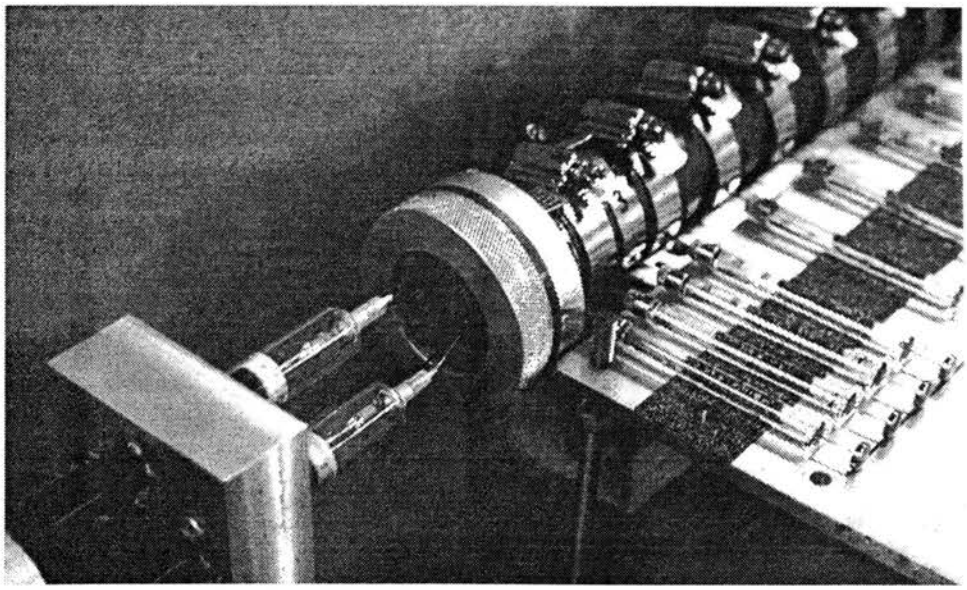

Figure 4-6. Close-up photo of the column with gas sampling syringes.

The inlet end was sealed with a two piece machined aluminum fitting to hold the gaskets. The fittings included a reducing flange and a cap. The reducing flange had an 0-ring shoulder to seal against the brass soil column end, and a wide surface on the male end of the fitting. The reducing fitting was sealed with an aluminum cap with a 4.5 cm diameter opening. The cap held two 5.8 cm diameter gaskets securely against the flat surface on the male end of the reducing flange. Gaskets were made from a 1.6 mm thick viton gasket against the soil, and a 3.2 mm thick red silicone gasket on the outside to seal around the injection syringe needles. All threaded fittings were wrapped with teflon tape to assure a tight seal, and the reducing flange and cap were tightened securely with a pipe wrench. The inlet fittings added 1.3 cm of length to the packed soil making total column length of 61.3 cm. Figure 4-7 shows the inlet fittings taken apart.

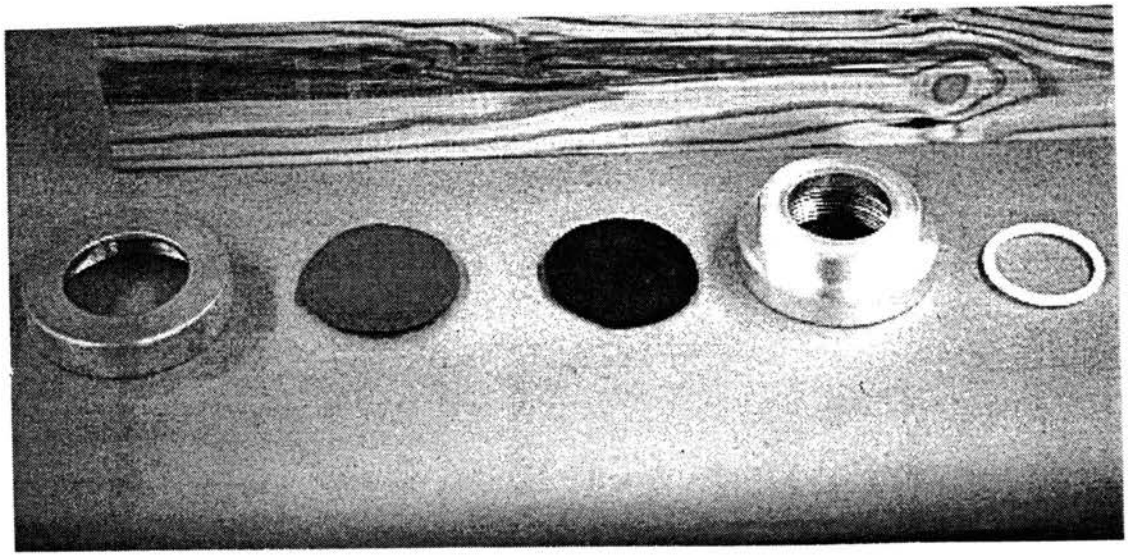

Figure 4-7. Inlet fittings for the column.

The outlet end of the soil column was sealed with a brass pipe cap and a teflon o-ring to fit inside the cap against the column end. The column end threads were wrapped with teflon tape and the cap tightened securely with a pipe wrench. The brass cap had a 3.2 mm Swagelok™ tubing fitting mounted in the center of the cap and soldered in place. The fitting provided an outlet for air displaced from the column by the injected toluene solution during a column test. Air from the column was routed through 1/8 inch copper tubing to a methanol trap where any toluene that might exit the end of the column could be collected. The copper tubing outlet was placed just below the methanol liquid surface to prevent significant backpressure within the column. The methanol in the trap could be analyzed for toluene presence any time during a test.

The holes in Column 4 fulfilled the requirements to sample soil air during the test and sample soil upon its conclusion. The column was pressure tested at 25 cm of water

prior to packing with all clamps and fittings then tightened to prevent leaks. Column 4 was gas tight, sampling was simple, and soil and gas samples came from the same location which made for better comparisons. The simplicity of the column made it easy to clean and prepare for a column test.

Soil Preparation and Column Packing

Prior to packing column 4, the Teller loam soil was oven dried at 105 °C for 24 hours. After drying, the soil was cooled in a desiccator and a known mass of dry soil placed in a one gallon zip lock plastic bag. Two more bags were placed around the bagged soil. The triple-bagged soil was wetted to equal a packed soil moisture content of approximately 10% (by volume) with 0.01 N calcium sulfate solution which had 0.01% sodium azide present to inhibit biological activity. The bags were sealed with air excluded and the soil and liquid mixed by hand kneading of the bags. The wetted soil sat overnight to allow the soil moisture to equilibrate before packing the column.

Progressing from the inlet to the outlet end, the column was packed to an approximate dry bulk density of 1.65 g cm^{-3}. Sufficient wetted soil to yield a two centimeter thick lift of soil at approximately 10% volumetric moisture content (compacted) was weighed and placed in the column. Then the soil was compacted using a steel rod until the lift reached its 2 centimeter compacted depth as measured with a meter stick. Prior to adding the next lift, the surface of the compacted soil in the column was scarified. Filling the column required a total of 30 complete lifts and one partial lift. The outlet cap was replaced to seal the column. The column was weighed after packing

to determine the amount of wetted soil and actual packed density was determined by dividing this value by the column volume. The column sat overnight to allow moisture equilibration within prior to starting the test.

During packing, care was taken to keep the soil bag closed except when weighing soil to prevent moisture loss. After packing each lift, a stopper was placed on the end of the column to prevent moisture loss while the next lift was weighed. The packing operation was done quickly, but approximately an hour was required to pack the column. During packing the soil lost moisture, and the final packed moisture content in the column was about 8% by volume. The actual initial moisture content within the column was determined at completion of the column test by destructively sampling for moisture content. Initial soil moisture content was the average of all moisture samples beyond the wetting front.

Syringe Pump Injection to the Column

The computer controlled syringe pump used in the experiments is flexible and gives performance results similar to the Bruce/Klute techniques (Brown and Allred, 1992) for unsaturated flow tests. The pump system shown in Figure 4-8 is programmable to maintain unsaturated flow conditions at the column inlet with either a constant moisture potential or a constant moisture flux. This study used the constant moisture potential boundary condition with the final moisture content at the inlet measuring approximately 25% by volume. The initial moisture content in the column was constant throughout at about 8% by volume. The Bruce/Klute boundary conditions must be

maintained for validity of the horizontal column test. Test conditions require a homogeneous soil uniformly packed at a constant initial moisture level, and the final moisture content at the inlet must be constant. In addition, the soil column requires enough length to be considered semi-infinite, so that the wetting front remains in the column.

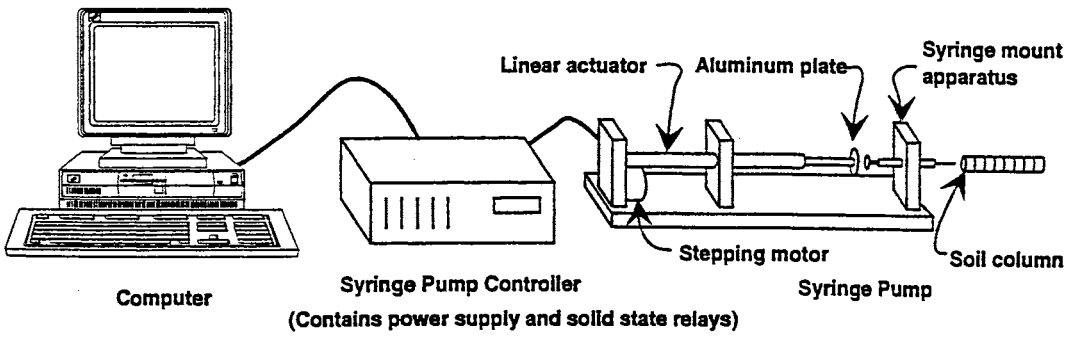

Figure 4-8. Syringe pump apparatus (after Brown and Allred, 1992)

Numeric procedures calculate the sorptivity and Boltzman variable using Teller loam's diffusivity at the packing density, the initial moisture content and the final moisture content. The sorptivity and Boltzman values determine test duration, expected travel distance of the wetting front, and total injection volume using

$$x = \lambda\sqrt{t} \ , \qquad \textbf{(4-13)}$$

and

$$V = SA\sqrt{t} \ , \qquad \textbf{(4-14)}$$

where x is the horizontal distance (cm) from the inlet, λ the Boltzman variable (cm $t^{-1/2}$), t the total time (sec), V the total volume injected (cm^3), S the sorptivity (cm $t^{-1/2}$) and A the cross-sectional area of the column (cm^2). Using the Boltzman variable and the total

length of the column, the rate of advance of the wetting front is calculated with Equation 4-13. Column experiments must be shorter than the time required for the front to reach the column end in order for the Bruce/Klute boundary conditions to be valid.

A convenient test time duration less than breakthrough time was chosen and the expected wetting front travel distance calculated from Equation 4-13. The column experiments were designed to advance the wetting front into the column as far as possible without the toluene gas phase breaking through into the methanol trap. Column experiment duration of 6, 12, and 24 hours met this requirement. One advantage of using the Boltzman transformation is that it allows comparison of different time length column tests at the same packing density and moisture boundary conditions. Using Equation 4-13, different test lengths are compared by plotting moisture content or concentration along the column length against the Boltzman variable at that distance. Self similar tests should plot closely. After choosing the test duration, Equation 4-14 calculates the total volume of solution to inject into the soil column using the syringe pump apparatus.

Procedures to make the injection solution and deliver the solution were developed. The syringe pump apparatus uses a syringe mount clamp to hold a milled aluminum disk with the syringes containing the injection solution. Previous experiments with more conservative contaminants used disposable 10 mL syringes in the disk but these were not suitable for use with the toluene due to adsorption problems. A new disk was milled to hold four Hamiliton 10 mL gas-tight glass syringes to eliminate the undesirable adsorption. Each syringe had a Luer fitting and used new, 18 gauge,

disposable needles for each test. All syringes and needles were thoroughly cleaned, rinsed with methanol and oven dried prior to loading the injection solution.

All tests were conducted in the linear concentration range for toluene so stock saturated toluene solution was diluted to approximately 90 mg L^{-1} to make the injection solution. Dilution was accomplished using a 500 mL aspirator bottle with a bottom spigot covered with a red rubber sleeve type serum bottle stopper. The bottle was weighed empty with a teflon coated magnetic stirring rod and cap in place. Then the bottle was partially filled with 0.01 N calcium sulfate solution and reweighed. Finally the bottle was topped off quickly with saturated toluene solution, capped without headspace air present and weighed again. The injection solution was stirred overnight before loading the syringes. The actual concentration of the diluted solution was determined by analysis instead of calculation based on the dilution weights because of adsorption by the serum sleeve and possible volatilization losses around the stopper.

The injection syringes were loaded just prior to starting a column test. The syringes were filled through the serum stopper on the bottom spigot of the aspirator bottle. Each syringe was overfilled, then inverted and any air bubbles ejected from the syringe. Next weighed samples of the solution in each syringe were placed in separate vials with known masses of hexane for analysis of the solution concentration in each injection syringe. In addition, weighed solution from each syringe was placed in individual EPA vials containing 20 mL of 0.01 N calcium sulfate solution. These samples were analyzed by EPICS headspace methods as a backup to the toluene concentration determined by hexane extraction. At the conclusion of a column test, remaining solution

in each syringe was placed in vials with 0.01 N calcium sulfate solution and analyzed for toluene concentration by headspace methods. The toluene concentration values for the syringes were averaged and this value plus the injection volume determined the total toluene mass added to the column during a test.

The disk with filled syringes was clamped tightly into the syringe mount apparatus. The sealed soil column was then carefully worked against the syringe needles until all needles were positioned with the opening just inside the innermost gasket in the soil. The column test began shortly after insertion of the injection syringes. At the beginning of a column test the syringes were checked closely to make sure that all solution was going into the column. If leaks occurred, they were corrected immediately or the test was canceled and all preparations started from scratch. Occasional problems occurred when an injection syringe needle opening plugged with soil when pushed into the column. The syringe leaked around the Luer connection when plugged, and normally reseating the needle to the Luer connection corrected this problem. The glass syringes were subject to breakage if a needle remained plugged.

Column Sampling and Analysis

Gas samples were taken from the soil using syringes with removable needles by pushing the needle through the viton septum directly into the center of the soil column. The 22s gauge needles of the gas-tight syringes were modified by adding four additional holes along the needle barrel. The holes were drilled through the needle wall to the center opening using a micro-drill. To aid drilling and to give a cleaner hole, the needle had a

cleaning wire inserted which was of different hardness than the needle. The operator could sense when the drill reached the wire and cease drilling. The holes were drilled in a spiral pattern around the needle barrel.

Commercially available side hole needles were tested and both the single or double hole opening styles tended to plug when inserted into the soil. Since a cleaning wire could not be run through the needle completely, these needles were almost impossible to clean after plugging. The needles with extra holes drilled had a standard needle point opening which could usually be cleaned satisfactorily after use. The modified needles had some problems with soil plugging of the openings, but generally the modified needles performed well in collecting soil air samples.

Figures 4-5 and 4-6 showed the column with syringes inserted. When a sample was taken from a location the syringe plunger was pushed in and out slowly three or more times prior to collecting the sample. The plunger was then drawn out slowly to about 20 μL gas volume, and the needle barrel unscrewed from the needle. A clean barrel was immediately screwed onto the needle in the soil. The sample taken had an unmodified needle screwed on and the gas volume reduced to 10 μL for immediate injection into the GC for analysis. The sample location, time of sampling, and the time of injection were recorded to assist analyzing the chromatogram. After injection, the gas syringe was flushed with methanol and dried with the heated vacuum syringe cleaner for additional use during the test.

Gas sampling commenced close to the column inlet right after the test began. Sampling was done along the column length with approximately one sample every five

minutes. Care was required during sampling to assure that when the gas sample was taken, water was not drawn into the syringe. Injection of water into the GC capillary column unsettled the chromatogram baseline making the results difficult if not impossible to interpret. As the wetting front advanced it was sometimes difficult to get a good gas sample as the air pores became less continuous in the wetter soil. This was exhibited when the gas concentration at a sampling point dropped significantly from the previous analysis. At this time the modified needle was rotated or in extreme cases replaced with a clean needle and another sample taken.

Soil air samples were collected intermittently throughout the column tests and the gas chromatograph analysis program ran almost continuously during a test. The chromatograms were very clean for the gas samples and times of retention consistent throughout a test. Gas standards were analyzed during the test to assure accuracy and retention time consistency. During the 12-hour and 24-hour tests the inlet septum on the GC was changed during the short downtime between GC programs to maintain the instrument accuracy. Gas sampling required at least two people sharing the duties because of the need to sample continuously over an extended time frame.

The soil sampling occurred at the conclusion of the test and this worked best with three people cooperating. Just prior to the end of injection all gas syringes were removed. As soon as injection stopped, the soil column was pulled away from the injection syringes and sampling started. Starting at the inlet end a power screwdriver was used to remove the steel hose clamp over the first hole. A soil sample for total toluene was taken with the brass tube and immediately placed in a centrifuge tube with the hexane extractant. The

hole was plugged with a stopper and the next hole sampled in a similar manner. All sixteen soil samples for toluene analysis were taken within ten minutes, and then the samples for soil moisture were taken from the same holes plus one at the inlet.

The moisture samples were placed in tins, immediately weighed after collection and placed in the oven at 105 °C` for 24-hours. The extraction samples were then placed on the tumbler overnight. The following morning the extraction samples were removed from the tumbler and put in the refrigerator to cool. After cooling the samples were centrifuged to settle the solids and the samples replaced in the refrigerator prior to GC analysis. Extracted toluene analysis started within 24 to 36 hours of sample collection.

CHAPTER 5

RESULTS AND DATA ANALYSIS

Introduction

The experimental results are discussed in the narrative and compiled in either tabular format, graphical format or both for additional clarity. Prior to conducting the column experiments the GC analytic procedures were developed and parameters affecting toluene transport were determined. These parameters included: the Teller loam soil properties, the soil-water solution properties and the toluene equilibrium phase partitioning coefficients. The majority of this chapter is devoted to the column experiments. Their results are compared to and evaluated against the theory presented in Chapter 3.

Soil Properties

The Teller loam soil was analyzed as outlined in Chapter 4 to provide baseline quality data for the soil. Both batches of Teller loam soil used in the experiments were collected from the same general area, and after collection the soil was air dried, ground with a hammer mill, mixed and stored in 15-gallon barrels. Depending on laboratory usage, a batch of soil lasted between one to three years. Since the soil was collected in the same location each time, the soil properties were similar between batches. Table 5-1

lists the physical and chemical properties for the two batches of Teller loam soil used in this study.

TABLE 5-1

Physical and Chemical Properties of Teller Loam Soil

Property	Unit	Measured Value
Texture classification†	loam loam	50% sand, 34% silt, 16% clay* 52% sand, 31% silt, 17% clay**
Extractable bases†	$cmol_c\ kg^{-1}$	$Na^+ = 0.8$, $K^+ = 1.0$, $Ca^{2+} = 6.3$, $Mg^{2+} = 2.4$**
Cation exchange capacity†	$cmol_c\ kg^{-1}$	19.5* & 14.0**
pH	--------	6.0*, 6.1** (1:1 soil:distilled water) 6.7** (1:2 soil:distilled water) 5.8** (1:2 soil:0.01M $CaCl_2$ solution)
Organic carbon content	%‡	0.7* & 0.9**
Soil organic matter††	%‡	1.2* & 1.5**
Ferric oxide content	%‡	4.9*
Specific surface area†	$M^2\ g^{-1}$	37.8**
Particle density	$g\ cm^{-3}$	2.65*

† Allred (1995)
* Measurement on the soil used up until May, 1993 (first batch)
** Measurement on the soil used after May, 1993 (second batch)
‡ Percentage by weight of dry soil
†† calculated as 1.72 times the organic carbon content

The first batch of soil was used during procedures and technique development, while the second batch was used for the actual partitioning and column experiments. Organic carbon content of the first batch of Teller loam soil was 0.7% by weight with the second batch slightly higher at 0.9%. Texture, CEC and pH of the soil were similar for

each batch. The measured values for soil properties in Table 5-1 are comparable to representative values for Teller loam reported by Henley et al. (1987). The Teller loam soil did not have any properties that might affect toluene transport in an unusual manner.

Soil Water Solution Properties

The soil water solution pH, density and surface tension were assessed for their potential effect on toluene transport in the Teller loam. Solution pH influences the soil particle surface charge, speciation of ionic compounds and microbial activity. Concentrated solutions in the ground water system cause density gradients, thereby increasing the contaminant transport rate. Liquid surface tension influences capillary effects in the soil. Interfacial tension between two immiscible or slightly miscible liquids such as water and toluene affects residual saturation within the soil.

Solution pH was measured according to the procedures listed in Chapter 4. A Fisher tensiometer (Tensomat model 21) determined surface tension by measuring the force required to pull a platinum ring through the surface film of the column injection solution. The solution's total dissolved solid (TDS) concentration was calculated based on the concentration of the calcium sulfate, sodium azide and toluene added to distilled water. Table 5-2 lists the pH, surface tension values and TDS of the distilled water and injection solution used in the column tests.

The pH of the 0.01 N calcium sulfate solution was 6.4, and after adding 0.01% sodium azide, it increased slightly to 6.5. Adding approximately 75 mg L^{-1} of toluene to the calcium sulfate and sodium azide solution did not change the pH of 6.5. The solution

pH and the soil pH levels are at similar levels, so solution pH's effect on transport is expected to be negligible.

TABLE 5-2

Water Solution Properties

Water Solution	Property[†]	Measured Value
distilled water	pH	5.4
0.01 N calcium sulfate solution	pH	6.4
0.01 N calcium sulfate solution with 0.01% sodium azide added	pH	6.5
0.01 N calcium sulfate solution with 0.01% sodium azide and approx. 75 mg L^{-1} of toluene	pH	6.5
distilled water	surface tension[‡]	72.3
0.01 N calcium sulfate solution	surface tension[‡]	72.8
0.01 N calcium sulfate solution with approx. 75 mg L^{-1} of toluene	surface tension[‡]	58.1
0.01 N calcium sulfate solution with 0.01% sodium azide and approx. 75 mg L^{-1} of toluene	total dissolved solids*	860

[†] all values measured at room temperature 23 ± 1^{0}C
[‡] dynes cm^{-1}
* mg L^{-1} (calculated from chemicals added)

The surface tension of the distilled water was 72.3 dynes cm^{-1} and the 0.01 N calcium sulfate solution was 72.8 dynes cm^{-1}. This slight increase with the addition of salt to the distilled water was expected. Pure toluene liquid has a surface tension of approximately 28.5 dynes cm^{-1}. The addition of 75 mg L^{-1} of toluene to the calcium

sulfate solution reduced its surface tension to 58.1 dynes cm^{-1}. According to Mercer and Cohen (1990) and Camp (1963) a decrease is expected. When a solute and solvent that have dissimilar surface tensions are combined, the surface tension of the solution is less than the higher of the two liquids. This is attributed to increased amounts of the solute concentrating near the water-air interface. If the toluene in solution concentrates near the water-air interface, it increases the concentration gradient near the surface, and increased toluene vaporization is possible. An increase in vaporization could evidence itself by increased toluene gaseous diffusion ahead of the wetting front. Lower solution surface tension could result in less capillary advancement of the wetting front than expected. Less advancement of the calcium sulfate solution with toluene than one without toluene would be evidence of lower surface tension.

Gas Chromatograph Calibration

Accurate calibration of the gas chromatograph at the toluene concentration levels of the experiments was critical to this study. Also the GC analysis required freedom from interference and repeatability as well as sensitivity. In this study external standards fit the requirements described above, and they were used to develop the calibration curve for gas phase toluene and toluene dissolved in hexane samples.

Analysis for Toluene Gas Phase

Toluene gas phase standards and batch samples were determined using EPICS headspace techniques described in Chapter 4. A calibration curve was developed for GC response area versus gas phase concentration, and this was used to determine

concentration levels of unknowns. Soil air samples were directly injected into the GC for analysis. Throughout the study, the toluene gas phase samples were free from interference, sensitive and reliable.

Appendix B lists the calibration data for the gas phase standards used in column tests #8 through #11. The fitted calibration curves for each test were excellent with high R-squared values varying from 0.982 to 0.997. The sensitivity of the toluene in air samples was excellent. Toluene concentrations as low as 0.01 mg L^{-1} (10 ppb) were routinely measured at the gas diffusion front during the column tests.

Analysis for Toluene Dissolved in Hexane Solvent

Toluene dissolved in hexane was analyzed using the GC as outlined in Chapter 4. A calibration curve was developed for GC response area versus concentration of toluene dissolved in hexane. Appendix B lists the calibration data for the column tests. The fitted calibration curves for the experiments were excellent, with R-squared values ranging from 0.992 to 0.997. The analysis for toluene did not exhibit significant interference, but the sensitivity of toluene measurement in hexane was limited to about 0.20 mg L^{-1} of toluene in hexane versus 0.01 mg L^{-1} for toluene gas in air. When hexane was used to extract toluene from the soil the sensitivity of the extraction procedure was limited to approximately 1.5 mg L^{-1} (1 ppm) of toluene in the soil matrix.

Equilibrium Partitioning Coefficients

The equilibrium batch test method described in Chapter 4 determined the partitioning coefficients for toluene and the Teller loam soil. First, the Henry coefficient

and activity coefficient were determined. Then the linear adsorption coefficient and maximum adsorption of toluene by Teller loam were analyzed and their values determined using the previously determined Henry and activity coefficient values. Table 5-3 lists the coefficient values and maximum adsorption capacity.

TABLE 5-3

Equilibrium Partitioning Coefficients for Toluene

Coefficient	Measured Value	Units
Henry (K_H)	0.27	none
Activity (γ)	1.04	none
Linear Adsorption (K_d) by Teller Loam soil	0.43	mL g^{-1} *
Maximum Adsorption ($C_{sm(max)}$) by Teller Loam soil	6 **	mL g^{-1} *

* mL of toluene per g of organic carbon

** calculated value based on fitted Freundlich Model and C_{sl} close to saturation (~500 mg L^{-1})

Henry Coefficient and Activity Coefficient

The Henry coefficient was 0.27 which is the same as determined by Ong et al. (1992) in their research. The activity coefficient was 1.04 for the calcium sulfate solution which is in general agreement with values Garbarini and Lion (1985) measured for sodium, calcium and aluminum chloride solutions. Appendix C lists the data for the Henry and activity coefficient measurements.

Linear Adsorption Coefficient

The adsorption coefficient for the Teller Loam soil was determined on four different samples from three different batches of Teller loam using the procedures outlined in Chapter 4. The result from each soil sample was related to its fraction of organic carbon (f_{oc}) by

$$K_{oc} = \frac{K_d}{f_{oc}} \quad , \tag{5-1}$$

where K_{oc} is the organic carbon partition coefficient. The average K_{oc} value from the four adsorption batch tests was determined and this value multiplied by the fraction of organic carbon for the Teller Loam soil used in each column test to yield the K_d for that particular test. The results of the adsorption studies are tabulated in Appendix D and shown in Figure 5-1.

All four samples shown in Figure 5-1 were within the linear adsorption range and the slope of the fitted line for each test equals its K_d value. The average K_{oc} value for the four tests was 47.8 mL g^{-1} of organic carbon. The Teller Loam used in the column tests (#8 through #11) had a f_{oc} of 0.009 g g^{-1}. This gave a calculated K_d value of 0.43 mL g^{-1} of organic carbon to use for the column test analyses. The measured K_{oc} is lower than the value of 300 predicted by Karickhoff et al.'s (1979) empirical formula based on the K_{ow} value for toluene. However, the K_{oc} value of 48 for the Teller loam was similar to values of 77 to 191 measured by Garbarini and Lion (1985) for soils from several Air Force Bases. Garbarini and Lion (1986) concluded that the variation of organic carbon matrices and its properties in natural systems results in dissimilarities in their ability to adsorb organic compounds. Relying on Karickhoff et al.'s (1979) empirical equation based on a single measured soil property (f_{oc}) to estimate K_d may therefore be misleading.

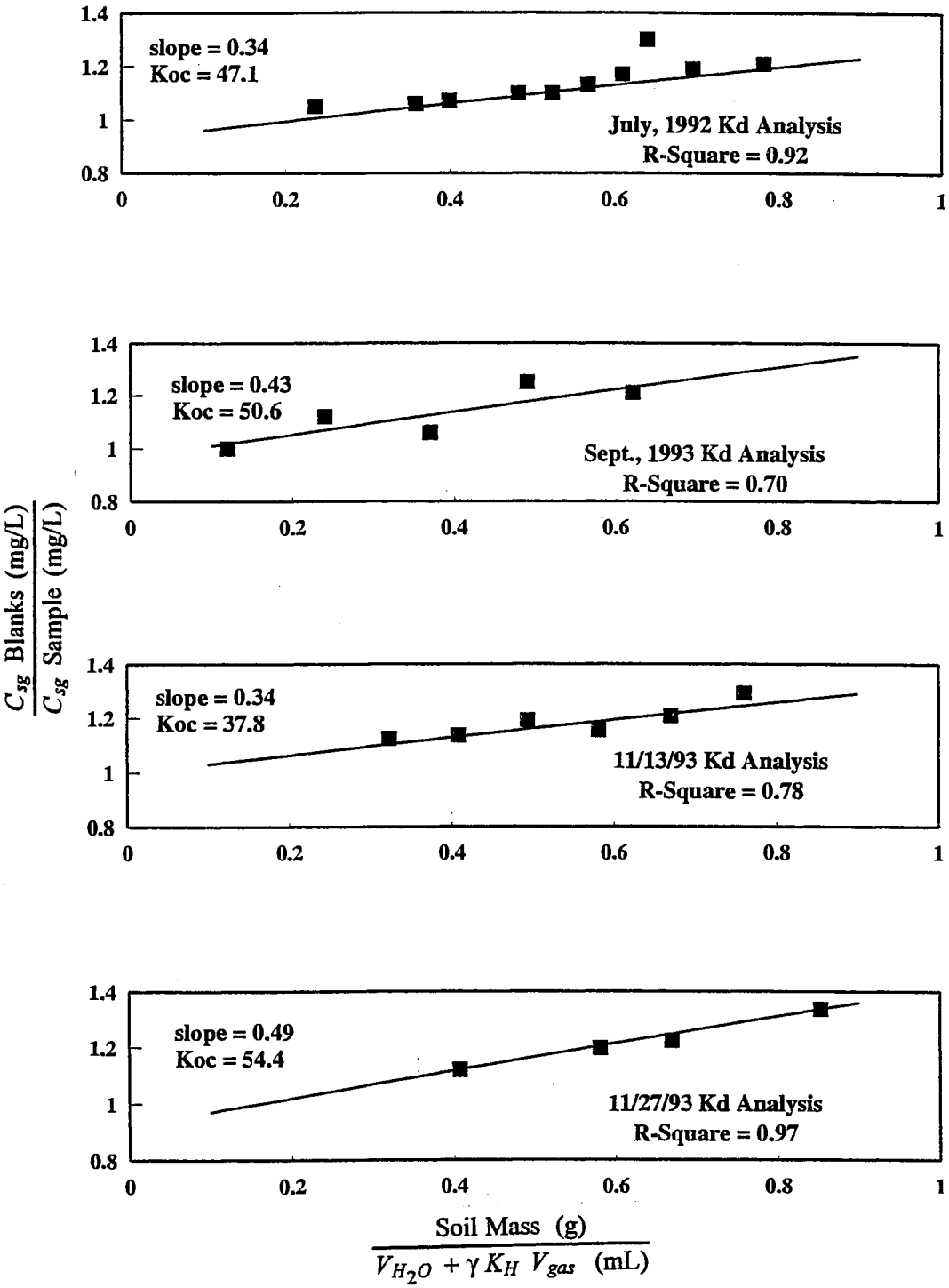

Figure 5-1. Adsorption of toluene by Teller loam soil.

Maximum Adsorption of Toluene by Teller Loam Soil

Data from the batch tests within the linear range and beyond the linear range were plotted for sample sizes of 12, 14 and 16 grams of soil to give an estimate of the maximum adsorption capacity of the Teller Loam. The data are shown in Figure 5-2 as toluene mass adsorbed per soil mass (X/M) versus toluene concentration in solution (C_{sl}).

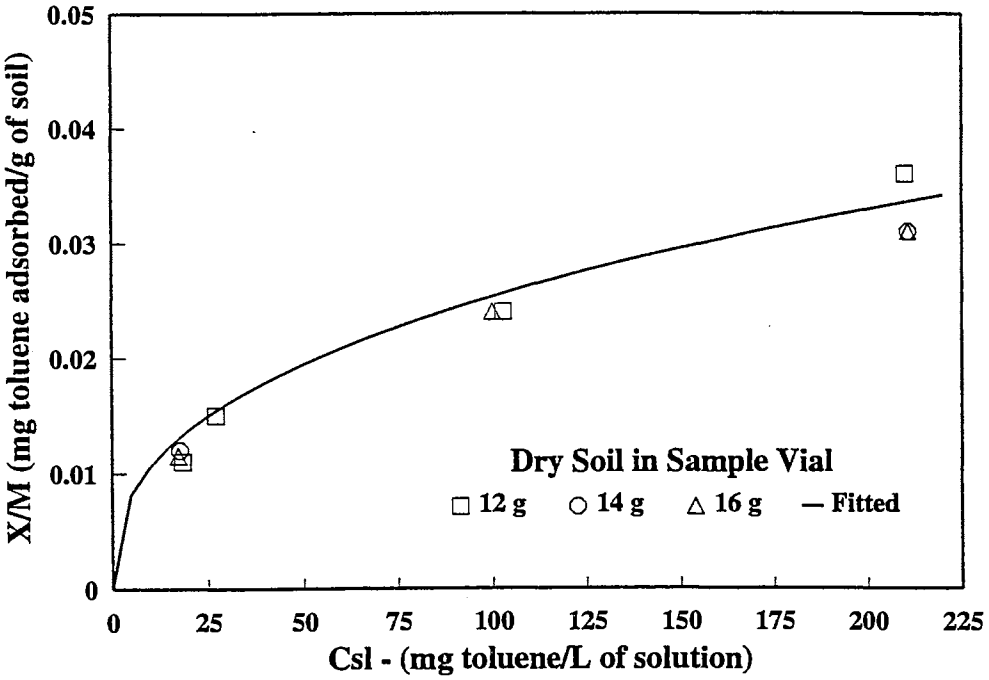

Figure 5-2. Maximum adsorption of toluene by the Teller loam soil.

The Freundlich model was fitted to the data and the resulting equation was

$$\frac{X}{M} = 0.0044 C_{sl}^{0.38} \quad . \qquad \textbf{(5-2)}$$

The data for Figure 5-2 are listed in Appendix E. Assuming the soil was exposed to a saturated toluene solution at approximately 500 mg L^{-1} yields a maximum toluene adsorption capacity of approximately 6 mL g^{-1} of organic carbon.

Preliminary Column Tests #1 to #7

The preliminary column tests described in Chapter 4 were important in developing the methodology used for column tests #8 to #11. Horizontal column tests are most often used (Klute and Dirksen, 1986; Brown and McWhorter, 1990; Brown and Allred, 1992; Allred, 1995) to study water movement and transport of relatively conservative contaminants in unsaturated soil. Limited use of horizontal tests for multi-phase and biodegradable contaminants was found in the literature. Extending the unsaturated horizontal column tests to toluene required solving several challenges: volatile loss from column leaks, adsorption by the column, prevention of biodegradation, prevention of chemical loss during and after sample collection, preparing injection solution at the same concentration level for each test and controlling the initial moisture during column packing to attain a similar initial moisture content from test-to-test. The first seven column tests produced relatively little usable data for this chapter, but they were invaluable in developing the methods and procedures used in analyzing column tests #8 through #11.

Column Tests #8 to #11

Methods and procedures for column tests #8 through #11 are discussed in Chapter 4 and only a brief description is given here. Each column test had toluene solution injected at a constant inlet moisture potential for the following lengths-of-time: 6 hours for test #8, 12 hours for test #9, 24 hours for test #10 and 12 hours for test #11. During test #9 one of the four glass syringes holding the injection solution broke at 5.7 hours into

the twelve hour test. The boundary condition at the inlet changed after the syringe broke, and the moisture potential at the inlet decreased after 5.7 hours. The gas phase data collected for test #9 showed similar trends to the other tests for the first 5.7 hours and after that it was not comparable. Test #9 was run to completion and destructively sampled to check moisture and toluene mass balances. Since the boundary conditions were violated for column test #9, it was difficult to compare its results against the other column tests, and the remainder of the chapter concentrates on the results of tests #8, #10 and #11. Table 5-4 lists column test data, moisture recovery and toluene recovery for all four tests.

Table 5-4 shows that the packing density was the same for each test. The initial moisture contents were similar for tests #8, #9 and #11, but that of test #10 was slightly lower. The final moisture contents at the inlet were similar for tests #9, #10 and #11 with that of test #8 slightly higher. The toluene injection concentrations for all tests were within the linear range. Injection concentration was close to the same for tests #9, #10 and #11, but approximately 23% higher for column test #8.

Moisture recovery and total toluene recovery were calculated from relatively small samples taken at points along the column. Moisture recovery was excellent, ranging from 97% to 103% for the four tests. Toluene recovery for the tests was very good with a range from 71% for test #10 to 94% for test #11 with tests #9 and #10 around 83% toluene recovery. Plots of the moisture and total concentration versus location along the column, or lambda, are not particularly smooth due to the fact that a small sample of soil represented a much larger volume for the mass balance calculations. The remainder of

this chapter discusses just tests #8, #10 and #11, and to make the narrative clearer, the tests are identified by their injection time duration of 6 hours, 12 hours or 24 hours respectively.

TABLE 5-4

Column† Test Data

Parameter	Test Number, Test Date, & Test Duration #8 5/21/93 6 hr	 #9 6/1/93 12 hr	 #10 7/21/93 24 hr	 #11 8/4/93 12 hr
Packing Density (g cm^{-3})	1.66	1.67	1.67	1.67
Theta Initial (cm^3 cm^{-3})	0.088	0.086	0.078	0.088
Theta Final (cm^3 cm^{-3})	0.268	0.240	0.247	0.249
Injection Solution Toluene Concentration (mg L^{-1})	86.6	68.9	69.2	70.4
Injection Volume (mL)	17.9	23.1	35.8	25.3
Toluene Mass Injected (mg)	1.56	1.59	2.47	1.78
Moisture Recovery‡ (%)	102.7	98.8	96.9	98.1
Toluene Recovery‡ (%)	82.9	82.7	70.9	93.5

† Column Dimensions (internal) - 4.0 cm diameter. by 61.3 cm in length
‡ Based on mass recovered divided by total mass within the column

Column Moisture Content and Moisture Recovery

Initial moisture content, final moisture content and mass recovery of moisture were important to test similarity and confidence in the test results. One advantage of the unsaturated horizontal column tests is that when all conditions (soil, packing density, moisture contents, injection concentration and boundary conditions) are similar, the

Boltzman Transformation allows direct comparison of tests conducted for different injection time lengths. Thus the horizontal column tests should have similar moisture versus lambda and concentration versus lambda curves.

Since each test was prepared independently of the others, maintaining similarity required careful preparation. The same batch of soil was used for all tests, and the packing density for all tests was the same. Initial moisture content was determined by averaging the moisture values beyond the wetting front. The initial moisture content of the 6 hour and 12 hour tests was the same at 0.088 mL of water per mL of soil with the 24 hour test at 0.078 mL mL^{-1} . At test conclusion moisture content at the inlet was 0.268, 0.249 and 0.247 mL mL^{-1} for the 6, 12 and 24 hour tests, respectively. Appendix F lists the moisture content data versus distance from the inlet and the transformed Boltzman variable (lambda). The normalized moisture content for each test was calculated by subtracting the initial moisture content from the moisture content at a sample site and then dividing this value by the difference of the inlet moisture content and the initial moisture content.

Figures 5-3a, 5-3b and 5-3c show water content versus distance, water content versus lambda and normalized water content versus lambda, respectively. The water content versus lambda curves look very similar for the 12 and 24 hour tests, but the 6 hour test has a higher moisture content at the inlet and through the wetting front. When the curves are normalized the 12 and 24 hour tests are even more similar with the 6 hour test still slightly higher. The curves are not smooth which may be due to the fact that a small point sample was analyzed to represent moisture content of a large soil volume.

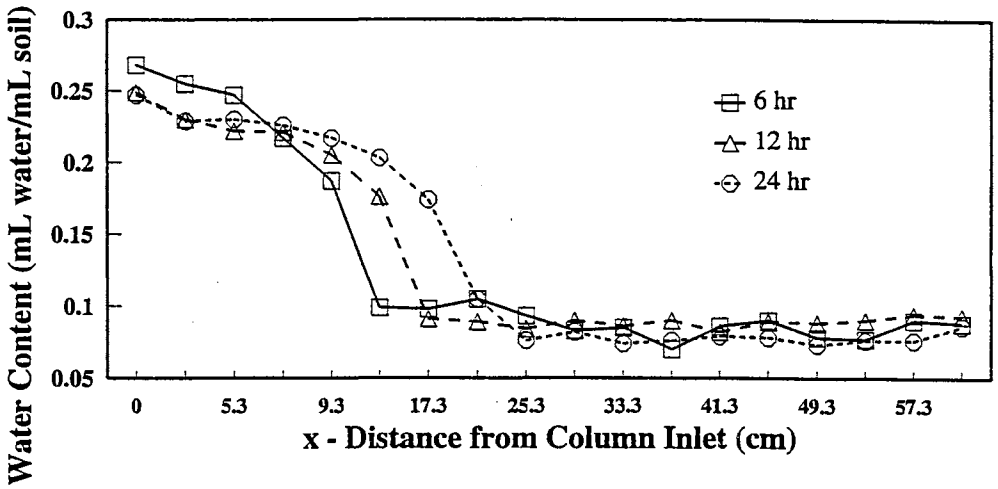

Figure 5-3a. Water content versus distance from the column inlet.

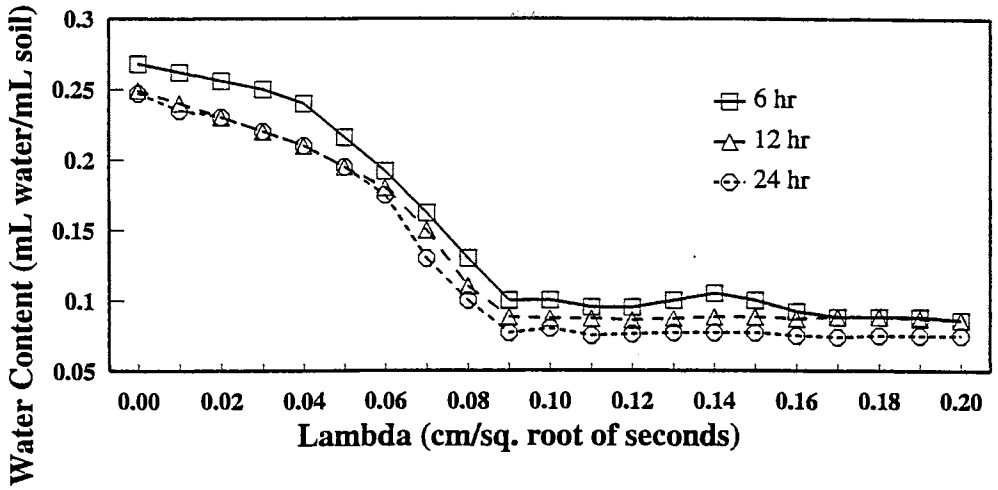

Figure 5-3b. Water content versus lambda.

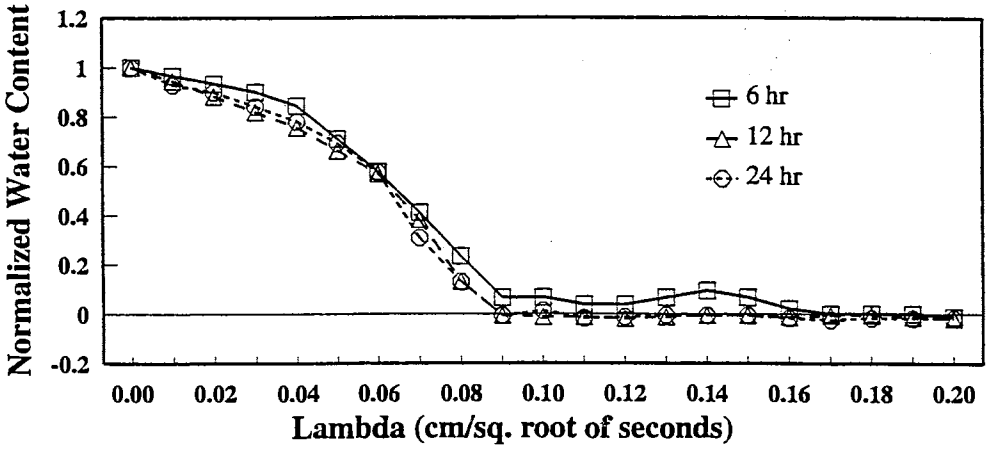

Figure 5-3c. Normalized water content versus lambda.

Figure 5-3a indicates that the wetting front advanced 13.3, 17.3 and 21.3 cm into the column for the 6, 12 and 24 hour tests, respectively. In Figure 5-3b the wetting front reached a lambda value of 0.09 cm per square root of seconds for all tests. Assuming a piston displacement by the injected liquid, the maximum extent of the injected water would occur at a lambda value of approximately 0.04 for all tests. Both gas and total phase toluene were analyzed well beyond the 0.04 lambda value.

Appendix G lists the data for the moisture recovery determination for each test. The moisture mass balance was determined using the point sample results and an average ends calculation method to determine the moisture within a section of the soil column. Moisture recovery was excellent for the 6, 12 and 24 hour tests with 102.7%, 98.1% and 96.9%, respectively. The moisture results were important for quality control (mass recovery) and assessing statistical similarity among the tests

The moisture values at each sampling distance along with the packing density and injection volume can be used to calculate the actual sorptivity value for each test. Based upon a 0.01 N calcium sulfate solution and an anticipated initial moisture content of 0.10 mL mL^{-1} with a final moisture content of 0.25 mL mL^{-1}, the expected sorptivity was calculated to be 0.00968 cm per square root of seconds. Actual sorptivity values were 0.015, 0.0085 and 0.00939 cm per square root of seconds for the 6, 12 and 24 hour tests, respectively. The large difference in the expected and actual 6 hour test sorptivity values makes it appear that the 6 hour test was not conducted close to the anticipated moisture levels. Since the actual sorptivity values are based on the point samples for the 12 and 24 hour tests the difference between anticipated and actual is inconclusive.

Total Toluene Content and Toluene Mass Recovery

Total toluene within the column was determined immediately upon test conclusion by removing a small soil sample from the same location used for the moisture samples. These samples had total toluene extracted using hexane as described in Chapter 4. Appendix H lists the toluene mass recovered at a each sampling site and the mass recovered between two sample sites. The total toluene mass between two sites was summed to determine mass recovered. Mass of toluene injected was determined by multiplying the injection volume by the solution concentration. Recovery of toluene mass was 82.9%, 93.5% and 70.9% for the 6, 12 and 24 hour tests, respectively. Figures 5-4a and 5-4b show total concentration versus distance and lambda.

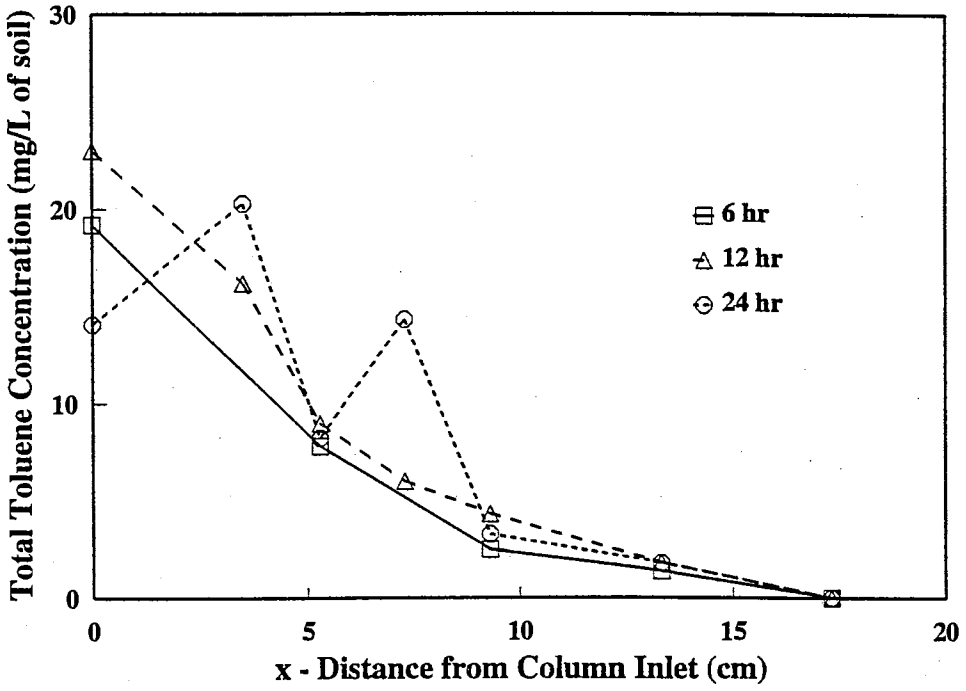

Figure 5-4a. Total toluene concentration versus distance from inlet.

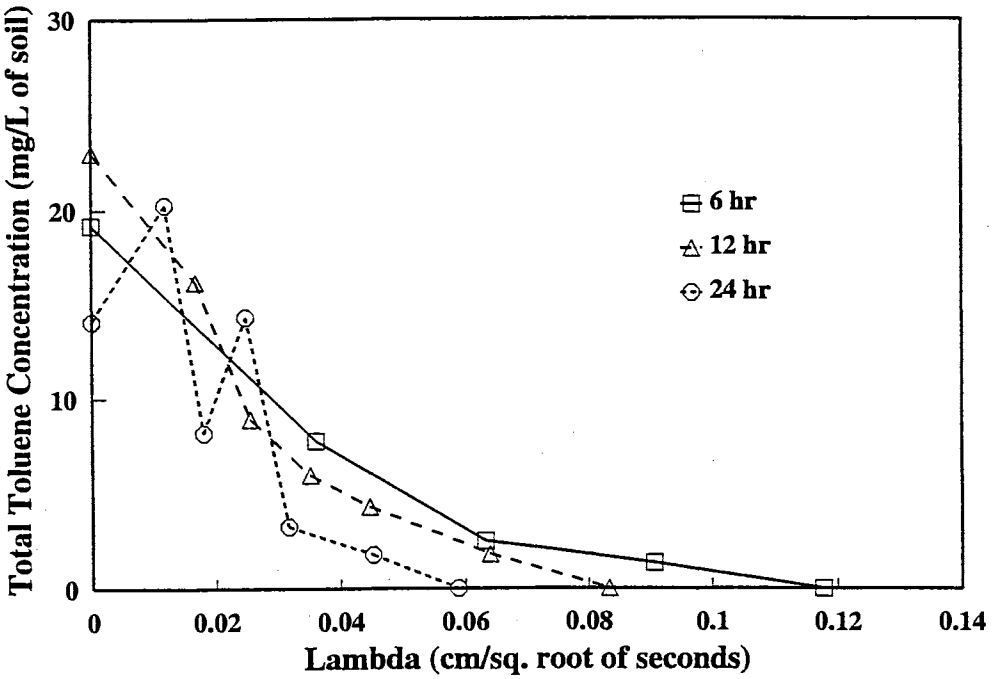

Figure 5-4b. Total toluene concentration versus lambda.

The recovery for the 6 and 12 hour tests was excellent, and the 70.9% recovery for the 24 hour test is good for toluene. Similar to the moisture data, the curves are not smooth due to small samples representing a much larger volume. As explained in Chapter 4 loss of toluene by exposure to the air was a significant concern. It was impossible to section the column and collect larger soil samples without significant toluene losses. A compromise was required, and rapid removal of a small soil volume with immediate placement in a vial with hexane was used. The sensitivity limit of the extraction method was slightly less than 1.5 mg of toluene per liter of in-place soil, which meant that samples beyond the wetting front were below the analysis limit. The curve for the 24 hour test is particularly noisy and uneven, and this may be part of the reason for the lower recovery than the other two tests. .The total toluene samples were only used as quality control values. High recovery gave confidence that factors such as leaks,

biodegradation and adsorption on the column materials were not skewing the results of the toluene gas samples.

Toluene Gas Phase Concentration versus Distance and Lambda

Toluene gas phase samples were collected periodically along the length of the column throughout a test and analyzed immediately using the GC. A total of 56, 63 and 79 gas samples had measurable toluene for the 6, 12 and 24 hour tests, respectively. Since the samples were collected and analyzed in real time they were valuable in determining the equilibrium status within the column. Appendix I lists the gas phase concentration at a location, its time of collection and its respective lambda value for the 6, 12 and 24 hour column tests.

Figure 5-5a shows the data from Appendix I for gas concentration versus lambda, and Figure 5-5b shows the same data using the log of gas concentration. The log of toluene gas concentration versus lambda was modeled by linear regression of the data for each test, and the fitted values plotted as lines on Figure 5-5a. The fitted equations are discussed in more detail in the next section. All of the data collected were modeled except for samples without measurable toluene gas and obvious outlier results due to plugged syringe needles or incomplete samples. As the profile became wetter, the soil air was less continuous and sometimes a sample pulled a partial vacuum and was not complete. In general there were only a few outliers in each test with plugged needles the most common cause.

The curves in Figures 5-5a and 5-5b clearly show diffusion of the gas phase. This is also seen in Figures 5-6a, b and c showing number of gas samples collected and

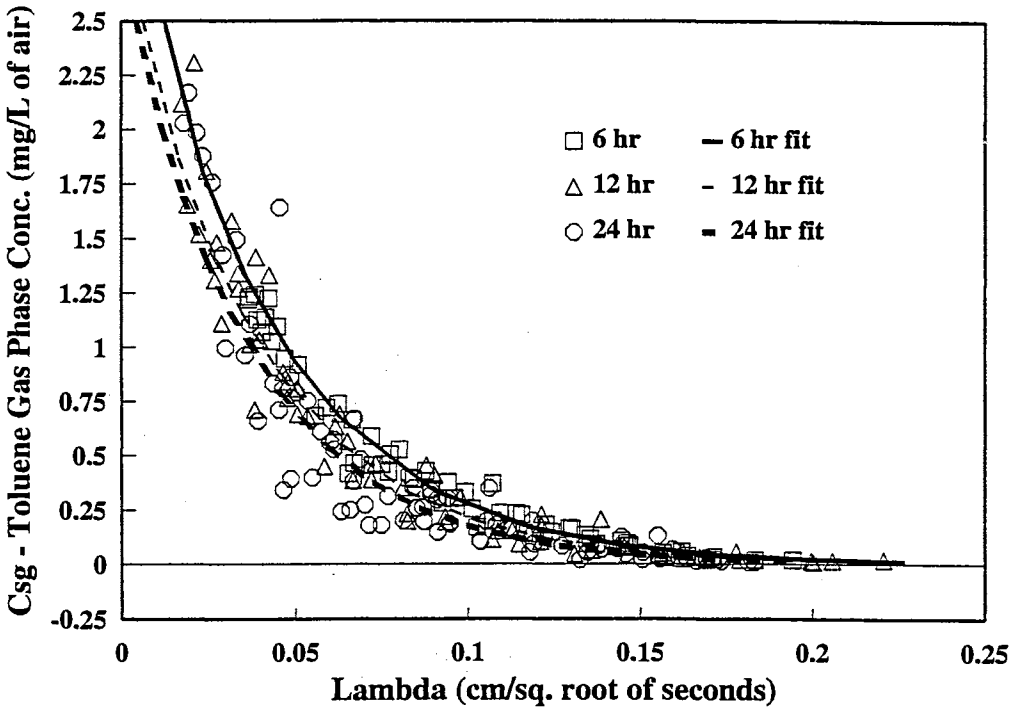

Figure 5-5a. Toluene gas phase concentration versus lambda.

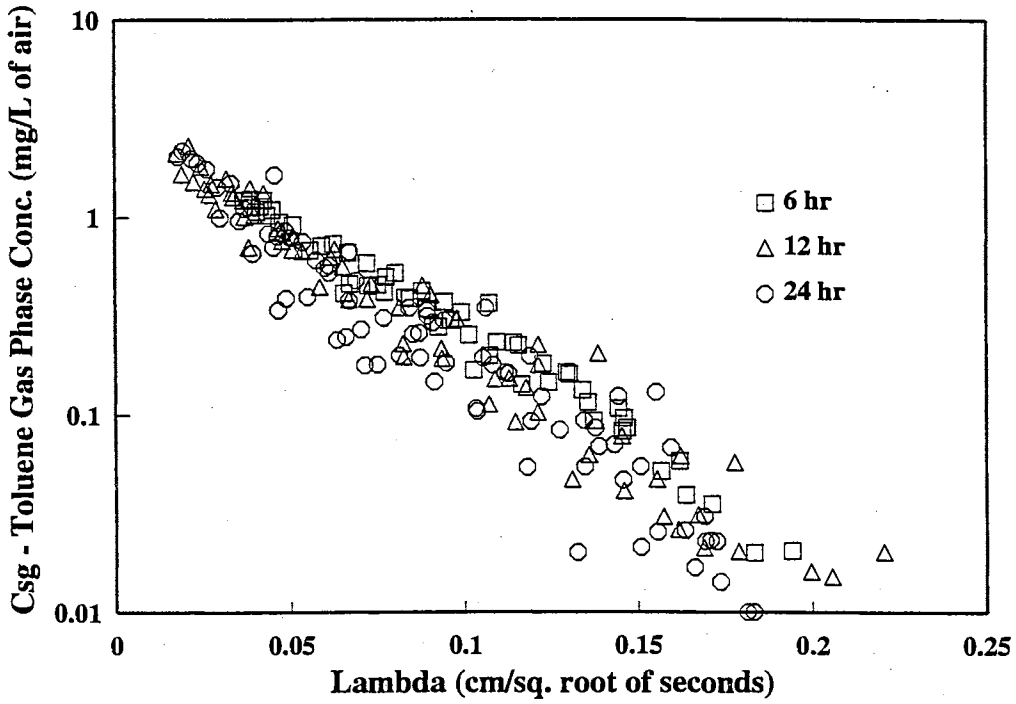

Figure 5-5b. Log of toluene gas phase concentration versus lambda.

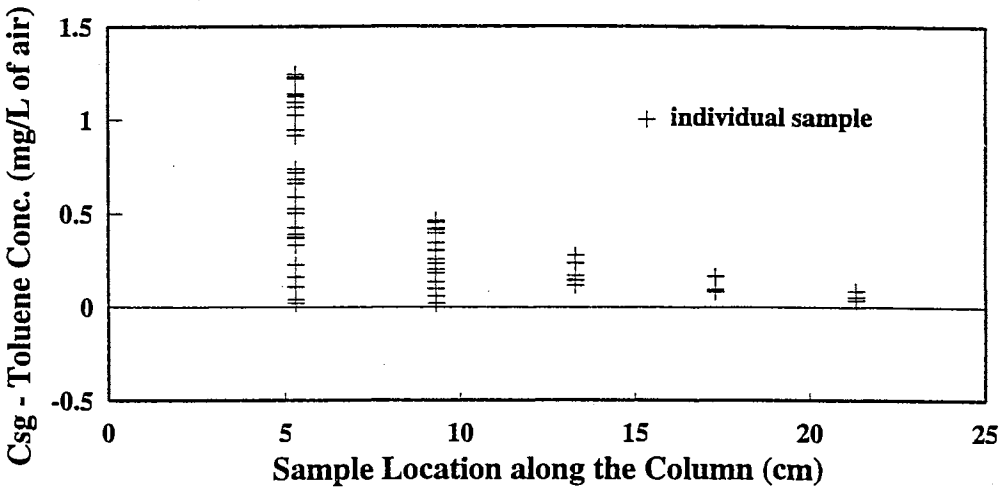

Figure 5-6a. Individual toluene gas samples collected during 6 hr test.

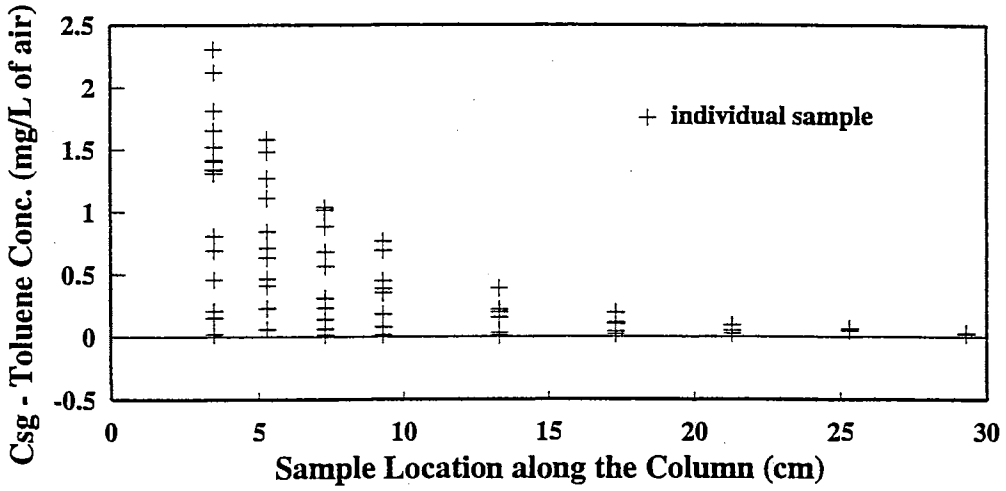

Figure 5-6b. Individual toluene gas samples collected during 12 hr test.

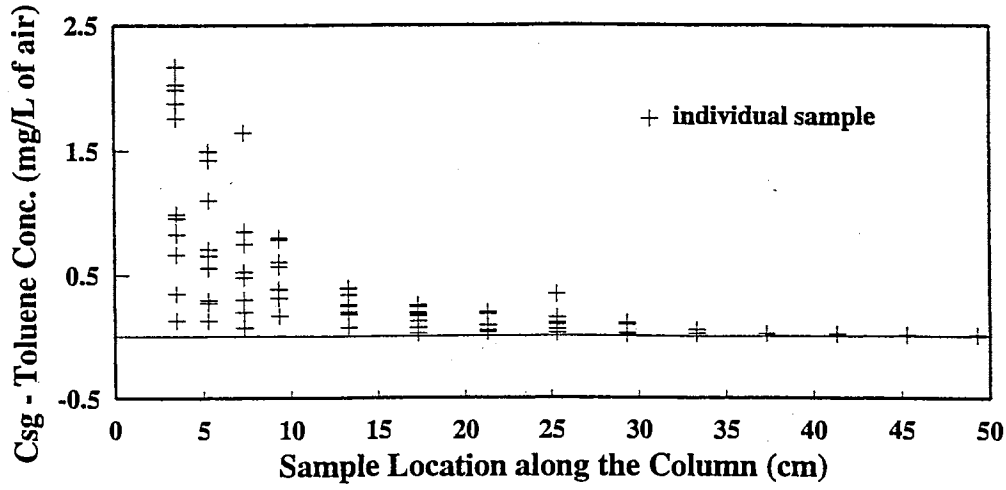

Figure 5-6c. Individual toluene gas samples collected during 24 hr test.

concentration collected at each site along the column length for the 6, 12 and 24 hour test, respectively. The data clearly shows how far ahead of the wetting front the gas phase was found. The wetting front of each test advanced to a lambda value of approximately 0.09, and in all tests the gas phase toluene was found at measurable concentrations at lambda values of 0.20. Therefore the gas phase toluene traveled twice as far into the soil column as the water. Although the gas concentrations ahead of the wetting front were low, they still resulted in significant spreading of the toluene plume, contaminating a much larger soil volume than by liquid advection and dispersion alone.

Linear Regression of Gas Phase Concentration versus Lambda

The gas phase data in Appendix I was broken into different time increments and evaluated by linear regression on the log of C_{sg} versus lambda from the beginning of a test until the interim time period. The results of one test are compared against the same period for a different test. Appendix J contains the regression output data for the fitted toluene gas phase curves, and Table 5-5 lists the fitted gas phase equations for the different time increments of each test.

The R-squared values for the fitted equations are very good with only the 0.87 value for increment 24a below 0.90. The rest of the R-squared values for the equations in Table 5-5 are around 0.94 to 0.95. The values for the first six hours of the 24 hour test (24a and 24b) both are considerably lower than the 6 and 12 hour tests. This is an artifact created by sampling. Most of the sampling during the first 6 hours of the 24 hour test tracked the leading edge of the gas front. At the conclusion of each test (increment 6b,

12d and 24f), the 12 and 24 hour tests are similar, as can be seen in Figure 5-5a. The 6 hour test is not similar to either the 12 or 24 hour test.

TABLE 5-5

Fitted Gas Phase Equations for the 6, 12 and 24 Hour Tests

Increment Symbol	Time Incr. (hr)	Fitted Equation Toluene Gas Phase, Csg = 6 hr	12 hr	24 hr
6a, 12a, 24a†	0 to 3	$3.11(10)^{-11.24\lambda}$	$3.50(10)^{-11.31\lambda}$	$2.27(10)^{-9.66\lambda}$
6b, 12b, 24b	0 to 6	$3.29(10)^{-10.96\lambda}$	$3.05(10)^{-11.27\lambda}$	$2.45(10)^{-10.41\lambda}$
12c, 24c	0 to 9		$3.01(10)^{-11.43\lambda}$	$3.02(10)^{-11.58\lambda}$
12d, 24d	0 to 12		$2.90(10)^{-11.38\lambda}$	$3.02(10)^{-11.71\lambda}$
24e	0 to 18			$2.97(10)^{-12.00\lambda}$
24f	0 to 24			$2.79(10)^{-12.05\lambda}$

† 6a represents the 6 hour test data for the increment (a) from 0 to 3 hours, with 12a the 12 hour test from 0 to 3 hours and 24a the 24 hour test from 0 to 3 hr

Paired Sample Statistical Analysis of the Moisture Data

One advantage of using unsaturated horizontal column tests is that tests conducted for different duration time periods can be compared. If the physical conditions (soil type, soil density, initial moisture content, inlet moisture potential, etc.) are similar and the test boundary conditions are not violated, then plots of moisture content versus the Boltzman variable lambda should be similar for each. Also if LPE is present, it follows that the plots of concentration versus lambda should be similar. Figures 5-3c, 5-4b and 5-5a show the normalized moisture, total toluene concentration and toluene gas phase concentration versus lambda, respectively. The moisture curves appear similar but both total and gas phase concentration versus lambda are noisy and difficult to evaluate by appearance

alone. Therefore another method of evaluating test similarity other than by appearance is required for the experimental data.

Snedecor and Cochran (1980) in their text present methods to statistically compare two paired samples or two independent samples, and the horizontal column tests fit the paired test requirements. Snedecor's and Cochran's (1980) paired test uses the following relationships to compare paired values such as moisture from two different tests where both have the same value of lambda:

$$Dm = \sum_{i=1}^{n} \frac{D_i}{n} , \tag{5-3}$$

and

$$D_i = \theta_{1i} - \theta_{2i} . \tag{5-4}$$

The terms are defined as follows: Dm the mean sample difference, n the number of paired comparisons, D_i the difference between the paired values, θ_{1i} the moisture value from one test at a given lambda value and θ_{2i} the moisture value from the second test at the same lambda value. The hypothesis that there is no difference between results due to test physical conditions (soil type, soil density, initial moisture content, inlet moisture potential, etc.) and equilibrium status is rejected if:

$$\left|\frac{Dm}{SDm}\right| \geq \hat{t}_{1-\alpha/2,n-1} , \tag{5-5}$$

where SDm is the standard deviation of D_i, $\hat{t}$ the Student t distribution value and α the significance level.

The paired comparison was done on the normalized moisture content at test conclusion for the 6, 12 and 24 hour tests. The normalized moisture content was used instead of the actual moisture content to counteract bias from the greater number of samples beyond the wetting front. The small soil moisture samples gave a noisy baseline

for initial moisture content, but normalizing the data muted its effect on the paired analysis. The results of the paired analyses for moisture are listed in Appendix K and compiled in Table 5-6. The null hypothesis was rejected for the 6 hour test compared to either the 12 hour or 24 hour test and it was accepted for the 12 hour test compared to the 24 hour test. This meant that the 12 hour and 24 hour tests were considered not statistically different at a 5% significance level, but the 6 hour test was statistically different from either the 12 hour or 24 hour test.

TABLE 5-6

Paired Test Results for Theta versus Lambda

Paired Tests Compared	n	Dm	Test Statistic	t-statistic	Ho Accepted	t-test Probability
6b vs 12d	21	0.048	6.63	2.08	no	1E-06
6b vs 24f	21	0.048	6.95	2.08	no	7E-07
12d vs 24f	21	0.013	-0.05	2.08	yes	0.957

Liquid to Solid Net Phase Transfer Non-equilibrium (*P*) versus Lambda

In Chapter 3 two non-equilibrium phase terms were defined and a mathematical relationship developed for each using LPE theory, transport equations and the Boltzman Transformation. One term was considered an adsorption functional relationship where the net phase non-equilibrium for toluene going from the liquid phase to the adsorbed phase was defined and represented as *P*. The mathematical relationship for *P* is given by Equation 3-62 in Chapter 3. Values of *P* were calculated directly using partitioning coefficients, the fitted gas phase equations in Table 5-5 and theta values at specific

lambda values extrapolated using Figure 5-3b. Table 5-7 lists the constants and their values.

TABLE 5-7

Constants used in Calculations for 6, 12 and 24 Hour Tests

Parameter	Symbol	Value	Units
Dry bulk density	ρ_b	1.67	g cm^{-3}
Porosity	ϕ	0.37	cm^3 cm^{-3}
Henry coefficient	K_H	0.27	------
Linear Adsorption coef.	K_d	0.43	mL g^{-1}
Sorptivity	S	0.00968	cm $seconds^{-0.5}$
Toluene gas diffusion in air	$D_{g(air)}$	0.076	cm^2 $second^{-1}$

Appendix L lists the calculated values of *P* versus lambda for the fitted gas phase transport interim time period equations listed in Table 5-5. Figure 5-7a shows the net mass transfer non-equilibrium value (*P*) in units of mg of toluene per liter of soil water plotted against lambda at the completion of the 6, 12 and 24 hour tests. The *P* values for Figure 5-7a were multiplied by moisture content corresponding to a lambda value to convert *P* into mg of toluene per liter of in-place soil. Figure 5-7b shows the information after it has been normalized to a representative volume (RVE). The values for the 12 and 24 hour tests match well, but the 6 hour test is slightly different. Figures 5-8, 5-9 and 5-10 show plots of *P* versus lambda (not normalized to a RVE) for all time periods of the 6, 12 and 24 hour tests, respectively. Figure 5-11 shows all time periods for the three

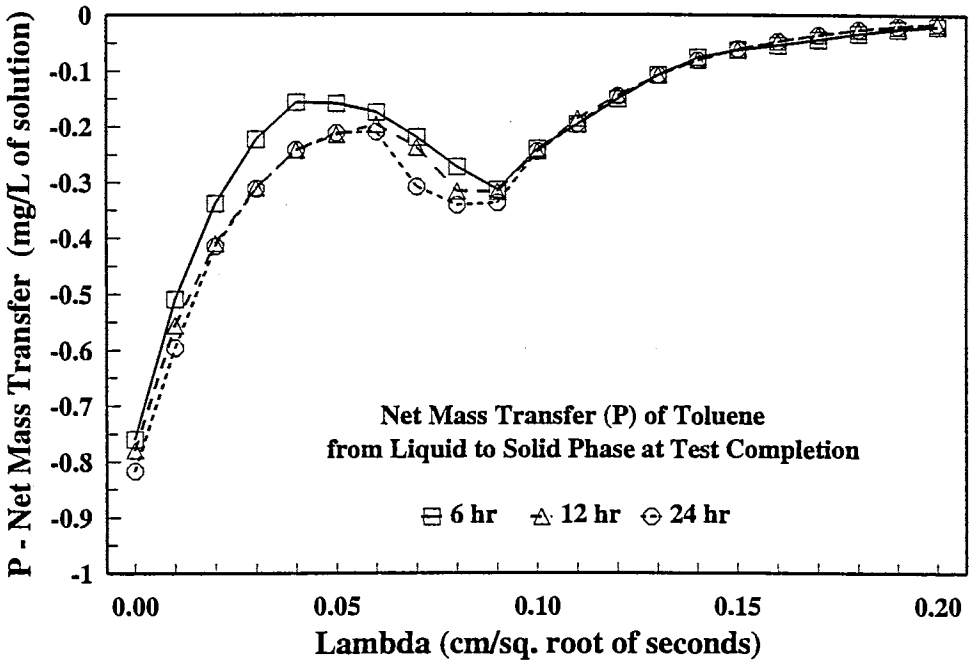

Figure 5-7a. Net mass transfer of toluene from liquid to solid phase at completion of 6, 12 and 24 hour tests.

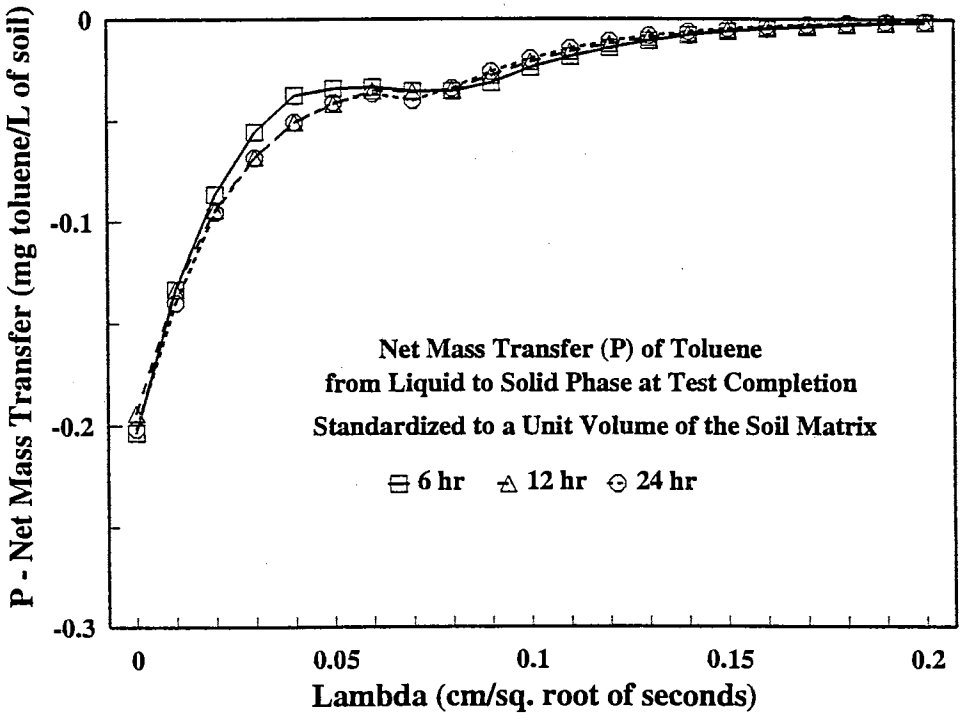

Figure 5-7b. Net mass transfer of toluene from liquid to solid phase standardized to a unit volume of in-place soil at completion of 6, 12 and 24 hour tests.

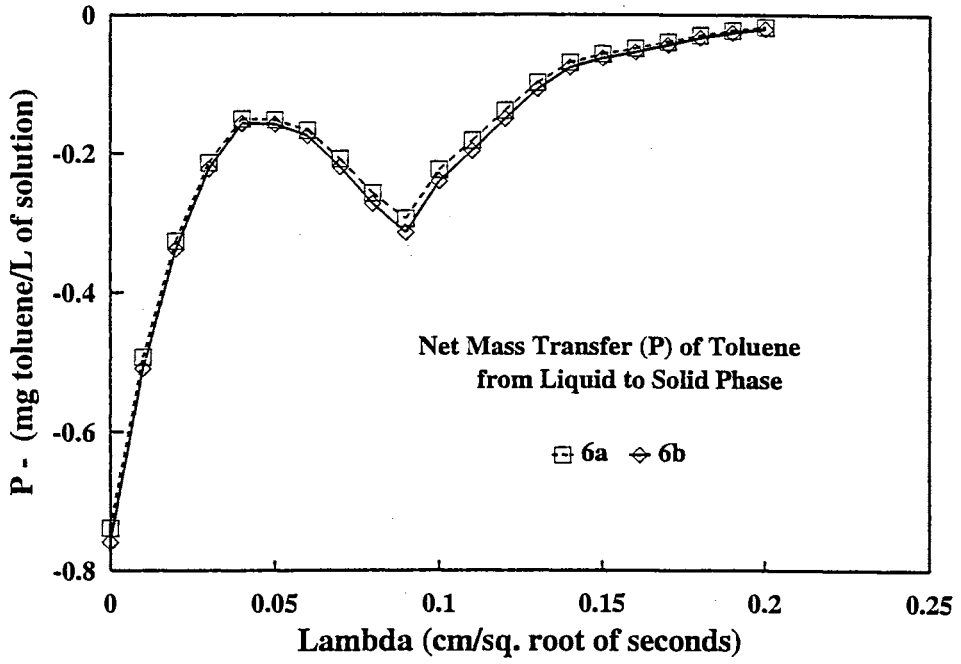

Figure 5-8. Net mass transfer of toluene from liquid to solid phase for segments of the 6 hour test.

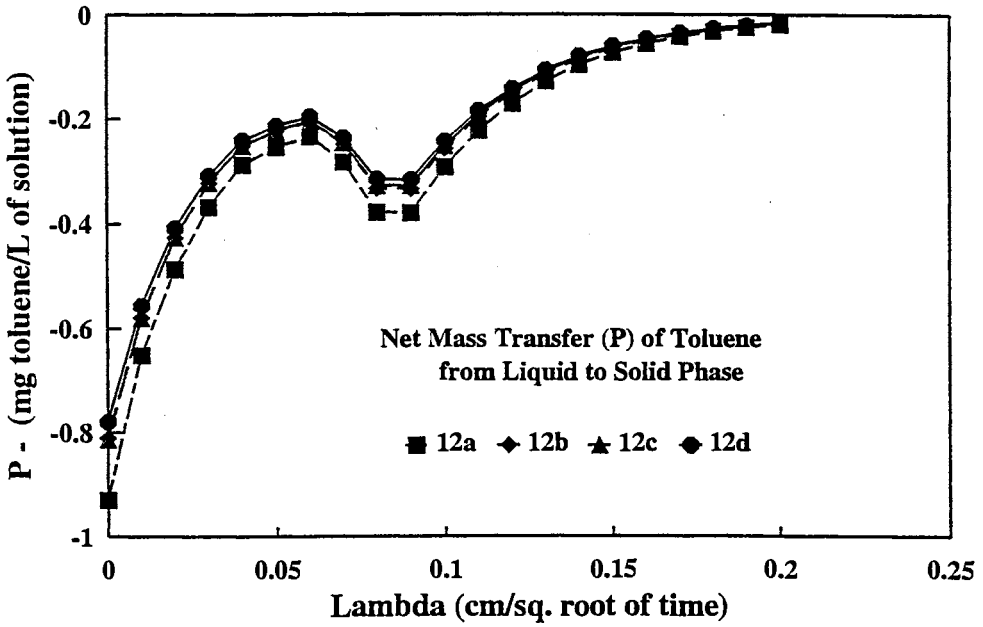

Figure 5-9. Net mass transfer of toluene from liquid to solid phase for segments of the 12 hour test.

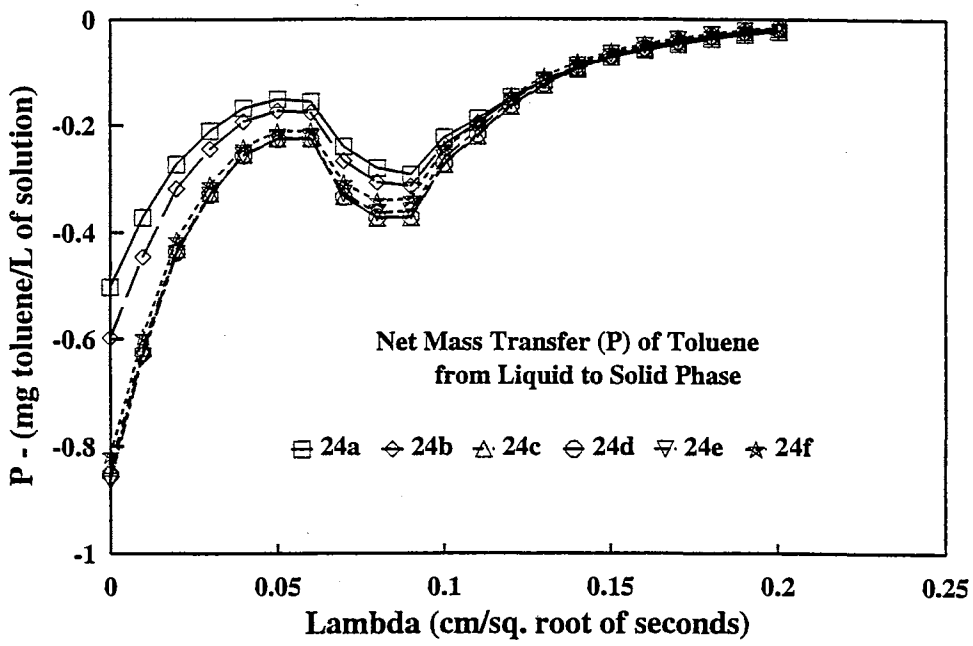

Figure 5-10. Net mass transfer of toluene from liquid to solid phase for segments of the 24 hour test.

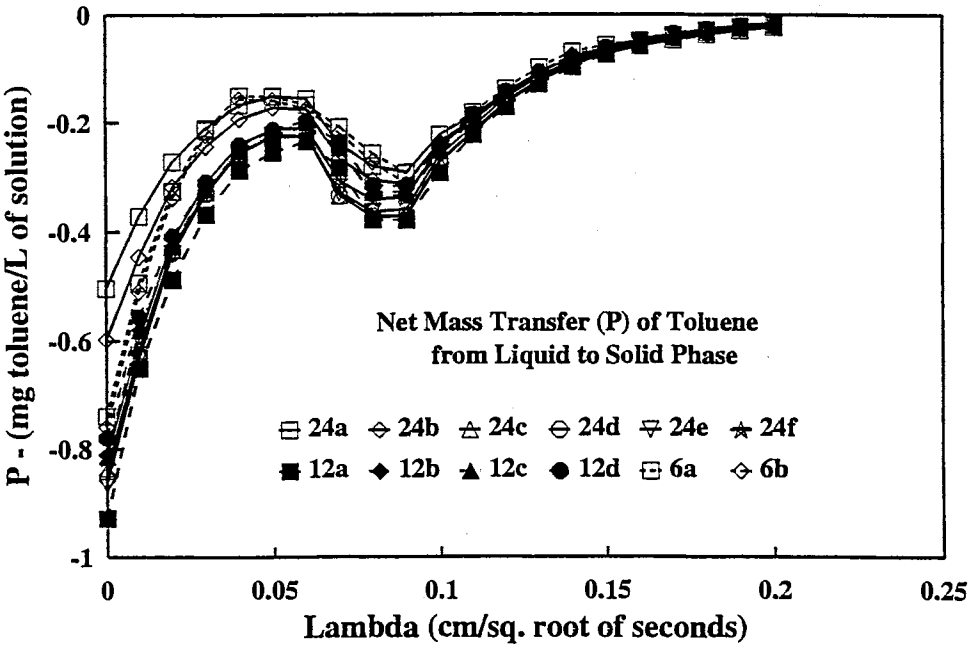

Figure 5-11. Net mass transfer of toluene from liquid to solid phase for segments of all tests.

tests on the same plot and it shows that all interim time periods are close in value except for 0 to 3 hr and 0 to 6 hours periods. The plot of P versus lambda by itself is not enough to quantify equilibrium status within the column.

Variance of Solid Phase Adsorption from Equilibrium (Δ) versus Lambda

In Chapter 3 the non-equilibrium phase term for the variance of solid phase adsorption was considered a disequilibrium functional relationship where the net phase non-equilibrium for toluene going from the adsorbed phase to the liquid phase was defined and represented as Δ. The mathematical relationship in Equation 3-63 was determined using LPE theory, transport equations and the Boltzman Transformation. The mathematical relationship in Equation 3-63 can not be used to calculate Δ directly since Δ is within the differential. Equation 3-63 can be solved numerically using the boundary conditions for Δ, or integrated to find if an analytic solution exists. An analytic solution was found for Equation 3-63 and the solution is given by Equations 3-66, 3-67 and 3-68 in Chapter 3. Using these equations, values for Δ were calculated directly using the constants in Table 5-7, the fitted gas phase equations in Table 5-5 and theta values extrapolated from Figure 5-3b.

Appendix M lists the calculated values of Δ versus lambda for fitted gas phase transport interim time period equations listed in Table 5-5. Figure 5-12 shows the variance of solid phase toluene adsorption (Δ) determined through integration in units of mg of toluene per gram of organic carbon plotted against lambda at the completion of the 6, 12 and 24 hour tests. Figure 5-13 shows the shows the same plot as Figure 5-12 but its

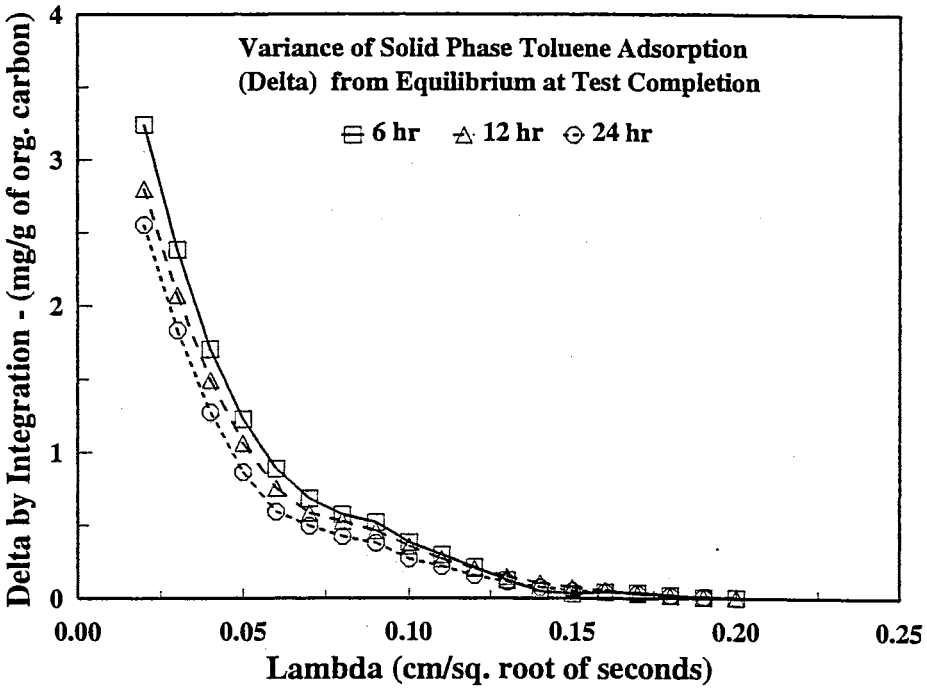

Figure 5-12. Toluene solid phase adsorption variance from equilibrium determined by integration at completion of 6, 12 and 24 hour tests.

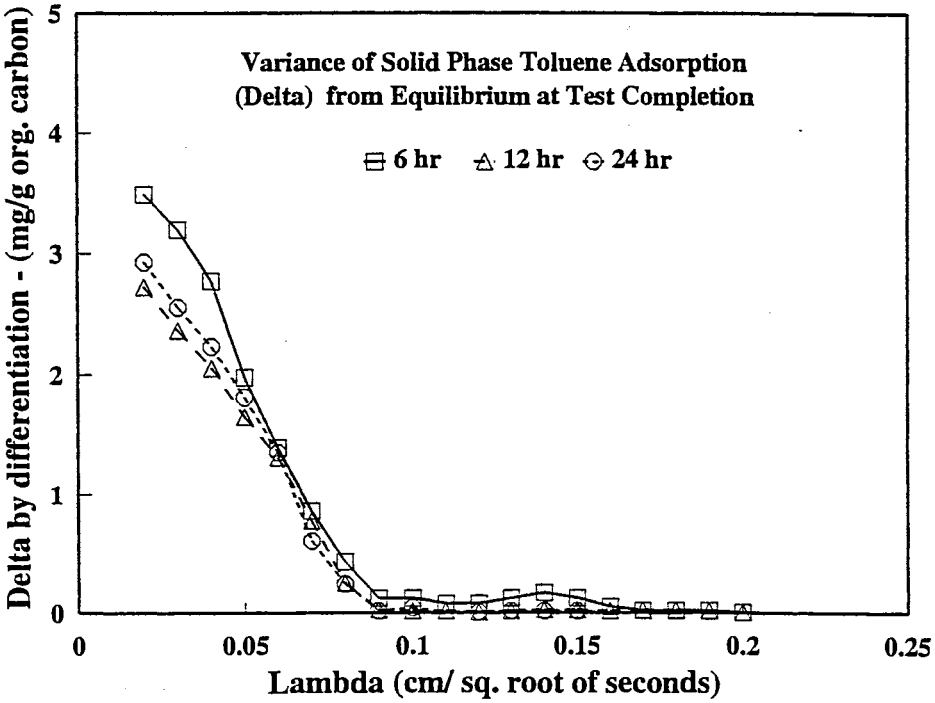

Figure 5-13. Toluene solid phase adsorption variance from equilibrium determined by differentiation at completion of 6, 12 and 24 hour tests.

values for Δ were determined by central-difference numeric methods for the differential relationship instead of using the analytic solution. The shape and magnitude of Δ versus λ in Figures 5-12 and 5-13 are in general agreement with each other, and this provides confidence in the accuracy of the integration.

As in the previous section for P, the Δ values were normalized to a RVE to convert them into mg of toluene per liter of in-place soil. The bulk density and the soil organic carbon content are constant and the actual Δ values were multiplied by

$$\Delta(\text{in mg/g})\left[\frac{1}{f_{oc}(\rho_b)}\right] = \Delta(\text{of a RVE}), \qquad \textbf{(5-6)}$$

where f_{oc} of the Teller loam equals 0.009 gram of organic carbon per gram of soil and ρ_b equals 1670 grams of soil per liter of in-place soil. Figure 5-14 shows the plot of Δ for a RVE versus lambda for the 6, 12 and 24 hour tests.

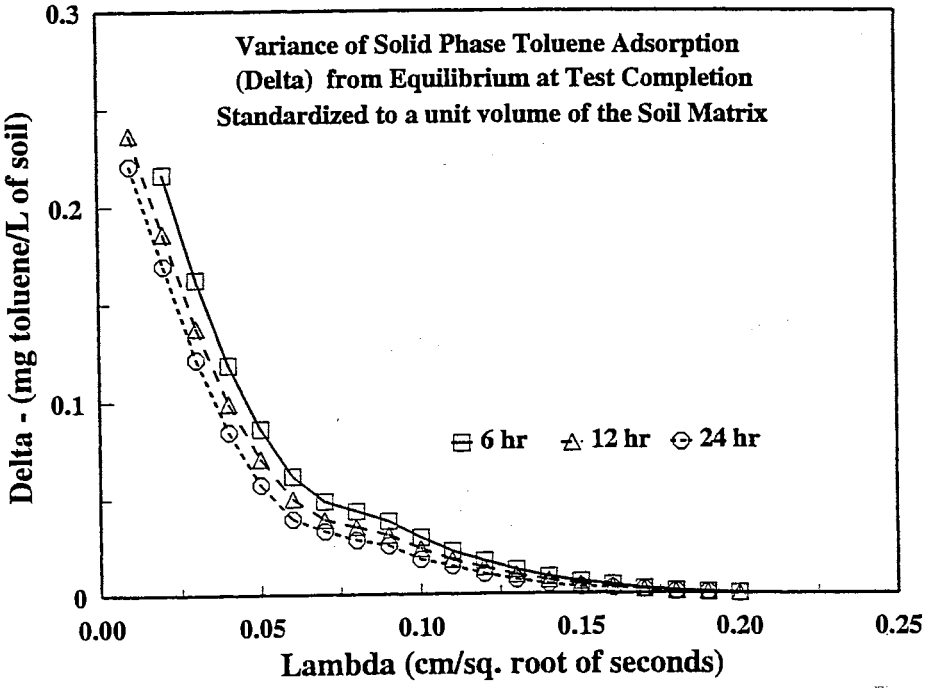

Figure 5-14. Toluene solid phase adsorption variance from equilibrium determined by integration and standardized to a unit volume of in-place soil for the 6, 12 and 24 hour tests.

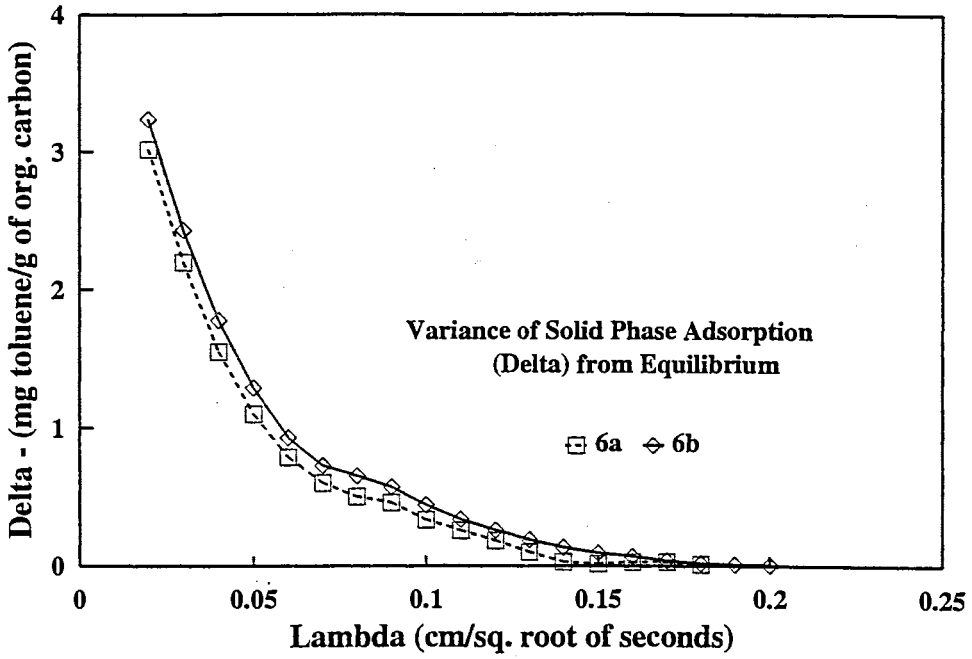

Figure 5-15. Toluene solid phase adsorption variance from equilibrium for segments of the 6 hour test.

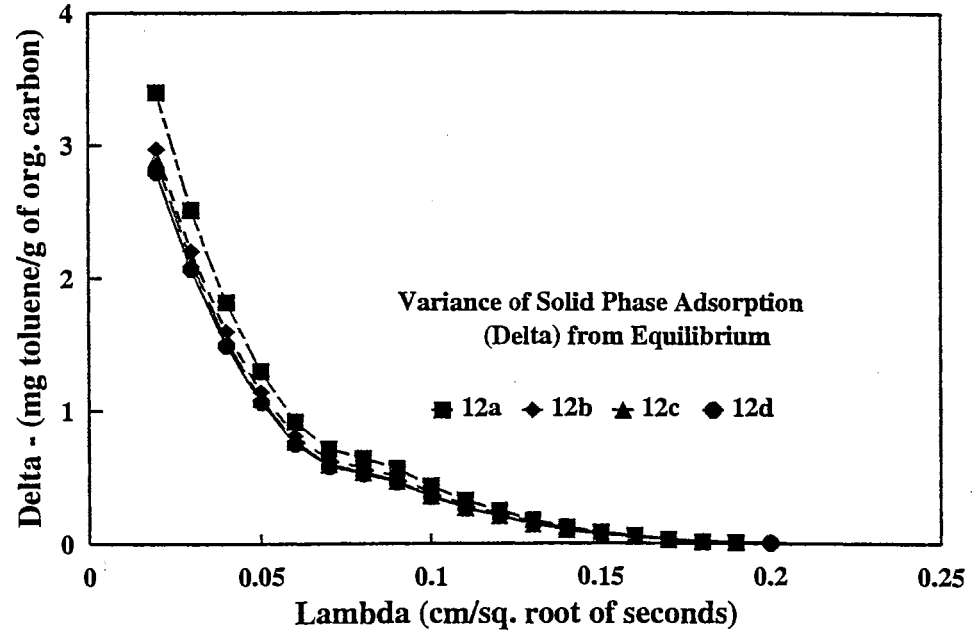

Figure 5-16. Toluene solid phase adsorption variance from equilibrium for segments of the 12 hour test.

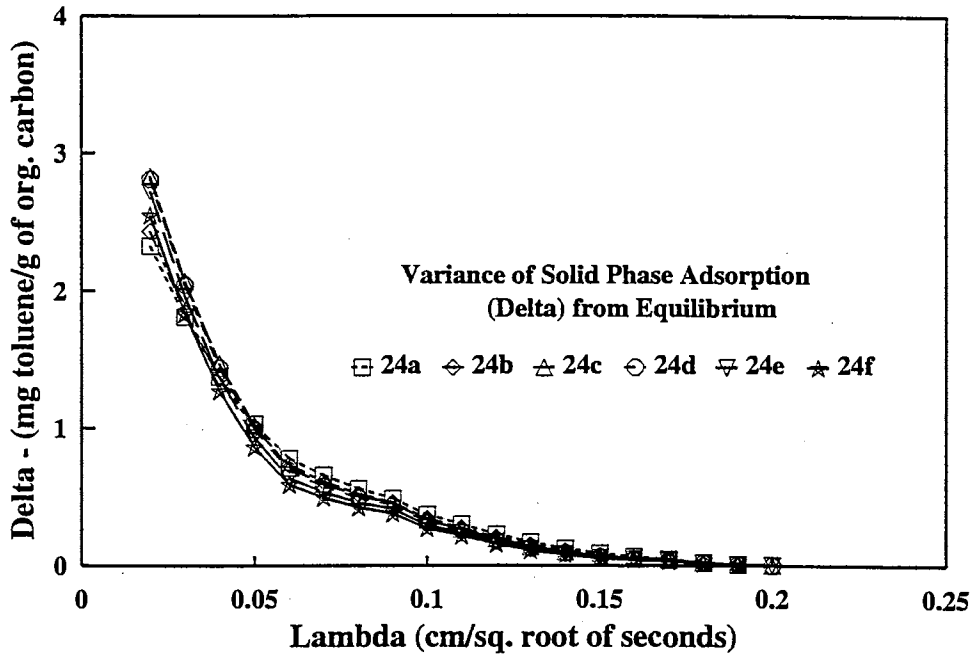

Figure 5-17. Toluene solid phase adsorption variance from equilibrium for segments of the 24 hour test.

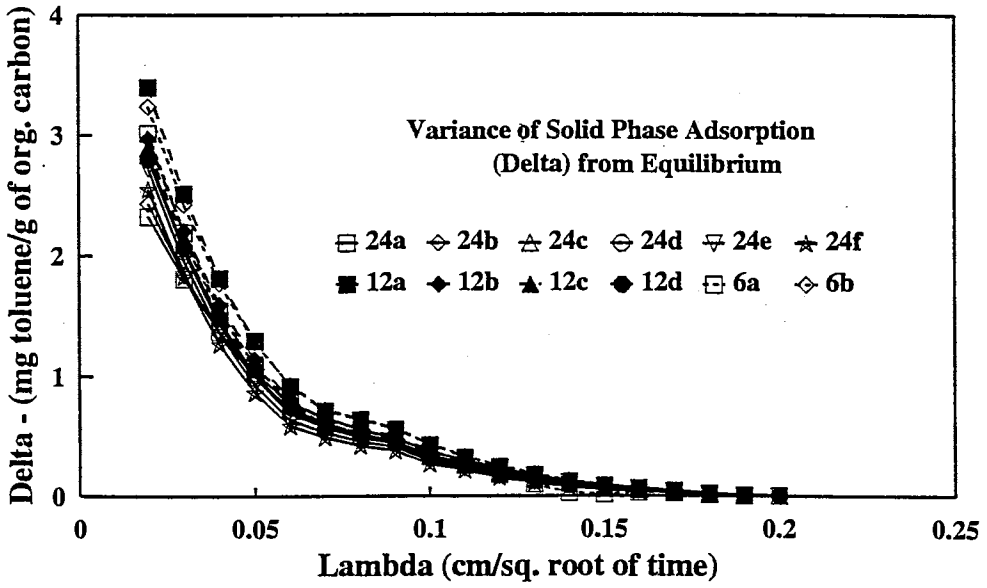

Figure 5-18. Toluene solid phase adsorption variance from equilibrium for segments of all tests.

Figures 5-15, 5-16 and 5-17 show plots of Δ versus lambda (not normalized to a RVE) for all time periods of the 6, 12 and 24 hour tests, respectively. Figure 5-18 shows all time periods for the three tests on the same plot.

Δ versus *P*

The Δ versus lambda curves in Figures 5-18 for the 6, 12 and 24 hour tests are similar, but it is difficult to make a conclusive observation about their equilibrium status. Another approach is to plot Δ and *P* values for the same lambda value against each other and see if it is more definitive. Appendix N lists the data for Δ versus *P*. Figures 5-19a and 5-19b show the plots for the 6, 12 and 24 hour test for the data as-calculated and for the values normalized to a RVE, respectively. The 12 and 24 hour plots are close together and the 6 hour test definitely appears to be at a different equilibrium status. The 12 and 24 hour tests were previously determined as statistically similar. The 6 hour test was significantly different from either the 12 or 24 hour test, so the difference in the plots may be a result of the 6 hour test being different. This is evaluated by breaking the tests into time periods as done for *P* and Δ versus lambda.

The results for the individual time periods are shown in Figures 5-20, 5-21 and 5-22 for the 6, 12 and 24 hour tests, respectively. Figure 5-23 shows all time periods for the three tests on the same plot. Figure 5-23 shows that the results for the first six hours of each test appear to be different from the other time periods after six hours. Even though the 6 hour test was significantly different from the other tests, its results tended to agree with the data for the first six hours of the 12 and 24 hour tests. Further

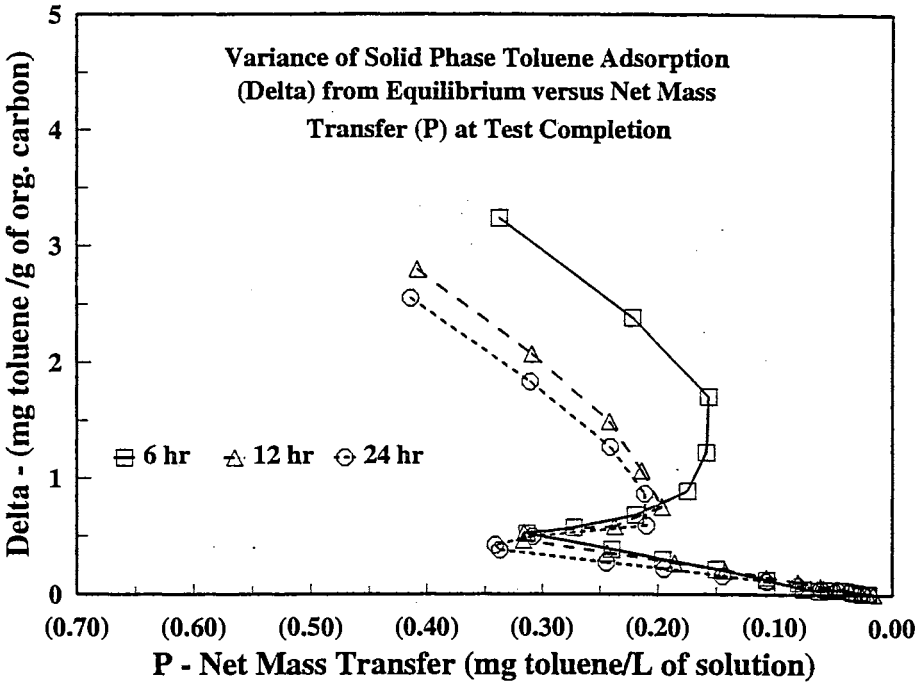

Figure 5-19a. Toluene solid phase adsorption variance from equilibrium versus net mass transfer from liquid to solid phase at completion of 6, 12 and 24 hour tests.

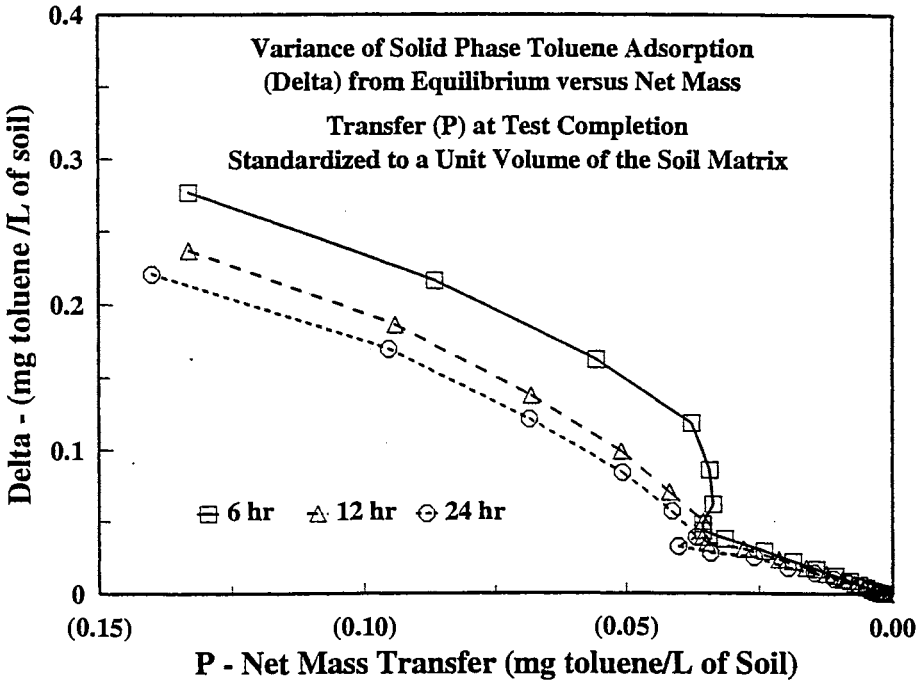

Figure 5-19b. Toluene solid phase adsorption variance from equilibrium versus net mass transfer from liquid to solid phase standardized to unit volume of in-place soil.

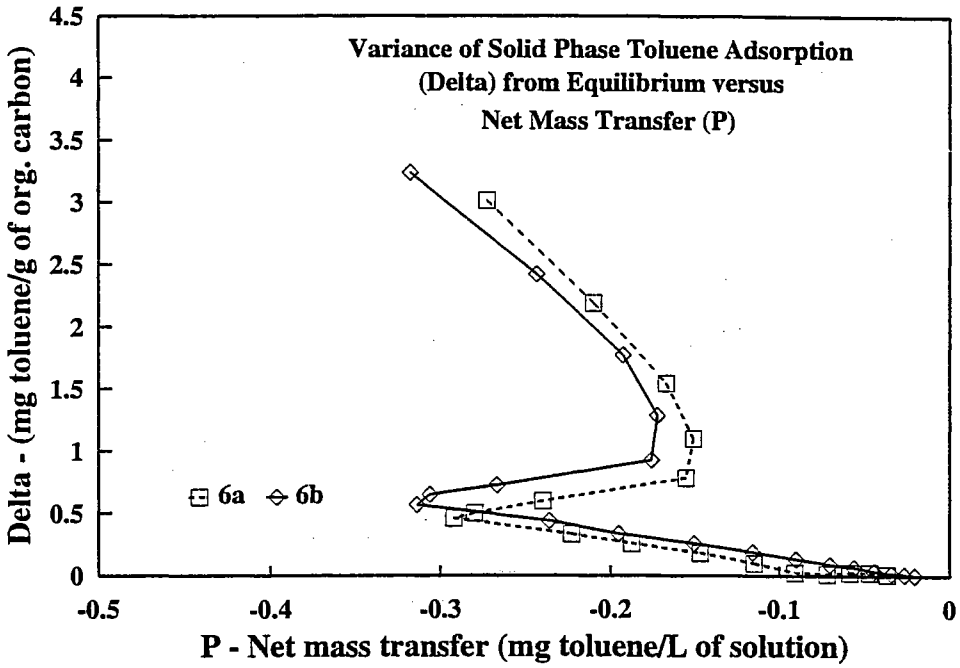

Figure 5-20. Toluene solid phase adsorption variance from equilibrium versus net mass transfer from liquid to solid phase for segments of the 6 hour test.

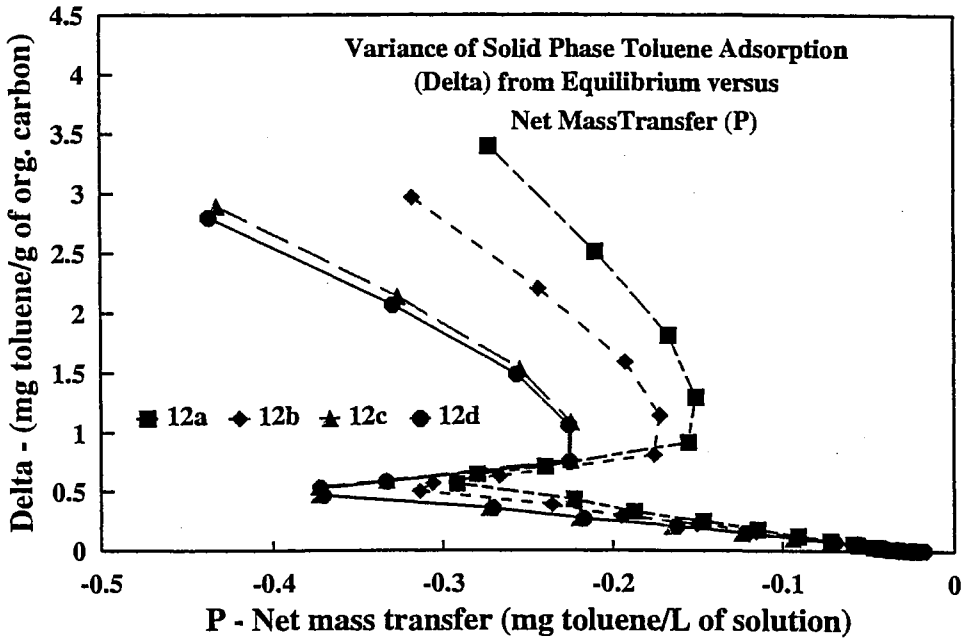

Figure 5-21. Toluene solid phase adsorption variance from equilibrium versus net mass transfer from liquid to solid phase for segments of the 12 hour test.

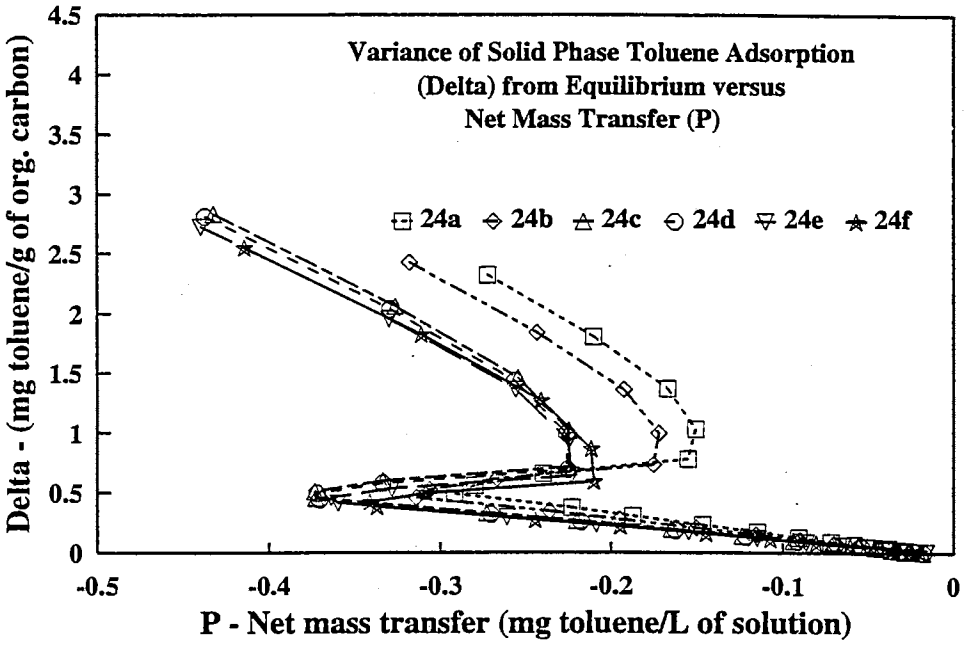

Figure 5-22. Toluene solid phase adsorption variance from equilibrium versus net mass transfer from liquid to solid phase for segments of the 24 hour test.

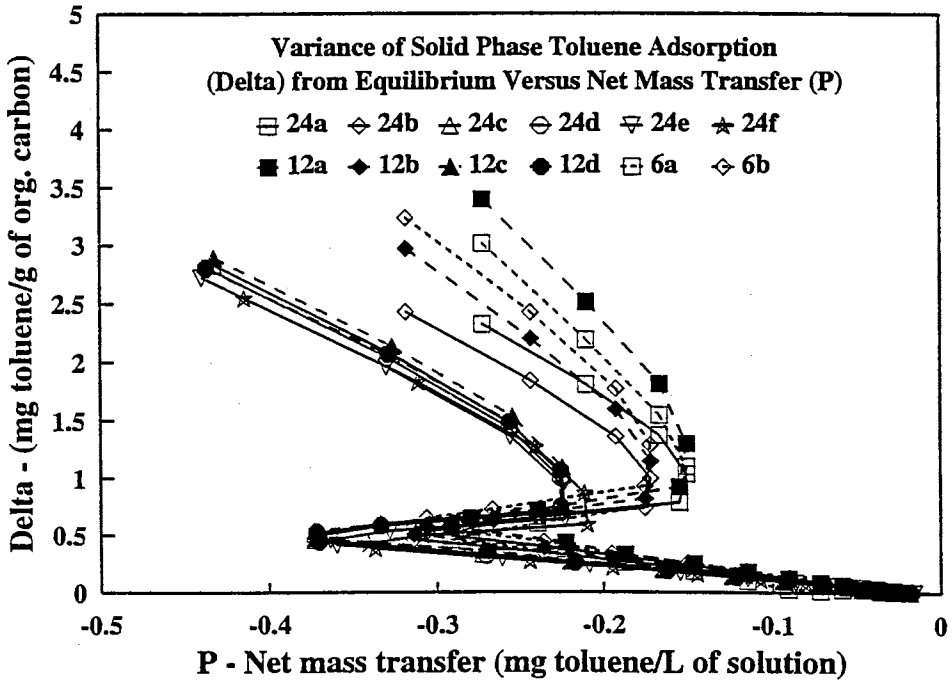

Figure 5-23. Toluene solid phase adsorption variance from equilibrium versus net mass transfer from liquid to solid phase for segments of all tests.

analysis of Figures 5-20 to 5-23 to quantify the equilibrium situation and statistical similarity of different time periods is difficult. A statistical evaluation is completed in the next section. The section following takes a slightly different approach to the equilibrium question.

Paired Sample Statistical Analysis of *P* and Δ

Paired sample statistical analysis was completed on *P* versus lambda, Δ versus lambda and Δ versus *P*, with the test results shown in Appendix O, Appendix P and Appendix Q, respectively. The paired test results are compiled in Appendix R for easier comparison. A high percentage of the statistical analysis on the calculated results for Δ and *P* fail the null hypothesis which means that they are significantly different at the 5% significance level. The values for Δ and *P* were calculated using fitted equations for the gas phase versus lambda and these equations fail the null hypothesis in a statistical analysis. It appears that the method of calculation biases the paired tests for Δ and *P* and a statistical analysis on the calculated non-equilibrium terms is of little value in determining similarity.

Net Non-equilibrium (*P* + Δ) versus Lambda

Both Δ and *P* are non-equilibrium terms calculated at values of lambda for the 6, 12 and 24 hour tests. As originally defined, their magnitude can not be compared except when normalized to a RVE; then their magnitudes are comparable. Figure 5-19b shows Δ

versus P for the normalized values. As this graph is difficult to evaluate, a different approach is needed. The introduction of the contaminant into the clean soil at the column inlet creates concentration gradients which drive the equilibrium. As time elapses, the effective gradient at the inlet would change. It stands to reason that the overall non-equilibrium status is changing also. What properly needs to be evaluated is a net non-equilibrium status represented as $\Delta + P$ for the column tests.

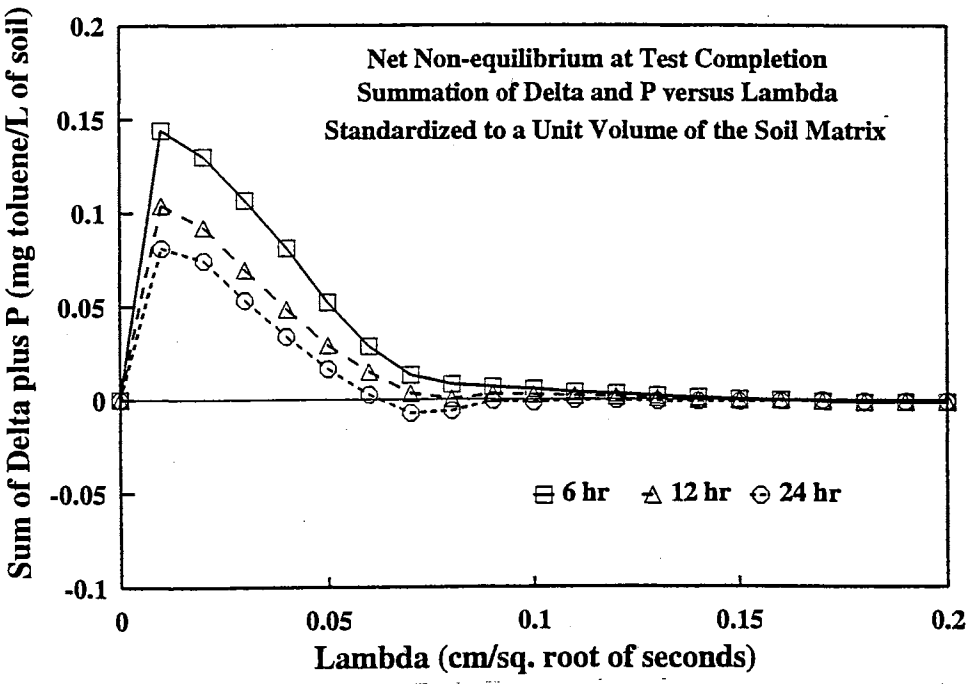

Figure 24. Net toluene mass transfer versus lambda at test completion.

In the theoretical analysis of Chapter 3, the relationship between liquid and gas phase toluene was considered to be at equilibrium instantaneously. Non-equilibrium was related to liquid-to-solid phase adsorption (which is negative in these calculations) or a variance in adsorption (which is positive for this calculations) by the solid phase. For these unsaturated horizontal column tests a net non-equilibrium for a RVE equals the sum

of Δ and P for the respective lambda values. Figure 24 shows the relationship of $\Delta + P$ (standardized to a RVE) versus lambda for the 6, 12 and 24 hour tests.

The sum of $\Delta + P$ in Figure 5-24 shows a trend towards zero with increasing test times. The values of $\Delta + P$ at lambda value of 0.01 (from Figure 5-24) are 0.144, 0.104 and 0.081 for the 6 , 12 and 24 hour tests, respectively. Plotting these net non-equilibrium values against test length gives a reaction rate relationship for the decay of $\Delta + P$. This relationship can be modeled conservatively as a second order reaction or less conservatively as a zero order equation. When it is considered a zero order reaction it takes approximately two days for the net non-equilibrium to reach zero. Modeled as a second order relationship requires approximately fourteen days to reach zero. Thus the data from Figure 24 projects that between two to fourteen days are required for the decay shown in Figure 24 to reach zero.

The magnitude of the non-equilibrium values can be approximated by comparing their RVE values to the toluene mass adsorbed and dissolved at equilibrium for each test. Using the injection solution concentration and inlet moisture content (θ_0) the total toluene concentration (C_T) in a RVE is calculated. Then using equation 3-15 with the K_d, K_H and θ values the amounts of toluene mass adsorbed (C_{sm}) and dissolved (C_{sl}) at equilibrium per RVE are calculated. Table 5-8 lists the values for the equilibrium and non-equilibrium terms.

TABLE 5-8

Values of Non-equilibrium Terms Δ and P Compared to C_{sm} and C_{sl} at Equilibrium

Parameter†	Test Duration 6 Hour	12 Hour	24 Hour
Δ	0.277	0.237	0.221
P	-0.133	-0.133	-0.140
$\Delta + P$	0.144	0.104	0.081
C_T	23.2	17.4	17.2
C_{sm}	16.5	12.4	12.4
C_{sl}	6.1	4.3	4.3

† All parameters are in units of mg toluene per unit volume of in-place soil at $\lambda = 0.01$

The values of Δ are 1.7%, 1.9% and 1.8% of the equilibrium values for C_{sm} and the values of P are 2.2%, 3.1% and 3.3% of the equilibrium values for Csl for the 6, 12 and 24 hour tests, respectively. The net non-equilibrium values are positive which indicates that adsorption is dominating the non-equilibrium within the column. It also implies that the soil adsorbed more toluene than it should at equilibrium. The soil may have acted as a sink as the contaminated plume initially invaded the clean soil, where the affinity for adsorption overshot the equilibrium values with desorption occurring more slowly than adsorption. The rate difference between adsorption and desorption could account for the excess adsorbed toluene. Even though non-equilibrium exists, its magnitude and effect is small when compared to soil and flow heterogeneity where the effect may be orders of magnitude. So the assumption of equilibrium among phases is reasonable for transport calculations in models.

CHAPTER 6

SUMMARY AND CONCLUSIONS

Summary

The primary objective of the study was to evaluate local phase equilibrium (LPE) assumptions for toluene under unsaturated, transient flow conditions. Unsaturated horizontal column tests were conducted to simulate a toluene contaminated plume advancing into uncontaminated soil. In this situation toluene is present in the gas phase, liquid phase and adsorbed on the soil organic matter. The dynamic conditions at the advecting front are difficult to study without sample collection shifting the equilibrium among phases, and this has limited research in this area. This study developed the procedures and methods to evaluate the validity of the LPE assumptions.

Since effect of adsorption on equilibrium at the wetting front was a significant part of the study, a low organic matter soil or sand was not considered. A Teller loam soil was chosen because it represents a good Oklahoma agricultural soil with an organic matter content high enough to exhibit significant adsorption of toluene. Teller soil has a sandy loam texture, good unsaturated permeability and an organic carbon content of 0.7% to 0.9% by weight. The soil adsorbed toluene in significant quantities and held measurable quantities in the liquid and gas phases within the soil.

Before beginning the column experiments all soil and soil water properties affecting toluene phase equilibrium were determined. Soil properties measured were:

organic carbon content, texture, particle density, pH, CEC, AEC, extractable bases, ferric oxide content and particle surface area. Soil water properties measured included: pH, TDS and surface tension. Twenty-four hour batch tests at room temperature (25 ± 2 °C) gave a Henry coefficient of 0.27, activity coefficient of 1.04 and linear adsorption coefficient of 0.43 mL g^{-1} of organic carbon. Specific gas chromatography procedures and methodology were developed for this research to analyze toluene in the gas phase, and dissolved in a solvent after extraction from the soil. The procedures and methodology are readily transferable to other chemicals and experiments.

After collecting the preliminary data, the horizontal soil column design and sample collection methods were determined. Several different columns were tested before finding a design that was easy to sample, gas tight and non-adsorbing. The column soil was packed to a dry bulk density of 1.67 g cm^{-3} at an initial moisture content in the column of about 0.08 mL mL^{-1}. Toluene solution at approximately 70 mg L^{-1} was injected into the soil column using a computer controlled syringe pump to maintain a constant moisture content at the column inlet of about 0.25 mL mL^{-1}. Three different injection time lengths, of 6, 12 and 24 hour duration were used in the experiments to enable comparison of final total water and toluene contents for similarity.

Periodically during the column test, soil gas samples were removed along the length of the column using gas tight 25 µL syringes with a modified syringe needle. The gas samples were immediately injected into the GC for toluene analysis. These samples yielded a gas phase profile at different times and locations along the column length. At the conclusion of the test, the column soil was sampled for moisture and total toluene

concentration. These concentrations were used in mass balance analyses. Mass recovery of moisture varied from approximately 97% to 103% with mass recovery of toluene varying from 71% to 94%.

The horizontal column tests used Bruce-Klute unsaturated boundary conditions which enabled further analysis on the collected gas data. The data was transformed from functions of time and distance to single value functions of the Boltzman variable. Equilibrium partitioning theory and the advective-dispersive equations were analyzed at the experimental boundary conditions. The transformation, along with the boundary conditions, allowed direct comparison of the different time duration tests.

Equilibrium was assumed between the toluene liquid and gas phases, and it was speculated that non-equilibrium was due to either liquid-to-solid net phase transfer (P) or variance of the solid phase adsorption (Δ) from equilibrium. Equations were developed for the defined non-equilibrium terms, using the Boltzman transformation to convert them into single variable functions. Gas phase equations were fitted to the measured gas samples, and measured values for all other parameters were used in the equations for P and Δ. The liquid-to-solid net phase transfer term (P) was calculated directly. The variance of solid phase adsorption from equilibrium (Δ) equation was first integrated for the boundary conditions to find an analytic solution, and the solution was used to calculate Δ. The calculated non-equilibrium (P and Δ) terms allow conclusions about the equilibrium state of the experiments.

Conclusions

The methods and procedures to collect and analyze small gas samples worked well, as samples appear consistent during and between tests. The soil parameters and ground water quality were typical with no unusual effects observed. The surface tension of the toluene injection solution was approximately 20% lower than 0.01 N calcium sulfate solution without toluene, and this probably resulted in slower advancement of the wetting front than expected from water only tests. The effect of surface tension on the wetting front advancement into the column was inconclusive. A paired statistical comparison was done on the normalized moisture content profiles for the 6, 12 and 24 hour column tests. The 12 and 24 hour tests were not significantly different but the 6 hour test was significantly different from the 12 or 24 hour tests at a 5% confidence level. The equilibrium status of the 6 hour test, based on Δ and P, was still compared to the 12 and 24 hour tests, since the curves for Δ versus P for the first six hours of all three tests were similar in appearance and magnitude.

The gas samples plotted as a diffusion curve and the curves were consistent among the tests. The gas phase advanced beyond the wetting front, and for all tests gas phase toluene was measured at more than twice the distance ($\lambda = 0.20$) that the wetting front traveled ($\lambda = 0.09$). Although gas concentrations were low ahead of the wetting front, they still resulted in significant spreading of the toluene beyond that due to only advection and dispersion. Initial arrival of toluene gas at a particular distance within the column was consistently near a Boltzman lambda value of 0.20.

The two non-equilbrium terms (P and Δ) were plotted against the Boltzman variable (λ) and Δ versus P was plotted at equivalent lambda values. The plots suggested that equilibrium was not present in the 6, 12 or 24 hour column tests, but the disequilibrium could not be quantified directly from the plots. The P and Δ values were summed to define a net non-equilibrium value, and the net non-equilibrium value gave a clearer relationship to analyze. The sums of P and Δ were positive which indicated that adsorption was dominating the non-equilibrium within the column.

The net non-equilibrium plots ($P+\Delta$ versus λ) exhibited a decreasing functional relationship, where the net non-equilibrium curve flattened out and approached zero with increasing test duration. A reaction rate equation was fitted to $P+\Delta$ values near the column inlet and then analyzed as a zero order and more conservatively as a second order equation to determine the time to reach zero. The zero order model predicted that a value of zero was reached in two days and the second order model predicted that it would take fourteen days. Thus, between two and fourteen days will be required for the column tests to reach equilibrium.

Even though equilibrium was not present for the 6, 12 or 24 hour tests it was not far from equilibrium conditions. The net non-equilibrium values were positive, and all were within two percent of the equilibrium values. Considering all the normal variability in soil properties and flow conditions, the variance from equilibrium does not have a significant effect on prediction of contaminant transport. Therefore, using equilibrium coefficients and LPE assumptions is a realistic and acceptable approach for contaminant transport models.

Recommendations for Further Research

These column tests require precise procedures and are relatively difficult to prepare and conduct when compared to more commonly used column tests. Because of this, I would not recommend using these tests for analyses which are readily completed with the simpler steady-state tests. The methodology is transferable to other chemicals and soils, but it should be used to study specific multi-phase transient transport situations, which can not be evaluated otherwise. One possible area for future research is to evaluate gas phase movement by a mixture of similar volatile organics (eg. toluene, benzene and xylene) to evaluate their behavior according to Raoult's Law. Another study area is to treat the Teller Loam soil to remove its organic carbon and then conduct tests on the now non-adsorbing soil. The gas phase movement and equilibrium status results for the non-adsorbing Teller could be compared against the results of this study. The 6 hour duration test is probably unnecessary, and 12 hour, 24 hour and multiples of 24 hour tests would be better.

A redesigned column would allow collection of larger samples for moisture and possibly total chemical analysis. One possibility is to split a brass column lengthwise, mill the edges for gaskets along the length and thread each end to tighten the two halves together. Small gas sampling holes could be located along the length of the column to give more sites for gas sampling than available with the current column design. Packing the soil within an aluminum foil sleeve inside the column would limit moisture loss during destructive sampling. At the conclusion of injection the column halves could be

separated, and the core sliced rapidly and placed into different containers for moisture and chemical analysis. The aluminum foil wrapping would prevent volatilization losses while the samples were collected.

BIBLIOGRAPHY

Abdul, A.S., and T.L. Gibson. 1986. Equilibrium batch experiments with six polycyclic aromatic hydrocarbons and two aquifer materials. Hazard. Waste Hazard. Mater. 3(2):125-137.

Abdul, A.S., T.L. Gibson, and D.N. Rai. 1990. Laboratory studies of the flow of some organic solvents and their aqueous solutions through bentonite and kaolin clays. Ground Water. 28:524-533.

Abriola, L.M., and G.F. Pinder. 1985a. A multiphase approach to the modeling of porous media contamination by organic compounds: 1. Equation development. Water Resour. Res. 21:11-18.

Abriola, L.M., and G.F. Pinder. 1985b. A multiphase approach to the modeling of porous media contamination by organic compounds: 2. Numerical simulation. Water Resour. Res. 21:19-26.

Acher, A.J., P. Boderie, and B. Yaron. 1989. Soil pollution by petroleum products: 1. Multiphase migration of kerosene components in soil columns. J. Contam. Hydrol. 4:333-345.

Ahlert, W.K., and C.G. Uchrin. 1990. Rapid and secondary sorption of benzene and toluene by two aquifer solids. J. Hazard. Mater. 23:317-330.

Allred, B. 1995. Surfactant mobility in unsaturated soil and the impact on saturated hydraulic conductivity and unsaturated diffusivity. Ph.D. dissertation in Biosystems Engineering at Oklahoma State University. Stillwater, OK.

Amali, S., and D.E. Rolston. 1993. Theoretical investigation of multicomponent volatile organic vapor diffusion: Steady-state fluxes. J. Environ. Qual. 22:825-831.

ASTM Standards. 1972. Standard method for particle-size analysis of soil. D422-63.

ASTM Standards. 1989. Standard test method of 24-h batch-type measurement of contaminant sorption by soils and sediments, SD4646-87. In *Annual book of ASTM standards*. 11.04:121-124.

Baehr, A.L., and M.Y. Corapcioglu. 1987. A compositional multiphase model for groundwater contamination by petroleum products: 2. Numerical solution. Water Resour. Res. 23:201-213.

Baehr, A.L. 1987. Selective transport of hydrocarbons in the unsaturated zone due to aqueous and vapor phase partitioning. Water Resour. Res. 23:1926-1938.

Baehr, A.L., G.E. Hoag, and M.C. Marley. 1989. Removing volatile contaminants from the unsaturated zone by inducing advective air-phase transport. J. Contam. Hydrol. 4:1-25.

Baehr, A.L., and C.J. Bruell. 1990. Application of the Stefan-Maxwell equations to determine limitations of Fick's Law when modeling organic vapor transport in sand columns. Water Resour. Res. 26:1155-1163.

Baker, J.A. 1989. Case studies in organic contaminant hydrogeology. Environ. Geol. Water Sci. 14:17-33.

Barbaro, J.R., J.F. Barker, L.A. Lemon, and C.I. Mayfield. 1992. Biotransformation of BTEX under anaerobic, denitrifying conditions: Field and laboratory observations. J. of Contam. Hydrol. 11:245-272.

Barone, F.S., R.K. Rowe, and R.M. Quigley. 1992. A laboratory estimation of diffusion and adsorption coefficients for several volatile organics in a natural clayey soil. J. Contam. Hydrol. 10:225-250.

Benson, D.A., D. Huntley, and P.C. Johnson. 1993. Modeling vapor extraction and general transport in the presence of NAPL mixtures and nonideal conditions. Ground Water. 31:437-445.

Bird, R.B., W.E. Stewart, and E.N. Lightfoot. 1960. *Transport Phenomena.* John Wiley & Sons, Inc. New York.

Brown, G.O., and D.B. McWhorter. 1990. Solute transport by a volatile solvent. J. Contam. Hydrol. 5:387-402.

Brown, G.O., and B. Allred. 1992. The performance of syringe pumps in unsaturated horizontal column experiments. Soil Sci. 154(3):243-249.

Brunauer, S.P., P.H. Emmett, and E. Teller. 1938. Adsorption of gases in multi-molecular layers. J. Am. Chem. Soc. 60:309-319.

Brusseau, M.L., R.E. Jessup and P.S.C. Rao. 1989. Modeling the transport of solutes influenced by multiprocess nonequilibrium. Water Resour. Res. 25:1971-1988.

Brusseau, M.L. 1991. Transport of organic chemical by gas advection in structured or heterogeneous porous media: Development of a model and application to column experiments. Water Resour. Res. 27:3189-3199.

Brusseau, M.L. 1992a. Nonequilibrium transport of organic chemicals: The impact of pore-water velocity. J. Contam. Hydrol. 9:353-368.

Brusseau, M.L. 1992b. Transport of rate-limited sorbing solutes in heterogeneous porous media: Application of a one-dimensional multifactor nonideality model to field data. Water Resour. Res. 28:2485-2497.

Camp, T.R. 1963. *Water and its impurities*. Reinhold Book Corporation. New York, NY.

Chiou, C.T., and T.D. Shoup. 1985. Soil sorption of organic vapors and effects of humidity in sorptive mechanism and capacity. Environ. Sci. Technol. 19:1196-1200.

Cho, H.J., and P.R. Jaffe. 1990. The volatilization of organic compounds in unsaturated porous media during infiltration. J. Contam. Hydrol. 6:387-410.

Cline, P.V., J.J. Delfino, and P.S.C. Rao. 1991. Partitioning of aromatic constituents into water from gasoline and other complex solvent mixtures. Environ. Sci. Technol. 25:914-920.

Cohen, Y., W. Tsai, S.L. Chetty and G.J. Mayer. 1990. Dynamic partitioning of organic chemicals in regional environments: A multimedia screening-level modeling approach. Environ. Sci. Technol. 24:1549-1558.

Corapcioglu, M.Y., and A.L. Baehr. 1987. A compositional multiphase model for groundwater contamination by petroleum products: 1. Theoretical considerations. Water Resour. Res. 23:191-200.

Corapcioglu, M.Y., and M.A. Hossain. 1990. Ground-water contamination by high-density immiscible hydrocarbon slugs in gravity-driven gravel aquifers. Ground Water. 28:403-412.

Crittenden, J.C., N.J. Hutzler, D.G. Geyer, J.L. Oravitz, and G. Friedman. 1986. Transport of organic compounds with saturated groundwater flow: Model development and parameter sensitivity. Water Resour. Res. 22:271-284.

Crittenden, J.C., T.J. Rigg, D.L. Perram, S.R. Tang, and D.W. Hand. 1989. Predicting gas-phase adsorption equilibria of volatile organics and humidity. J. Environ. Eng. 115:560-573.

Devitt, D.A., R.B. Evans, W.A. Jury, T.H. Starks, B. Eklund and A. Ghalsan. 1987. Soil gas sensing for detection and mapping of volatile organics. U.S. Environ. Prot. Agency-Environ. Monit. Systems Lab. EPA/600/8-87/036. Las Vegas, Nev.

Domenico, P.A., and F.W. Schwartz. 1990. *Physical and chemical hydrogeology.* John Wiley and Sons, Inc. New York, NY.

Dowdy, S., and S. Weardon. 1983. *Statistics for research.* John Wiley and Sons, Inc. New York, NY.

Eagle, D.J., J.L.O. Jones, E.J. Jewell, and R.P. Paxton. 1991. Determination of pesticides by gas chromatography and high-pressure liquid chromatography. p 548-552. In K. A. Smith (ed.) *Soil analysis. Modern instrumental techniques.* 2nd ed. Marcel Dekker, Inc. New York.

Falta, R.W., I. Javandel, K. Pruess, and P.A. Witherspoon. 1989. Density-driven flow of gas in the unsaturated zone due to the evaporation of volatile organic compounds. Water Resour. Res. 25:2159-2169.

Fetter, C.W. 1993. *Contaminant hydrogeology.* Macmillan Publishing Co. New York, NY.

Garbarini, D.R., and L.W. Lion. 1985. Evaluation of sorptive partitioning of nonionic pollutants in closed systems by headspace analysis. Environ. Sci. Technol. 19:1122-1128.

Garbarini, D.R., and L.W. Lion. 1986. Influence of the nature of soil organics on the sorption of toluene and trichloroethylene. Environ. Sci. Technol. 20:1263-1269.

Gerstl, Z. 1990. Estimation of organic chemical sorption by soils. J. Contam. Hydrol. 6:357-375.

Gierke, J.S., N.J. Hutzler, and J.C. Crittenden. 1990. Modeling the movement of volatile organic chemicals in columns of unsaturated soils. Water Resour. Res. 26:1529-1547.

Gierke, J.S., N.J. Hutzler, and D.B. McKenzie. 1992. Vapor transport in unsaturated soil columns: Implications for vapor extraction. Water Resour. Res. 28:323-335.

Hamaker, J.W. 1972. Diffusion and volatilization. p. 342-393. Goring, C.A.I., and J.W. Hamaker (eds.) In *Organic chemicals in the soil environment.* Marcel Dekker, Inc. New York, NY.

Hamaker, J.W., and J.M. Thompson. 1972. Adsorption. p. 51-132. Goring, C.A.I., and J.W. Hamaker (eds.). In *Organic chemicals in the soil environment.* Marcel Dekker, Inc. New York, NY.

Henley, J., R.D. Gelnar, and R.E. Mayhugh. 1987. Soil survey of Payne County, Oklahoma. USDA Soil Conservation Service in cooperation with the Oklahoma Agricultural Experiment Station.

Hillel, D. 1980. *Fundamentals of soil physics.* Academic Press, Inc. New York, NY.

Hughes, W.F. 1979. *An introduction to viscous flow.* McGraw-Hill. Washington, D.C.

Jury, W.A., W.F. Spencer, and W.J. Farmer. 1983. Behavior assessment model for trace organics in soil: I. Model description. J. Environ. Qual. 12:558-564.

Jury, W.A., W.F. Spencer, and W.J. Farmer. 1984a. Behavior assessment model for trace organics in soil: II. Chemical classification and parameter sensitivity. J. Environ. Qual. 13:567-572.

Jury, W.A., W.F. Spencer, and W.J. Farmer. 1984b. Behavior assessment model for trace organics in soil: III. Application of screening model. J. Environ. Qual. 13:573-579.

Jury, W.A., W.F. Spencer, and W.J. Farmer. 1984c. Behavior assessment model for trace organics in soil: IV. Review of experimental evidence. J. Environ. Qual. 13:580-586.

Jury, W.A., and G. Sposito. 1985. Field calibration and validation of solute transport models for the unsaturated zone. Soil Sci. Soc. Am. J. 49:1331-1341.

Jury, W.A., D. Russo, G. Streile, and H. El Abd. 1990. Evaluation of volatilization by organic chemicals residing below the soil surface. Water Resour. Res. 26:13-20.

Jury, W.A., W.R. Gardner, and W.H. Gardner. 1991. *Soil Physics,* 5th Ed. John Wiley and Sons, Inc. New York, NY.

Jury, W.A., and H. Fluhler. 1992. Transport of chemicals through soil: mechanisms, models and field applications. Adv. Agron. 47:141-201.

Karickhoff, S.W., D.S. Brown, and T.A. Scott. 1979. Sorption of hydrophobic pollutants on natural sediments. Water Res. 13:241-248.

Karmi, A.A., W.F. Farmer, and M.M. Cliath. 1987. Vapor-phase diffusion of benzene in soil. J. Environ. Qual. 16:38-43.

Kerfoot, H.B. 1991. Subsurface partitioning of volatile organic compounds: Effects of temperature and pore-water content. Ground Water. 29:678-684.

Khondaker, A.N., R.I. Al-Layla, and T. Husain. 1990. Groundwater contamination studies - The state-of-the-art. Critical Reviews in Environ. Control. 20:231-256.

Klute, A., and C. Dirksen. 1986. Hydraulic conductivity and diffusivity: Laboratory methods. p. 691-693 In A. Klute (Ed.) *Methods of soil analysis. Part 1.* ed. 2. American Society of Agronomy. Madison, WI.

Kobayashi, H., and B.E. Rittmann. 1982. Microbial removal of hazardous organic compounds. Environ. Sci. Technol. 16:170a-183a.

Lewis, T.E., A.B. Crockett, R.L. Siegrist, and K. Zarrabi. 1991. Soil sampling and analysis for volatile organic compounds. USEPA Ground-Water Issue, doc. EPA/540/4-91/001. U.S. Government Printing Office. Washington, DC.

Li, C., and E.A. Voudrias. 1992. Difference in transport behavior between aliphatic and aromatic petroleum vapors in unsaturated soil. Water Sci. Technol. 26:89-98.

Lion, L.W., S.K. Ong, S.R. Linder, J.L. Swanger, S.J. Schwager, and T.B. Culver. 1990. Sorption equilibria of vapor phase organic pollutants on unsaturated soils and soil minerals. Cornell University rep. ESL-TR-90-05, Dept. of Civil and Environ. Eng. Ithaca, NY.

MacIntyre, W.G., T.B. Stauffer and C.P. Antworth. 1991. A comparison of sorption coefficients determined by batch, column, and box methods on a low organic carbon aquifer material. Ground Water. 29:908-913.

Mackay, D.M., W.Y. Shiu, and R.P. Sutherland. 1979. Determination of air-water Henry's Law constants for hydrophobic pollutants. Environ. Sci. Technol. 13:333-337.

Mackay, D.M., P.V. Roberts, and J.A. Cherry. 1985. Transport of organic contaminants in groundwater. Environ. Sci. Technol. 19:384-392.

Mackay, D.M., W.Y. Shiu, A. Maijanen, and S. Feenstra. 1991. Dissolution of non-aqueous phase liquids in groundwater. J. Contamin. Hydrol. 7:23-42.

MacQuarrie, K.T., E.A. Sudicky, and E.O. Frind. 1990. Simulation of biodegradable organic contaminants in groundwater 1. Numerical formulation in principal directions. Water Resour. Res. 26:207-222.

MacQuarrie, K.T., and E.A Sudicky. 1990. Simulation of biodegradable organic contaminants in groundwater 2. Plume behavior in uniform and random flow fields. Water Resour. Res. 26:223-239.

McCarty, P.L., M. Reinhard, and B.E. Rittmann. 1981. Trace organics in groundwater. Environ. Sci. and Technol. 15:40-51.

McLean, E.O. 1982. Soil pH and lime requirement. p. 199-224 *In* A.L. Page, R.H. Miller, and D.R. Keeney (Eds) *Methods of soil analysis. Part 2.* ed. 2. American Society of Agronomy. Madison, WI.

Mendoza, C.A., and E.O. Frind. 1990. Advective-dispersive transport of dense organic vapors in the unsaturated zone 1. Model development. Water Resour. Res. 26:379-387.

Mendoza, C.A., and T.A. McAlary. 1990. Modeling of ground-water contamination caused by organic solvent vapors. Ground Water. 28:199-206.

Mercer, J.W., and R.M. Cohen. 1990. A review of immiscible fluids in the subsurface: properties, models, characterization and remediation. J. Contam. Hydrol. 6:107-163.

Metcalfe, D.E., and G.J. Farquhar. 1986. Modeling gas migration through unsaturated soils from waste disposal sites. Water Air Soil Pollut. 32:247-259.

Miller, C.T., and E.G. Staes. 1992. Effect of vapor-phase mass transfer on aquifer restoration. Water Resour. Res. Instit. Rep. no. 262. University of North Carolina. Chapel Hill, NC.

Miller, C.T., J.A. Pedit, A.M. Levert, and A.J. Rabideau. 1992. Investigation of multicomponent sorption and desorption rates in saturated groundwater systems. Water Resour. Res. Instit. Rep. no. 263. University of North Carolina. Chapel Hill, NC.

Moreau, M. 1985. A regulator's perspective on prevention of leaks from underground storage systems. In *Proceedings of the NWWA/API Conference on Petroleum Hydrocarbons and Organic Chemicals in Groundwater.* National Water Well Association.

National Research Council. 1990. *Ground water models: scientific and regulatory applications.* National Academy Press. Washington, D.C.

Ong, S.K., T.B. Culver, L.W. Lion, and C.A. Shoemaker. 1992. Effects of soil moisture and physical-chemical properties of organic pollutants on vapor-phase transport in the vadose zone. J. Contam. Hydrol. 11:273-290.

Park, W., and G.G. Eichholz. 1990. Partitioning of organic materials in porous beds under unsaturated water flow conditions. Waste Mgmt. 10:125-139.

Peterson, M.S., L.W. Lion, and C.A. Shoemaker. 1988. Influence of vapor-phase sorption and diffusion on the fate of trichloroethylene in an unsaturated aquifer system. Environ. Sci. Technol. 22:571-578.

Priddle, M.W., and R.E. Jackson. 1991. Laboratory column measurement of VOC retardation factors and comparison with field values. Ground Water. 29:260-266.

Rao, P.S.C., A.G. Hornsby, and R.E. Jessup. 1985. Indices for ranking the potential for pesticide contamination of groundwater. Soil & Crop Sci. Soc. Fla. Proc. 44:1-8.

Rao, P.S.C., L.S. Lee and A.L. Wood. 1991. Solubility, sorption and transport of hydrophobic organic chemicals in complex mixtures. USEPA Environmental Research Brief. EPA/600/M-91/009 March 1991.

Reible, D.D., T.H. Illangasekare, D.V. Doshi, and M.E. Malhiet. 1990. Infiltration of immiscible contaminants in the unsaturated zone. Ground Water. 28:685-692.

Robinson , K.G., W.S. Farmer, and J.T. Novak. 1990. Availability of sorbed toluene in soils for biodegradation by acclimated bacteria. Water Res. 24:345-350.

Roe, V.D., M.J. Lacy, and J.D. Stuart. 1989. Manual headspace method to analyze for the volatile aromatics of gasoline in groundwater and soil samples. Anal. Chem. 61:2584-2585.

Roy, W.R., I.G. Krapac, S.F.J. Chou, and R.A. Griffin. 1987. Batch-type procedures for estimating soil adsorption of chemicals. USEPA Rep. EPA/530-SW-87-006-F. U.S. Government Printing Office. Washington, DC.

Shimizu, Y., N. Takei, and Y. Terashima. 1992. Sorption of organic pollutants from vapor phase: The effects of natural solid characteristics and moisture content. Water Sci. Technol. 26:79-87.

Shoemaker, C.A., T.B. Culver, L.W. Lion, and M.G. Peterson. 1990. Analytic models of the impact of two-phase sorption on subsurface transport of volatile chemicals. Water Resour. Res. 26:745-758.

Siegrist, R.L., and P.D. Jenssen. 1990. Evaluation of sampling method effects on volatile organic compound measurements in contaminated soils. Environ. Sci. Technol. 24:1387-1392.

Sleep, B.E., and J.F. Sykes. 1989. Modeling the transport of volatile organics in variably saturated media. Water Resour. Res. 25:81-92.

Snedecor, G.W., and W.G. Cochran. 1980. *Statistical methods.* 7th ed. Iowa State University Press. Ames, IA.

Sposito, G., W.A. Jury, and V.K. Gupta. 1986. Fundamental problems in the stochastic convection-dispersion model of solute transport in aquifers and field soils. Water Resour. Res. 22:77-88.

Stumm, W., and J.J. Morgan. 1981. The solid-solution interface. p. 579-679 In *Aquatic chemistry.* John Wiley and Sons, Inc. New York, NY.

Stumm, W. 1992. Adsorption. p. 87-155 In *Chemistry of the solid-water interface.* John Wiley and Sons, Inc. New York, NY.

Swanger, J.L. 1990. Vapor phase sorption of trichloroethylene and toluene on unsaturated soils. Masters thesis Cornell University. Ithaca, NY.

Swisher, R.D. 1970. *Surfactant Degradation.* Marcel Dekker, Inc. New York, NY.

Thomas, G.W. 1982. Exchangeable cations. p. 159-165 *In* A.L. Page, R.H. Miller, and D.R. Keeney (Eds) *Methods of soil analysis. Part 2. ed. 2,* American Society of Agronomy. Madison, WI.

Thorstenson, D.C., and D.W. Pollock. 1989. Gas transport in unsaturated zones: multicomponent systems and adequacy of Fick's Laws. Water Resour. Res. 25:477-507.

Verschueren, K. 1990. Toluene. p.1103-1108 In *Handbook of environmental data on organic chemicals.* Van Nostrand Reinhold Co. New York, NY.

Voice, T.C., and W.J. Weber Jr. 1983. Sorption of hydrophobic compounds by sediments, soils and suspended solids - I. Theory and background. Water Res. 17:1433-1441.

Walton, B.T., M.S. Hendricks, T.A. Anderson, W.H. Griest, R. Merriweather, J.J. Beauchamp and C.W. Francis. 1992. Soil sorption of volatile and semivolatile organic compounds in a mixture. J. Environ. Qual. 21:552-558.

Weber, W.J. Jr., T.C. Voice, M. Pirbazari, G.E. Hunt, and D.M. Ulanoff. 1983. Sorption of hydrophobic compounds by sediments, soils and suspended solids - II. Sorbent evaluation studies. Water Res. 17:1443-1452.

Yu, M. 1995. Personal communication. Ph.D. dissertation in Biosystems Engineering at Oklahoma State University. Stillwater, OK.

Zalidis, G.C., M.D. Annable, R.B. Wallace, N.J. Hayden, and T.C. Voice. 1991. A laboratory method for studying the aqueous phase transport of dissolved constituents from residually held NAPL in unsaturated soil columns. J. Contamin. Hydrol. 8:143-156.

Zhang, J. 1990. Dynamic simulation of water movement and uptake in unsaturated soil zones. Ph.D. dissertation in Agricultural Engineering at Oklahoma State University. Stillwater, Ok.

APPENDIX A

Integration to Determine an Analytic Solution for Delta

APPENDIX A

Integration to Determine an Analytic Solution for Delta

The equations to analyze are

$$P = -(\frac{\lambda}{2})\frac{d}{d\lambda}[C_{sg}(\frac{\theta}{K_H}+\varepsilon)] + (\frac{S}{2K_H})\frac{dC_{sg}}{d\lambda} - D_{g(air)}[\frac{d^2}{d\lambda^2}(\frac{\varepsilon^{3.33}}{\phi^2}C_{sg})] \quad (1)$$

and

$$\frac{d\Delta}{d\lambda} = (\frac{K_d}{K_H})\frac{dC_{sg}}{d\lambda} - (\frac{2}{\lambda\rho_b})P \ . \quad (2)$$

Fitted values for the experimentally measured gas phase data have the form

$$C_{sg} = a(10^{b\lambda}), \quad (3)$$

where a and b are constants determined by linear regression. In equations 1 and 2 the values of each term used in the analysis were determined as follows:

K_d	constant - experimentally measured using batch equilibrium tests
K_H	constant - experimentally measured using batch equilibrium tests
ρ_b	constant - determined from weight of dry soil packed in the column
ϕ	constant - calculated based on the dry bulk density
$D_{g(air)}$	constant - interpolated from a handbook based on the isothermal temperature and chemical vapor present in the air
S	constant - experimentally determined for the Teller loam soil through unsaturated flow tests at Bruce/Klutt boundary conditions
θ	variable - determined from the measured water content profile for each individual column test
ε	variable - determined by subtracting θ from ϕ
λ	variable - Boltzman variable determined by actual distance and time elapsed during an individual column test
C_{sg}	variable - gas phase values determined using relationship in equation 3 fitted to the actual measured gas phase concentrations
P	variable - calculated directly using equation 1
Δ	variable - calculated by integration or numeric analysis of equation 2

Boundary Conditions

The following boundary conditions were utilized to evaluate P and Δ.

$$\frac{dC_{sg}}{d\lambda} = ab(10)^{b\lambda} \text{ and } \frac{d^2C_{sg}}{d\lambda^2} = ab^2(10)^{b\lambda}, \text{ and at } (\lambda = 0) \text{ both terms equal zero} \quad , \tag{4}$$

$$C_{sg}(\lambda = 0) = C_{sg}^{o}, \Delta(\lambda = 0) = 0, P(\lambda = 0) = 0 \quad , \tag{5}$$

and

$$C_{sg}(\lambda = \infty) = C_{sg}^{i}, \Delta(\lambda = \infty) = 0, P(\lambda = \infty) = 0 \quad . \tag{6}$$

Integration Steps

Integration of equation 2 begins with multiplication by $d\lambda$

$$d\Delta = \frac{K_d}{K_H} dC_{sg} - \frac{2}{\lambda \rho_b} P d\lambda \quad . \tag{7}$$

Next equation 7 is integrated and evaluated over the range $\lambda = (0,\lambda)$, where the lower end of the range is close to zero at $\lambda = 0.0001$, but not zero. Equation 7 then becomes

$$\Delta|_0^{\lambda} = \frac{K_d}{K_H} C_{sg}|_0^{\lambda} - \frac{2}{\rho_b} \int_0^{\lambda} \frac{1}{\lambda} P d\lambda \quad . \tag{8}$$

The first two terms of equation 8 are simplified but the third term requires expansion and simplification. Substituting into the third term of equation 8 for P gives

$$-\frac{2}{\rho_b} \int_0^{\lambda} \frac{1}{\lambda} P d\lambda = -\frac{2}{\rho_b} \int_0^{\lambda} \frac{1}{\lambda} \left(-\left(\frac{\lambda}{2}\right) \frac{d}{d\lambda} \left[C_{sg}\left(\frac{\theta}{K_H} + \varepsilon\right)\right] + \left(\frac{S}{2K_H}\right) \frac{dC_{sg}}{d\lambda} - D_{g(air)} \left[\frac{d^2}{d\lambda^2} \left(\frac{\varepsilon^{3.33}}{\phi^2} C_{sg}\right)\right]\right) d\lambda \quad . \tag{9}$$

In equation 9, the terms on the right side are expanded and separated giving

$$= \int_0^{\lambda} \frac{1}{\rho_b} \frac{d}{d\lambda} \left[C_{sg}\left(\frac{\theta}{K_H} + \varepsilon\right)\right] d\lambda - \left(\frac{S}{\rho_b K_H}\right) \int_0^{\lambda} \frac{1}{\lambda} \frac{dC_{sg}}{d\lambda} d\lambda + \frac{2}{\rho_b} D_{g(air)} \int_0^{\lambda} \frac{1}{\lambda} \left[\frac{d^2}{d\lambda^2} \left(\frac{\varepsilon^{3.33}}{\phi^2} C_{sg}\right)\right] d\lambda \quad , \tag{10}$$

and continuing the expansion and solution of equation 10 yields

$$= \frac{1}{\rho_b} \left(\frac{\theta}{K_H} + \varepsilon\right) C_{sg}|_0^{\lambda} - \left(\frac{S}{\rho_b K_H}\right) \int_0^{\lambda} \frac{1}{\lambda} \left[\frac{dC_{sg}}{d\lambda}\right] d\lambda + \frac{2}{\rho_b} D_{g(air)} \left(\frac{\varepsilon^{3.33}}{\phi^2}\right) \int_0^{\lambda} \frac{1}{\lambda} \left[\frac{d^2}{d\lambda^2} C_{sg}\right] d\lambda \quad . \tag{11}$$

The first term of equation 11 is simplified but the last two terms require further simplification. Using the relationships from equation 4 and substituting into the last two terms of equation 11 gives

$$+\left[-\left(\frac{Sab}{\rho_b K_H}\right) + \frac{2ab^2}{\rho_b} D_{g(air)} \left(\frac{\varepsilon^{3.33}}{\phi^2}\right)\right] \int_0^{\lambda} \frac{1}{\lambda} \left[10^{b\lambda}\right] d\lambda \quad . \tag{12}$$

The integral in equation 12 requires simplification, and this is done by applying the integration by parts technique twice, which then gives

$$\int_0^{\lambda} \frac{1}{\lambda}[10^{b\lambda}]d\lambda = \frac{1}{1-b^2}[(\log\lambda - \frac{b}{\lambda})(10^{b\lambda})]|_0^{\lambda} \quad . \tag{13}$$

Substituting equation 13 into equation 12, then equation 12 into equation 11, and finally equation 11 into equation 9 gives

$$-\frac{2}{\rho_b}\int_0^{\lambda} \frac{1}{\lambda}Pd\lambda = \frac{1}{\rho_b}(\frac{\theta}{K_H} + \varepsilon)C_{sg}|_0^{\lambda} + [-(\frac{Sab}{\rho_b K_H}) + \frac{2ab^2}{\rho_b}D_{g(air)}(\frac{\varepsilon^{3.33}}{\phi^2})](\frac{1}{1-b^2})[(\log\lambda - \frac{b}{\lambda})(10^{b\lambda})]|_0^{\lambda}. \tag{14}$$

Next equation 14 is substituted into equation 8 and then each term is evaluated over the range from close to zero to λ. After simplification this gives the analytic solution in equation 15.

The analytic solution for the integration of Δ is

$$\Delta(\lambda) = [\frac{K_d}{K_H} + \frac{1}{\rho_b}(\frac{\theta}{K_H} + \phi - \theta)](a10^{b\lambda} - a) + [const][\log(\lambda) - \frac{b}{\lambda}](a10^{b\lambda}) + ki \tag{15}$$

where $$[const] = [\frac{b}{\rho_b(1-b^2)}][(2b)D_{g(air)}(\frac{(\phi-\theta)^{3.33}}{\phi^2}) - \frac{S}{K_H}], \tag{16}$$

with ki = integration constant .

and ki is determined based on the experimental boundary conditions, where beyond the extent of the contamination $\Delta = 0$.

APPENDIX B

Gas and Liquid Phase Calibration Data for Column Tests

APPENDIX B

Gas and Liquid Phase Calibration Data for Column Tests

Gas Phase Toluene Calibration Standards and Gas Chromatograph Response

Test Date	Vial or Bottle #	mL of 0.01 N calcium sulfate solution	mL of air in the sample	Toluene mass added to the sample (mg)	Calculated Csg (mg/L)	Avg GC response area per uuL of HS air injected (x1000)
May 20, 1993	JR 1	29.9	10.1	2.17	17.3	64.3
	JR 2	29.9	10.1	4.34	34.7	122.6
	JR 3	29.9	10.1	6.5	52	165.8
	JR 5	29.8	10.2	10.84	86.8	312.6
May 22, 1993	JR 16	19.9	20.1	2.17	22.4	85.8
	JR 17	19.9	20.1	4.34	44.9	157.5
	JR 18	19.9	20.1	6.5	67.4	240
	JR 19	19.9	20.1	8.67	89.7	288.6
May 30, 1993	JR 1	19.9	20.1	0.87	9	26.1
	JR 2	20	20	1.73	17.9	45.8
	JR 3	19.9	20.1	3.03	31.4	106.8
	JR 4	20	20	4.34	44.8	154.6
	JR 5	19.9	20.1	6.5	67.2	207
	JR 6	19.9	20.1	8.67	89.7	259.3
July 20, 1993	Bottle 1	282.6	223,9	2.17	1.7	7.1
	Bottle 2	294.7	209.2	4.34	3.2	13.3
	JR 1	19.9	20.1	0.87	9	35.1
	JR 2	19.9	20.1	1.73	17.9	87.4
	JR 3	20	20	2.6	26.8	123.9
Aug 3, 1993	Bottle 1	247.2	259.3	2.17	1.8	9
	Bottle 2	250.8	253.1	4.34	3.6	16.8
	JR 1	19.8	20.2	0.87	9	41.6
	JR 2	20	20	1.73	17.9	65.9
	JR 3	19.9	20.1	2.6	26.9	96.4
	JR 4	19.9	20.1	3.47	35.9	149.9
	JR 5	19.9	20.1	4.34	44.8	163.8
	JR 6	20	20	5.2	53.8	239.3
Nov 12, 1993	1	252.9	253.6	2.17	1.8	9
	2	242.8	261.1	4.34	3.7	17.4
	3	248.1	280.7	8.67	7.2	37.1
	4	245.2	258.8	13.01	11.1	49.6
Nov 26, 1993	1	256.1	250.4	0.87	0.72	4
	2	249.4	254.5	2.17	1.84	8.6
	3	245.5	283.3	4.34	3.63	16.4
	4	251.6	252.4	6.5	5.49	24.4

Linear Regression Output for the Gas Phase Calibration Results

Test Date	Constant	Std Err of Y Est	R Squared	X Coef.	Std Err of X Coef.	Formula
May 20, 1993	0	10.88	0.992	3.5	0.1	Csg = 3.50*A
May 22, 1993	0	12.86	0.982	3.38	0.1	Csg = 3.38*A
May 30, 1993	0	12.08	0.986	3.04	0.1	Csg = 3.04*A
July 20, 1993	0	4.08	0.991	4.64	0.12	Csg = 4.64*A
Aug 3, 1993	0	12.09	0.984	4.07	0.14	Csg = 4.07*A
Nov 12, 1993	0	2.41	0.983	4.65	0.17	Csg = 4.65*A
Nov 26, 1993	0	0.51	0.997	4.49	0.07	Csg = 4.49*A

A = GC response area per μL of air injected

Toluene Dissolved in Hexane Calibration Standards and Gas Chromatograph Response

Test Date	Vial or Bottle #	Toluene spike solution added (uuL)	Toluene mass added to the sample (mg)	Hexane plus toluene volume (mL)	Calculated Csl (mg/L)	Avg GC response area per 0.75 uuL injection of liquid (x1000)
May 20, 1993	JR 7	20	0.15	19.18	7.8	33.2
	JR 8	40	0.3	19.16	15.7	75.9
	JR 9	60	0.45	19.17	23.5	104
	JR 10	80	0.6	19.25	31.2	151.8
	JR 11	100	0.75	18.27	41.1	187.7
	JR 12	0	0	18.79	0	0
May 30, 1993	JR 7	5	0.03	18.7	1.67	8.2
	JR 8	10	0.06	18.61	3.35	16.4
	JR 9	20	0.12	18.43	6.77	34.7
	JR 10	40	0.25	18.69	13.35	75.4
	JR 11	60	0.37	18.55	20.18	106.3
	JR 12	80	0.5	4.34	26.68	147.8
July 20, 1993	JR 9	1	0.01	19.16	0.34	ND
	JR 10	5	0.03	19.04	1.69	8.9
	JR 11	10	0.06	18.68	3.45	16.9
	JR 12	20	0.13	18.74	6.89	36.4
	JR 13	40	0.26	18.7	13.81	78
	JR 14	60	0.39	18.35	21.1	113.1
	JR 15	80	0.52	18.75	27.54	146.1
Aug 3, 1993	JR 7	2.5	0.02	20.48	0.79	2.7
	JR 8	5	0.03	20.51	1.57	8.4
	JR 9	10	0.06	19.48	3.31	16
	JR 10	20	0.13	19.31	6.68	35.3
	JR 11	40	0.26	19.97	12.93	66.2
	JR 12	80	0.52	19.16	26.96	158.3

Linear Regression Output for the Toluene Dissolved in Hexane Calibration Results

Test Date	Constant	Std Err of Y Est	R Squared	X Coef.	Std Err of X Coef.	Formula
May 20, 1993	0	4.52	0.996	4.64	0.08	Csl = 4.64*A
May 30, 1993	0	2.66	0.997	5.45	0.07	Csl = 5.45*A
July 20, 1993	0	2.04	0.995	5.36	0.05	Csl = 5.36*A
Aug 3, 1993	0	4.41	0.993	5.7	0.14	Csl = 5.70*A

A = CG response area per 0.75 μL of solvent injected

APPENDIX C

Data for Henry Coefficient and Activity Coefficient Determination

APPENDIX C

Data for Henry Coefficient and Activity Coefficient Determination

Test Date	Vial or Bottle #	mL of 0.01 N calcium sulfate solution	mL of high purity distilled water	mL of air in the sample	Toluene mass added to the sample (mg)	Avg GC response area per uuL of HS air injected (x1000)
			Henry Coefficient Data			
Nov. 11, 1993	JR 7	20		20	1.3	612.2
	JR 8	20.1		19.9	1.3	631
	JR 9	20		20	1.3	664.3
	JR 10	10		30	1.3	831.2
	JR 11	10		30	1.3	890.2
	JR 12	10		30	1.3	936.7
			Activity Coeffficient Data			
Nov. 11, 1993	JR 1	20		20	1.3	698.6
	JR 2	20		20	1.3	647.2
	JR 3	20		20	1.3	623.4
	JR 4		20	20	1.3	611.3
	JR 5		20	20	1.3	639.4
	JR 6		20	20	1.3	658.7
	Henry Coef. =	0.273				
	Activity Coef. =	1.038				

APPENDIX D

Data for Linear Adsorption Coefficient Determination

APPENDIX D

Data for Linear Adsorption Coefficient Determination

Test Date Henry coef activity coef frac. of O.C.	Mass of Sorbent, M g	Avg. Sample Csg normalized to 20 mL mg/L	Sample gas vol., Vg mL	Sample Liq. vol., Vl mL	X-axis variable	Y-axis variable g/mL
July, 1992	5.86	4.72	17.53	20.11	0.24	1.05
Kh = 0.26	9.74	4.71	15.53	20.27	0.4	1.07
ac = 1.04	11.73	4.6	14.9	20.27	0.48	1.1
foc = 0.007	13.68	4.52	14.14	20.31	0.57	1.13
	15.63	3.87	15.54	20.24	0.64	1.3
	8.8	4.53	16.45	20.16	0.36	1.06
	12.7	4.44	14.84	20.23	0.52	1.1
	14.66	4.18	13.85	20.3	0.61	1.17
	16.61	4.15	13.08	20.35	0.7	1.19
	18.57	4.1	12.44	20.39	0.78	1.21
	blank	4.77	19.97	19.83		
	Kd = 0.34 mL/g		**Koc = 47.1**		**R-square = 0.92**	
Sept, 1993	3	9.13	18.87	20	0.12	1
Kh = .0.27	6	8.15	17.74	20	0.24	1.12
ac = 1.04	9	8.6	16.6	20	0.37	1.06
foc = 0.0085	12	7.31	15.47	20	0.49	1.25
	15	7.57	14.34	20	0.62	1.21
	blank	91.3	20	20		
	Kd = 0.43 mL/g		**Koc = 50.6**		**R-square = 0.70**	
11/13/93	8	12.96	16.98	20	0.32	1.12
Kh = .0.27	10	12.81	16.23	20	0.41	1.14
ac = 1.04	12	12.23	15.47	20	0.49	1.19
foc = 0.009	14	12.61	14.72	20	0.58	1.15
	16	12.06	13.96	20	0.67	1.21
	18	11.27	13.21	20	0.76	1.29
	blank	14.56	20	20		
	Kd = 0.34 mL/g		**Koc = 37.8**		**R-square = 0.78**	
11/27/93	10	4.97	16.23	20	0.41	1.12
Kh = .0.27	14	4.65	14.72	20	0.58	1.2
ac = 1.04	16	4.55	13.96	20	0.67	1.22
foc = 0.009	20	4.16	12.45	20	0.85	1.34
	blank	5.56	20	20		
	Kd = 0.49 mL/g		**Koc = 54.4**		**R-square = 0.97**	

APPENDIX E

Data to Determine Maximum Adsorption of Toluene by Teller Loam Soil

APPENDIX E

Data to Determine Maximum Adsorption of Toluene by Teller Loam Soil

Liquid Conc Csl	Sample Soil Mass of 12 g X/M	Sample Soil Mass of 14 g X/M	Sample Soil Mass of 16 g X/M	Fitted Freundlich X/M
209.9	0.036			
102.9	0.024			
27.1	0.015			
18.5	0.011			
210.7		0.031		
17.8		0.012		
210.7			0.031	
100			0.024	
17.4			0.012	
0				0
20				0.014
30				0.016
40				0.018
50				0.019
60				0.021
70				0.022
80				0.023
90				0.024
100				0.025
110				0.026
120				0.027
130				0.028
140				0.029
160				0.03
180				0.032
200				0.033
210				0.034
220				0.034

APPENDIX F

Data for Moisture Content versus Distance & Lambda

APPENDIX F

Data for Moisture Content versus Distance & Lambda

Moisture Content Theta (θ) Versus Distance from Column Inlet (*x*)

	Distance x (cm)	Theta 6 hr (mL/mL)	Theta 12 hr (mL/mL)	Theta 24 hr (mL/mL)
Inlet	0	0.268	0.249	0.247
	3.5	0.255	0.23	0.229
	5.3	0.247	0.222	0.23
	7.3	0.217	0.221	0.226
	9.3	0.187	0.205	0.217
	13.3	0.099	0.176	0.203
	17.3	0.098	0.091	0.174
	21.3	0.105	0.089	0.105
	25.3	0.093	0.084	0.076
	29.3	0.083	0.09	0.082
	33.3	0.085	0.086	0.074
	37.3	0.07	0.09	0.076
	41.3	0.086	0.082	0.079
	45.3	0.09	0.089	0.078
	49.3	0.078	0.088	0.073
	53.3	0.077	0.09	0.076
	57.3	0.09	0.094	0.076
Outlet	61.3	0.088	0.093	0.086

Moisture Content Theta (θ) Versus Lambda $(\frac{x}{\sqrt{T}})$

	Lambda x/(sqrt T) (cm/sqrt sec.)	Theta 6 hr (mL/mL)	Theta 12 hr (mL/mL)	Theta 24 hr (mL/mL)
Inlet	0	0.268	0.249	0.247
	0.01	0.262	0.24	0.235
	0.02	0.256	0.23	0.23
	0.03	0.25	0.22	0.22
	0.04	0.24	0.21	0.21
	0.05	0.216	0.195	0.195
	0.06	0.192	0.18	0.175
	0.07	0.162	0.15	0.13
	0.08	0.13	0.11	0.1
	0.09	0.1	0.088	0.077
	0.1	0.1	0.087	0.08
	0.11	0.095	0.087	0.075
	0.12	0.095	0.086	0.076
	0.13	0.1	0.087	0.077
	0.14	0.105	0.088	0.077
	0.15	0.1	0.088	0.077
	0.16	0.092	0.087	0.075
	0.17	0.088	0.088	0.074
	0.18	0.088	0.088	0.075
	0.19	0.088	0.087	0.075
	0.2	0.086	0.086	0.075

Normalized Moisture Content Theta (θ) Versus Lambda $(\frac{x}{\sqrt{T}})$

	Lambda x/(sqrt T) (cm/sqrt sec.)	Normalized Theta * 6 hr (mL/mL)	Normalized Theta 12 hr (mL/mL)	Normalized Theta 24 hr (mL/mL)
Inlet	0	1	1	1
	0.01	0.97	0.94	0.93
	0.02	0.93	0.88	0.9
	0.03	0.9	0.82	0.84
	0.04	0.84	0.76	0.78
	0.05	0.71	0.66	0.69
	0.06	0.58	0.57	0.57
	0.07	0.41	0.38	0.31
	0.08	0.23	0.13	0.13
	0.09	0.07	(0.01)	(0.01)
	0.1	0.07	(0.01)	0.01
	0.11	0.04	(0.01)	(0.02)
	0.12	0.04	(0.02)	(0.01)
	0.13	0.07	(0.01)	(0.01)
	0.14	0.09	(0.01)	(0.01)
	0.15	0.07	(0.01)	(0.01)
	0.16	0.02	(0.01)	(0.02)
	0.17	0	(0.01)	(0.02)
	0.18	0	(0.01)	(0.02)
	0.19	0	(0.01)	(0.02)
	0.2	(0.01)	(0.02)	(0.02)

* Normalized Water Content = $\frac{\theta-\theta_i}{\theta_0-\theta_i}$

θ_0 =	0.268	0.249	0.247
θ_i =	0.088	0.088	0.078

APPENDIX G

Data for Column Moisture Recovery Determination

APPENDIX G

Data for Column Moisture Recovery Determination

6 Hour Duration Column Test (#8)

Column Test Duration (hr)	Distance from Column Inlet (cm)	Lambda cm/s^1/2	Sample Soil Moisture (g/g)	Sample Soil Moisture (mL/mL)	Total Moisture Between Sample Sites (mL)
6	0	0	0.162	0.268	
	5.3	0.04	0.149	0.247	17.15
	9.3	0.06	0.113	0.187	10.91
	13.3	0.09	0.06	0.099	7.2
	17.3	0.12	0.059	0.098	4.96
	21.3	0.14	0.064	0.105	5.11
	25.3	0.17	0.056	0.093	4.97
	29.3	0.2	0.05	0.083	4.42
	33.3	0.23	0.052	0.085	4.24
	37.3	0.25	0.042	0.07	3.91
	41.3	0.28	0.052	0.086	3.92
	45.3	0.31	0.055	0.09	4.42
	49.3	0.34	0.047	0.078	4.24
	53.3	0.36	0.047	0.077	3.91
	57.3	0.39	0.054	0.09	4.21
	61.3	0.42		0.088	4.48
				Sum =	**88.06**

Average Initial Moisture Content =	0.088	mL/mL
Dry Bulk Density =	1.66	g/cm^3
Initial Water Volume Present in Column =	67.9	mL
Injection Volume =	17.9	mL
Final Water Volume Present in Column =	88.1	mL
Initial Volume + Injection Volume =	85.5	mL
Moisture Recovery in the Column =	102.7	%

12 Hour Duration Column Test (#11)

Column Test Duration (hr)	Distance from Column Inlet (cm)	Lambda cm/s^1/2	Sample Soil Moisture (g/g)	Sample Soil Moisture (mL/mL)	Total Moisture Between Sample Sites (mL)
12	0	0	0.15	0.249	
	3.5	0.02	0.139	0.23	10.53
	5.3	0.03	0.134	0.222	5.11
	7.3	0.04	0.134	0.221	5.57
	9.3	0.04	0.124	0.205	5.36
	13.3	0.06	0.107	0.176	9.57
	17.3	0.08	0.055	0.091	6.72
	21.3	0.1	0.054	0.089	4.53
	25.3	0.12	0.051	0.084	4.35
	29.3	0.14	0.054	0.09	4.37
	33.3	0.16	0.052	0.086	4.41
	37.3	0.18	0.054	0.09	4.41
	41.3	0.2	0.05	0.082	4.32
	45.3	0.22	0.054	0.089	4.3
	49.3	0.24	0.053	0.088	4.44
	53.3	0.26	0.054	0.09	4.47
	57.3	0.28	0.057	0.094	4.61
	61.3	0.29	0.056	0.093	4.7
				Sum =	**91.79**

Average Initial Moisture Content =	0.088	mL/mL
Dry Bulk Density =	1.67	g/cm^3
Initial Water Volume Present in Column =	68.3	mL
Injection Volume =	25.3	mL
Final Water Volume Present in Column =	91.8	mL
Initial Volume + Injection Volume =	93.6	mL
Moisture Recovery in the Column =	98.1	%

24 Hour Duration Column Test (#11)

Column Test Duration (hr)	Distance from Column Inlet (cm)	Lambda cm/s^1/2	Sample Soil Moisture (g/g)	Sample Soil Moisture (mL/mL)	Total Moisture Between Sample Sites (mL)
24	0	0	0.149	0.247	
	3.5	0.012	0.139	0.229	10.47
	5.3	0.018	0.139	0.23	5.2
	7.3	0.025	0.137	0.226	5.74
	9.3	0.032	0.131	0.217	5.57
	13.3	0.045	0.123	0.203	10.57
	17.3	0.059	0.105	0.174	9.5
	21.3	0.072	0.051	0.105	6.49
	25.3	0.086	0.046	0.076	4.01
	29.3	0.1	0.049	0.082	3.96
	33.3	0.113	0.045	0.074	3.91
	37.3	0.127	0.046	0.076	3.77
	41.3	0.141	0.047	0.079	3.89
	45.3	0.154	0.047	0.078	3.94
	49.3	0.168	0.044	0.073	3.8
	53.3	0.181	0.046	0.076	3.74
	57.3	0.195	0.046	0.076	3.83
	61.3	0.209	0.052	0.086	4.09
				Sum	**92.47**

Average Initial Moisture Content =	0.078	mL/mL
Dry Bulk Density =	1.67	g/cm^3
Initial Water Volume Present in Column =	59.7	mL
Injection Volume =	35.8	mL
Final Water Volume Present in Column =	92.5	mL
Initial Volume + Injection Volume =	95.5	mL
Moisture Recovery in the Column =	96.9	%

APPENDIX H

Data for Total Toluene Recovery and Total Toluene Concentration versus Distance & Lambda

APPENDIX H

Data for Total Toluene Recovery and Total Toluene Concentration versus Distance & Lambda

Total Toluene Recovery

Test Duration	Distance from Inlet x	Lambda	Extracted Toluene at the Site	In-place Soil Volume	Total Toluene Between Sample Sites
hr	cm	cm/sqrt sec.	mg	mL	mg
6	0	0	0.021	1.074	
	5.3	0.04	0.01	1.276	0.899
	9.3	0.06	0.003	1.058	0.259
	13.3	0.09	0.001	0.742	0.097
	17.3	0.12	0	0.475	0.034
12	0	0	0.007	0.632	
	3.5	0.02	0.008	1.019	0.862
	5.3	0.03	0.006	1.371	0.285
	7.3	0.04	0.002	0.699	0.188
	9.3	0.04	0.002	0.789	0.13
	13.3	0.06	0.001	0.846	0.154
	17.3	0.08	0	0.8	0.046
24	0	0	0.005	0.695	
	3.5	0.01	0.005	0.488	0.756
	5.3	0.02	0.006	1.371	0.322
	7.3	0.02	0.004	0.566	0.283
	9.3	0.03	0.002	1.108	0.222
	13.3	0.05	0.001	0.688	0.128
	17.3	0.06	0	0.877	0.045

Column Test	Toluene Mass Added (mg)	Toluene Mass Recovered (mg)	% Recovered
6 hr	1.56	1.29	82.9
12 hr	1.78	1.66	93.5
24 hr	2.47	1.76	70.9

Total Toluene Concentration Along the Column

Test Duration	Distance from Inlet	Lambda	Total Toluene Conc.	Total Toluene Conc.	Total Toluene Conc.
	x	λ	6 hr	12 hr	24 hr
seconds	cm	cm/sqrt sec.	mg/L	mg/L	mg/L
21,600	0	0	19.2		
	5.3	0.04	7.8		
	9.3	0.06	2.5		
	13.3	0.09	1.4		
	17.3	0.12	0		
43,200	0	0		23	
	3.5	0.02		16.2	
	5.3	0.03		8.9	
	7.3	0.04		6	
	9.3	0.04		4.3	
	13.3	0.06		1.8	
	17.3	0.08		0	
86,400	0	0			14.1
	3.5	0.01			20.3
	5.3	0.02			8.2
	7.3	0.02			14.3
	9.3	0.03			3.3
	13.3	0.05			1.8
	17.3	0.06			0

APPENDIX I

Data for Toluene Gas Phase Concentration versus Distance & Lambda

APPENDIX I

Data for Toluene Gas Phase Concentration versus Distance & Lambda

Distance from the Inlet	Elapsed Time at Sample Collection	Lambda	Csg for 6 hr Test	Csg for 12 hr Test	Csg for 24 hr Test
cm	hr	cm/sqrt sec.	mg/L	mg/L	mg/L
3.5	0.07	0.22		0.02	
3.5	0.18	0.139		0.21	
3.5	0.29	0.109		0.15	
3.5	0.44	0.088		0.45	
3.5	0.86	0.063		0.69	
3.5	1.32	0.051		0.81	
3.5	1.88	0.043		1.33	
3.5	2.26	0.039		1.42	
3.5	2.99	0.034		1.34	
3.5	4.6	0.027		1.31	
3.5	5.07	0.026		1.4	
3.5	5.53	0.025		1.81	
3.5	6.65	0.023		1.52	
3.5	7.51	0.021		2.31	
3.5	9.15	0.019		1.66	
3.5	10.87	0.018		2.12	
3.5	0.14	0.155			0.13
3.5	0.3	0.106			0.35
3.5	0.48	0.084			0.35
3.5	0.76	0.067			0.67
3.5	1.77	0.044			0.83
3.5	2.67	0.036			0.96
3.5	3.71	0.03			1
3.5	4.85	0.026			1.76
3.5	6	0.024			1.88
3.5	6.98	0.022			1.99
3.5	8.84	0.02			2.17
3.5	10.28	0.018			2.03

Distance from the Inlet cm	Elapsed Time at Sample Collection hr	Lambda cm/sqrt sec.	Csg for 6 hr Test mg/L	Csg for 12 hr Test mg/L	Csg for 24 hr Test mg/L
5.3	0.29	0.164	0.04		
5.3	0.37	0.144	0.11		
5.3	0.46	0.13	0.16		
5.3	0.58	0.116	0.23		
5.3	0.68	0.107	0.37		
5.3	0.79	0.099	0.33		
5.3	0.88	0.094	0.38		
5.3	1.01	0.088	0.43		
5.3	1.1	0.084	0.39		
5.3	1.21	0.08	0.53		
5.3	1.3	0.078	0.5		
5.3	1.5	0.072	0.59		
5.3	1.76	0.067	0.66		
5.3	2.01	0.062	0.74		
5.3	2.24	0.059	0.72		
5.3	2.51	0.056	0.68		
5.3	3.03	0.051	0.92		
5.3	3.53	0.047	0.95		
5.3	3.88	0.045	1.1		
5.3	4.16	0.043	1.03		
5.3	4.34	0.042	1.23		
5.3	4.53	0.042	1.14		
5.3	4.78	0.04	1.07		
5.3	5.07	0.039	1.13		
5.3	5.23	0.039	1.24		
5.3	5.69	0.037	1.23		
5.3	5.76	0.037	1.22		
5.3	0.25	0.178		0.06	
5.3	0.53	0.122		0.23	
5.3	0.95	0.09		0.41	
5.3	1.45	0.073		0.46	
5.3	2.05	0.062		0.63	
5.3	3.39	0.048		0.84	
5.3	5.28	0.038		0.71	
5.3	6.74	0.034		1.27	
5.3	7.58	0.032		1.58	
5.3	9.22	0.029		1.11	
5.3	10.08	0.028		1.48	
5.3	0.37	0.145			0.12
5.3	0.94	0.091			0.29
5.3	1.58	0.07			0.27
5.3	2.18	0.06			0.56
5.3	3.81	0.045			0.71
5.3	5.04	0.039			0.66
5.3	5.64	0.037			1.11
5.3	7.02	0.033			1.5
5.3	8.93	0.03			1.43

Distance from the Inlet cm	Elapsed Time at Sample Collection hr	Lambda cm/sqrt sec.	Csg for 6 hr Test mg/L	Csg for 12 hr Test mg/L	Csg for 24 hr Test mg/L
7.3	0.35	0.206		0.02	
7.3	0.56	0.162		0.06	
7.3	1.07	0.118		0.14	
7.3	1.55	0.098		0.31	
7.3	2.18	0.082		0.23	
7.3	3.5	0.065		0.56	
7.3	5.17	0.053		0.68	
7.3	6.83	0.047		0.88	
7.3	9.32	0.04		1.03	
7.3	10.68	0.037		1.01	
7.3	0.58	0.159			0.07
7.3	1.05	0.119			0.2
7.3	1.67	0.094			0.3
7.3	3.12	0.069			0.48
7.3	3.96	0.061			0.53
7.3	5.15	0.054			0.75
7.3	6.25	0.049			0.86
7.3	7.12	0.046			1.64

Distance from the Inlet	Elapsed Time at Sample Collection	Lambda	Csg for 6 hr Test	Csg for 12 hr Test	Csg for 24 hr Test
cm	hr	cm/sqrt sec.	mg/L	mg/L	mg/L
9.3	0.71	0.183	0.02		
9.3	0.92	0.162	0.06		
9.3	1.12	0.146	0.1		
9.3	1.33	0.134	0.13		
9.3	1.59	0.123	0.18		
9.3	1.84	0.114	0.23		
9.3	2.09	0.107	0.2		
9.3	2.34	0.101	0.25		
9.3	2.6	0.096	0.3		
9.3	3.01	0.089	0.35		
9.3	3.47	0.083	0.4		
9.3	4.04	0.077	0.42		
9.3	4.25	0.075	0.46		
9.3	4.59	0.072	0.45		
9.3	5.35	0.067	0.46		
9.3	5.63	0.065	0.42		
9.3	0.6	0.2		0.02	
9.3	1.13	0.145		0.08	
9.3	1.63	0.121		0.18	
9.3	3.63	0.081		0.35	
9.3	5.38	0.067		0.39	
9.3	7.03	0.058		0.45	
9.3	9.36	0.051		0.69	
9.3	10.51	0.048		0.76	
9.3	1.92	0.112			0.16
9.3	3	0.089			0.32
9.3	4.07	0.077			0.31
9.3	5.38	0.067			0.38
9.3	6.43	0.061			0.57
9.3	7.31	0.057			0.61
9.3	9.52	0.05			0.79
9.3	11.15	0.046			0.81

Distance from the Inlet cm	Elapsed Time at Sample Collection hr	Lambda cm/sqrt sec.	Csg for 6 hr Test mg/L	Csg for 12 hr Test mg/L	Csg for 24 hr Test mg/L
13.3	2.67	0.136	0.12		
13.3	3.18	0.124	0.15		
13.3	3.62	0.117	0.14		
13.3	4.11	0.109	0.24		
13.3	4.67	0.103	0.17		
13.3	5.73	0.093	0.28		
13.3	1.23	0.2		0.01	
13.3	1.76	0.167		0.03	
13.3	3.85	0.113		0.15	
13.3	5.63	0.093		0.22	
13.3	7.2	0.083		0.2	
13.3	9.44	0.072		0.39	
13.3	2.39	0.143			0.07
13.3	4.2	0.108			0.18
13.3	5.48	0.095			0.18
13.3	6.48	0.087			0.26
13.3	7.41	0.081			0.2
13.3	11.3	0.066			0.25
13.3	16.24	0.055			0.4
13.3	20.65	0.049			0.39
13.3	22.62	0.047			0.34
17.3	3.92	0.146	0.08		
17.3	4.41	0.137	0.09		
17.3	4.94	0.13	0.16		
17.3	2.91	0.169		0.02	
17.3	3.89	0.146		0.04	
17.3	5.66	0.121		0.1	
17.3	7.24	0.107		0.11	
17.3	9.47	0.094		0.19	
17.3	2.9	0.169			0.02
17.3	4.31	0.139			0.07
17.3	5.55	0.122			0.12
17.3	6.54	0.113			0.16
17.3	7.49	0.105			0.2
17.3	11.43	0.085			0.26
17.3	16.34	0.071			0.18
17.3	20.73	0.063			0.24

Distance from the Inlet cm	Elapsed Time at Sample Collection hr	Lambda cm/sqrt sec.	Csg for 6 hr Test mg/L	Csg for 12 hr Test mg/L	Csg for 24 hr Test mg/L
21.3	4.3	0.171	0.04		
21.3	5.14	0.157	0.05		
21.3	5.84	0.147	0.09		
21.3	4.83	0.162		0.03	
21.3	7.33	0.131		0.05	
21.3	9.55	0.115		0.09	
21.3	4.41	0.169			0.03
21.3	5.93	0.146			0.05
21.3	6.62	0.138			0.09
21.3	7.73	0.128			0.08
21.3	16.51	0.087			0.2
21.3	22.4	0.075			0.18
25.3	7.37	0.155		0.05	
25.3	9.59	0.136		0.06	
25.3	6.1	0.171			0.02
25.3	6.66	0.163			0.03
25.3	7.83	0.151			0.05
25.3	9.81	0.135			0.09
25.3	16.63	0.103			0.11
25.3	21.33	0.091			0.15
25.3	22.3	0.089			0.34
29.3	7.45	0.179		0.02	
29.3	9.64	0.157		0.03	
29.3	7.91	0.174			0.01
29.3	9.86	0.156			0.03
29.3	16.78	0.119			0.09
29.3	22.21	0.104			0.1
33.3	10.35	0.173			0.02
33.3	16.92	0.135			0.05
33.3	22.07	0.118			0.05
37.3	17.02	0.151			0.02
37.3	21.96	0.133			0.02
41.3	17.2	0.166			0.02
45.3	17.3	0.182			0.01
49.3	20.1	0.183			0.01

APPENDIX J

Data for Fitted Toluene Gas Phase Curves

APPENDIX J

Data for Fitted Toluene Gas Phase Curves

Key: 6a, 12a, & 24a = six, twelve, & twenty-four hour test data for time period from start to 3 hours
6b,12b, & 24b = six, twelve, & twenty-four hour test data for time period from start to 6 hours
12c, 24c = twelve, & twenty-four hour test data for time period from start to 9 hours
12d, 24d = twelve, & twenty-four hour test data for time period from start to 12 hours
24e, 24f = twenty-four hour test data for time period from start to 18 & 24 hours respectively

Regression Output:	**6a (0-3 hr)**	**12a (0-3 hr)**	**24a (0-3 hr)**
Log of Constant	0.493	0.544	0.357
Std Err of Y Est	0.099	0.164	0.156
R Squared	0.961	0.942	0.874
No. of Observations	28	25	17
Degrees of Freedom	26	23	15
X Coefficient(s)	(11.2405)	(11.3085)	(9.6587)
Std Err of Coef.	0.442	0.585	0.949
Constant	3.11	3.5	2.27

Regression Output:	**6b (0-6 hr)**	**12b (0-6 hr)**	**24b (0-6 hr)**
Log of Constant	0.517	0.485	0.388
Std Err of Y Est	0.082	0.158	0.137
R Squared	0.97	0.946	0.922
No. of Observations	56	40	34
Degrees of Freedom	54	38	32
X Coefficient(s)	(10.9614)	(11.2749)	(10.4145)
Std Err of Coef.	0.261	0.436	0.536
Constant	3.29	3.05	2.45

Regression Output:	**12c (0-9 hr)**	**24c (0-9 hr)**
Log of Constant	0.479	0.48
Std Err of Y Est	0.158	0.142
R Squared	0.947	0.938
No. of Observations	51	52
Degrees of Freedom	49	50
X Coefficient(s)	(11.4293)	(11.5676)
Std Err of Coef.	0.385	0.419
Constant	3.01	3.02

Regression Output:	**12d (0-12 hr)**	**24d (0-12 hr)**
Log of Constant	0.462	0.48
Std Err of Y Est	0.147	0.144
R Squared	0.95	0.94
No. of Observations	63	60
Degrees of Freedom	61	58
X Coefficient(s)	(11.3801)	(11.7070)
Std Err of Coef.	0.333	0.389
Constant	2.9	3.02

Regression Output:	**24e (0-18 hr)**	**24f (0-24 hr)**
Log of Constant	0.473	0.446
Std Err of Y Est	0.161	0.186
R Squared	0.93	0.905
No. of Observations	70	79
Degrees of Freedom	68	77
X Coefficient(s)	-12.001	-12.052
Std Err of Coef.	0.401	0.45
Constant	2.97	2.79

APPENDIX K

Data & Statistical Analysis for Moisture versus Lambda

APPENDIX K

Data & Statistical Analysis for Moisture versus Lambda

DATA FOR STATISTICAL ANALYSIS
6, 12, & 24 hr column tests

Theta versus Lambda
Normalized by (theta - theta initial)/(theta final-theta initial)

Lambda	theta 6 hr	theta 12 hr	theta 24 hr
0	1	1	1
0.01	0.97	0.94	0.93
0.02	0.93	0.88	0.9
0.03	0.9	0.82	0.84
0.04	0.84	0.76	0.78
0.05	0.71	0.66	0.69
0.06	0.58	0.57	0.57
0.07	0.41	0.38	0.31
0.08	0.23	0.13	0.13
0.09	0.07	(0.01)	(0.01)
0.1	0.07	(0.01)	0.01
0.11	0.04	(0.01)	(0.02)
0.12	0.04	(0.02)	(0.01)
0.13	0.07	(0.01)	(0.01)
0.14	0.09	(0.01)	(0.01)
0.15	0.07	(0.01)	(0.01)
0.16	0.02	(0.01)	(0.02)
0.17	0	(0.01)	(0.02)
0.18	0	(0.01)	(0.02)
0.19	0	(0.01)	(0.02)
0.2	(0.01)	(0.02)	(0.02)

PAIRED TEST DATA FOR NORMALIZED THETA VERSUS LAMBDA

Calculations

#1	6b vs 12d	where: n = number of comparisons
#2	6b vs 24f	D = difference btw values 1 and 2
#3	12d vs 24f	Dm = mean difference = D/n
		d = deviation = D - Dm
		SD = std dev of D = Sq rt[d^2/(n-1)]
		SDm = std dev of Dm = SD/(Sq rt[n])
		test statistic = t = absolute value (Dm/SDm)
		mean absolute difference = (total of absol. dif)/n

1 **Paired Data for a = 6 hr versus b = 12 hr tests**

Pair no.	theta a	theta b	Difference D=a-b	Absol. Dif. | a-b |	Deviation d=D-Dm	Sqrd. Dev. d^2
1	1	1	0	0	(0.048)	0.002
2	0.97	0.94	0.026	0.026	(0.022)	0
3	0.93	0.88	0.049	0.049	0	0
4	0.9	0.82	0.081	0.081	0.033	0.001
5	0.84	0.76	0.084	0.084	0.035	0.001
6	0.71	0.66	0.047	0.047	(0.001)	0
7	0.58	0.57	0.011	0.011	(0.037)	0.001
8	0.41	0.38	0.029	0.029	(0.020)	0
9	0.23	0.13	0.099	0.099	0.05	0.003
10	0.07	(0.01)	0.076	0.076	0.028	0.001
11	0.07	(0.01)	0.083	0.083	0.034	0.001
12	0.04	(0.01)	0.053	0.053	0.004	0
13	0.04	(0.02)	0.059	0.059	0.01	0
14	0.07	(0.01)	0.083	0.083	0.034	0.001
15	0.09	(0.01)	0.096	0.096	0.048	0.002
16	0.07	(0.01)	0.076	0.076	0.028	0.001
17	0.02	(0.01)	0.033	0.033	(0.016)	0
18	0	(0.01)	0.006	0.006	(0.042)	0.002
19	0	(0.01)	0.006	0.006	(0.042)	0.002
20	0	(0.01)	0.013	0.013	(0.036)	0.001
21	(0.01)	(0.02)	0.009	0.009	(0.040)	0.002
Total	7.03	6.013	1.018	1.018	0	0.022
Mean	0.33	0.29	0.048			

TABLE VALUES
Paired Data for a = 6 hr versus b = 12 hr tests

SD^2	0.001		
SD	0.034	**Dm**	0.048
SDm	0.007	**mean absolute difference**	0.048
Sq rt n	4.58	**t = test statistic**	6.63

2 **Paired Data for a = 6 hr versus b = 24 hr tests**

	theta	theta	Difference	Absol. Dif.	Deviation	Sqrd. Dev.
Pair no.	**a**	**b**	**D=a-b**	**| a-b |**	**d=D-Dm**	**d^2**
1	1	1	0	0	(0.048)	0.002
2	0.97	0.93	0.041	0.041	(0.007)	0
3	0.93	0.9	0.031	0.031	(0.018)	0
4	0.9	0.84	0.06	0.06	0.012	0
5	0.84	0.78	0.059	0.059	0.011	0
6	0.71	0.69	0.018	0.018	(0.031)	0.001
7	0.58	0.57	0.006	0.006	(0.042)	0.002
8	0.41	0.31	0.102	0.102	0.054	0.003
9	0.23	0.13	0.1	0.1	0.052	0.003
10	0.07	(0.01)	0.076	0.076	0.028	0.001
11	0.07	0.01	0.058	0.058	0.01	0
12	0.04	(0.02)	0.058	0.058	0.01	0
13	0.04	(0.01)	0.052	0.052	0.004	0
14	0.07	(0.01)	0.076	0.076	0.028	0.001
15	0.09	(0.01)	0.096	0.096	0.048	0.002
16	0.07	(0.01)	0.076	0.076	0.028	0.001
17	0.02	(0.02)	0.038	0.038	(0.010)	0
18	0	(0.02)	0.024	0.024	(0.025)	0.001
19	0	(0.02)	0.018	0.018	(0.030)	0.001
20	0	(0.02)	0.018	0.018	(0.030)	0.001
21	(0.01)	(0.02)	0.008	0.008	(0.040)	0.002
Total	7.03	6.018	1.012	1.012	0	0.02
Mean	0.33	0.29	0.048			

TABLE VALUES
Paired Data for a = 6 hr versus b = 12 hr tests

SD^2	0.001		
SD	0.032	**Dm**	0.048
SDm	0.007	**mean absolute difference**	0.048
Sq rt n	4.58	**t = test statistic**	6.95

3 **Paired Data for a = 12 hr versus b = 24 hr tests**

Pair no.	theta a	theta b	Difference D=a-b	Absol. Dif. | a-b |	Deviation d=D-Dm	Sqrd. Dev. d^2
1	1	1	0	0	0	0
2	0.94	0.93	0.015	0.015	0.015	0
3	0.88	0.9	(0.018)	0.018	(0.018)	0
4	0.82	0.84	(0.021)	0.021	(0.021)	0
5	0.76	0.78	(0.025)	0.025	(0.025)	0.001
6	0.66	0.69	(0.030)	0.03	(0.030)	0.001
7	0.57	0.57	(0.005)	0.005	(0.005)	0
8	0.38	0.31	0.074	0.074	0.074	0.005
9	0.13	0.13	0.001	0.001	0.001	0
10	(0.01)	(0.01)	(0.000)	0	(0.000)	0
11	(0.01)	0.01	(0.024)	0.024	(0.024)	0.001
12	(0.01)	(0.02)	0.005	0.005	0.006	0
13	(0.02)	(0.01)	(0.007)	0.007	(0.007)	0
14	(0.01)	(0.01)	(0.007)	0.007	(0.006)	0
15	(0.01)	(0.01)	(0.000)	0	(0.000)	0
16	(0.01)	(0.01)	(0.000)	0	(0.000)	0
17	(0.01)	(0.02)	0.005	0.005	0.006	0
18	(0.01)	(0.02)	0.017	0.017	0.018	0
19	(0.01)	(0.02)	0.012	0.012	0.012	0
20	(0.01)	(0.02)	0.005	0.005	0.006	0
21	(0.02)	(0.02)	(0.001)	0.001	(0.001)	0
Total	6.013	6.018	-0.005	0.273	0	0.009
Mean	0.29	0.29	(0.000)			

TABLE VALUES
Paired Data for a = 6 hr versus b = 12 hr tests

SD^2	0		
SD	0.021	**Dm**	(0.0003)
SDm	0.005	**mean absolute difference**	0.013
Sq rt n	4.58	**t = test statistic**	(0.054)

APPENDIX L

Data for P versus Lambda

APPENDIX L

Data for P versus Lambda

Calculated Values for P versus Lambda
6, 12, & 24 hr column tests

	24a	24b	24c	24d	24e	24f
Lambda	P (0-3)	P (0-6)	P (0-9)	P (0-12)	P (0-18)	P (0-24)
0	(0.503)	(0.598)	(0.840)	(0.853)	(0.865)	(0.817)
0.01	(0.372)	(0.446)	(0.617)	(0.625)	(0.632)	(0.596)
0.02	(0.273)	(0.318)	(0.432)	(0.437)	(0.439)	(0.414)
0.03	(0.210)	(0.244)	(0.327)	(0.330)	(0.330)	(0.311)
0.04	(0.167)	(0.193)	(0.255)	(0.257)	(0.256)	(0.241)
0.05	(0.151)	(0.172)	(0.225)	(0.226)	(0.225)	(0.211)
0.06	(0.155)	(0.176)	(0.225)	(0.226)	(0.223)	(0.210)
0.07	(0.240)	(0.267)	(0.334)	(0.334)	(0.328)	(0.308)
0.08	(0.280)	(0.306)	(0.373)	(0.372)	(0.364)	(0.341)
0.09	(0.292)	(0.314)	(0.373)	(0.371)	(0.360)	(0.337)
0.1	(0.223)	(0.236)	(0.273)	(0.271)	(0.261)	(0.244)
0.11	(0.188)	(0.195)	(0.220)	(0.217)	(0.208)	(0.195)
0.12	(0.147)	(0.150)	(0.165)	(0.163)	(0.155)	(0.145)
0.13	(0.115)	(0.116)	(0.124)	(0.122)	(0.115)	(0.107)
0.14	(0.091)	(0.090)	(0.094)	(0.092)	(0.087)	(0.081)
0.15	(0.072)	(0.070)	(0.071)	(0.070)	(0.065)	(0.061)
0.16	(0.059)	(0.056)	(0.056)	(0.054)	(0.050)	(0.047)
0.17	(0.047)	(0.044)	(0.043)	(0.041)	(0.038)	(0.036)
0.18	(0.037)	(0.034)	(0.032)	(0.031)	(0.028)	(0.026)
0.19	(0.029)	(0.027)	(0.024)	(0.023)	(0.021)	(0.020)
0.2	(0.023)	(0.021)	(0.018)	(0.018)	(0.016)	(0.015)

	12 a	12b	12c	12d	6a	6b
Lambda	**P (0-3)**	**P (0-6)**	**P (0-9)**	**P (0-12)**	**P (0-3)**	**P (0-6)**
0	(0.929)	(0.810)	(0.814)	(0.780)	(0.739)	(0.760)
0.01	(0.651)	(0.579)	(0.580)	(0.556)	(0.493)	(0.509)
0.02	(0.487)	(0.426)	(0.426)	(0.409)	(0.326)	(0.338)
0.03	(0.369)	(0.323)	(0.322)	(0.310)	(0.214)	(0.222)
0.04	(0.288)	(0.253)	(0.252)	(0.242)	(0.150)	(0.157)
0.05	(0.255)	(0.224)	(0.223)	(0.214)	(0.152)	(0.158)
0.06	(0.234)	(0.206)	(0.204)	(0.197)	(0.167)	(0.175)
0.07	(0.283)	(0.249)	(0.246)	(0.237)	(0.208)	(0.219)
0.08	(0.378)	(0.333)	(0.328)	(0.316)	(0.257)	(0.273)
0.09	(0.380)	(0.334)	(0.328)	(0.317)	(0.294)	(0.314)
0.1	(0.293)	(0.258)	(0.252)	(0.244)	(0.223)	(0.240)
0.11	(0.223)	(0.197)	(0.192)	(0.185)	(0.181)	(0.196)
0.12	(0.172)	(0.152)	(0.147)	(0.143)	(0.138)	(0.150)
0.13	(0.129)	(0.114)	(0.111)	(0.107)	(0.098)	(0.107)
0.14	(0.097)	(0.086)	(0.083)	(0.080)	(0.069)	(0.076)
0.15	(0.074)	(0.065)	(0.063)	(0.061)	(0.056)	(0.062)
0.16	(0.057)	(0.051)	(0.048)	(0.047)	(0.048)	(0.054)
0.17	(0.043)	(0.038)	(0.036)	(0.035)	(0.039)	(0.044)
0.18	(0.033)	(0.029)	(0.027)	(0.027)	(0.030)	(0.033)
0.19	(0.025)	(0.022)	(0.021)	(0.021)	(0.023)	(0.026)
0.2	(0.019)	(0.017)	(0.016)	(0.016)	(0.018)	(0.020)

APPENDIX M

Data for Delta versus Lambda

APPENDIX M

Data for Delta versus Lambda

Calculated Values for Delta versus Lambda
6, 12, & 24 hr column tests

Delta versus Lambda determined through integration

	24a	24b	24c	24d	24e	24f
Lambda	Delta (0-3)	Delta (0-6)	Delta (0-9)	Delta (0-12)	Delta (0-18)	Delta (0-24)
0.02	2.33	2.43	2.83	2.81	2.72	2.55
0.03	1.81	1.84	2.07	2.04	1.96	1.83
0.04	1.37	1.36	1.46	1.44	1.36	1.27
0.05	1.03	1	1.02	0.99	0.93	0.86
0.06	0.78	0.73	0.71	0.69	0.64	0.59
0.07	0.66	0.62	0.6	0.58	0.54	0.49
0.08	0.56	0.52	0.51	0.49	0.46	0.42
0.09	0.49	0.46	0.45	0.44	0.41	0.38
0.1	0.37	0.34	0.33	0.32	0.3	0.27
0.11	0.3	0.28	0.26	0.25	0.24	0.22
0.12	0.23	0.21	0.19	0.19	0.17	0.16
0.13	0.17	0.15	0.14	0.13	0.12	0.11
0.14	0.12	0.11	0.1	0.09	0.09	0.08
0.15	0.09	0.07	0.07	0.06	0.06	0.05
0.16	0.07	0.06	0.05	0.05	0.05	0.04
0.17	0.05	0.04	0.04	0.04	0.04	0.03
0.18	0.02	0.02	0.02	0.02	0.02	0.01
0.19	0.01	0.01	0.01	0.01	0.01	0.01
0.2	(0.00)	(0.00)	0	0	0	(0.00)

	12 a	12b	12c	12d	6a	6b
Lambda	**Delta (0-3)**	**Delta (0-6)**	**Delta (0-9)**	**Delta (0-12)**	**Delta (0-3)**	**Delta (0-6)**
0.02	3.4	2.97	2.89	2.8	3.02	3.24
0.03	2.52	2.21	2.14	2.07	2.19	2.43
0.04	1.82	1.6	1.53	1.49	1.55	1.78
0.05	1.3	1.14	1.09	1.06	1.1	1.29
0.06	0.92	0.81	0.77	0.75	0.79	0.93
0.07	0.71	0.63	0.59	0.58	0.6	0.72
0.08	0.64	0.57	0.54	0.53	0.5	0.65
0.09	0.57	0.5	0.47	0.46	0.46	0.57
0.1	0.43	0.39	0.36	0.36	0.33	0.44
0.11	0.33	0.29	0.27	0.27	0.26	0.33
0.12	0.25	0.22	0.21	0.21	0.18	0.26
0.13	0.18	0.16	0.15	0.15	0.1	0.19
0.14	0.12	0.11	0.1	0.1	0.03	0.13
0.15	0.08	0.08	0.07	0.07	0.02	0.09
0.16	0.06	0.06	0.05	0.05	0.03	0.07
0.17	0.03	0.03	0.03	0.03	0.03	0.04
0.18	0.01	0.02	0.01	0.01	0.01	0.02
0.19	0	0.01	0	0.01	(0.00)	0.01
0.2	(0.00)	0	(0.00)	0	(0.00)	0

APPENDIX N

Data for Delta versus *P*

APPENDIX N

Data for Delta versus *P*

Calculated Values for P versus Delta
6, 12, & 24 hr column tests

		24f		12d		6b
	P	**Delta (0-24)**	**P**	**Delta (0-12)**	**P**	**Delta (0-6)**
all	(0.414)	2.55	(0.437)	2.8	(0.318)	3.24
	(0.311)	1.83	(0.330)	2.07	(0.244)	2.43
	(0.241)	1.27	(0.257)	1.49	(0.193)	1.78
	(0.211)	0.86	(0.226)	1.06	(0.172)	1.29
	(0.210)	0.59	(0.226)	0.75	(0.176)	0.93
	(0.308)	0.49	(0.334)	0.58	(0.267)	0.72
	(0.341)	0.42	(0.372)	0.53	(0.306)	0.65
	(0.337)	0.38	(0.371)	0.46	(0.314)	0.57
	(0.244)	0.27	(0.271)	0.36	(0.236)	0.44
	(0.195)	0.22	(0.217)	0.27	(0.195)	0.33
	(0.145)	0.16	(0.163)	0.21	(0.150)	0.26
	(0.107)	0.11	(0.122)	0.15	(0.116)	0.19
	(0.081)	0.08	(0.092)	0.1	(0.090)	0.13
	(0.061)	0.05	(0.070)	0.07	(0.070)	0.09
	(0.047)	0.04	(0.054)	0.05	(0.056)	0.07
	(0.036)	0.03	(0.041)	0.03	(0.044)	0.04
	(0.026)	0.01	(0.031)	0.01	(0.034)	0.02
	(0.020)	0.01	(0.023)	0.01	(0.027)	0.01
	(0.015)	(0.00)	(0.018)	0	(0.021)	0

		24a	12 a	6a
	P	Delta (0-3)	Delta (0-3)	Delta (0-3)
0-3 hr	(0.273)	2.33	3.4	3.02
	(0.210)	1.81	2.52	2.19
	(0.167)	1.37	1.82	1.55
	(0.151)	1.03	1.3	1.1
	(0.155)	0.78	0.92	0.79
	(0.240)	0.66	0.71	0.6
	(0.280)	0.56	0.64	0.5
	(0.292)	0.49	0.57	0.46
	(0.223)	0.37	0.43	0.33
	(0.188)	0.3	0.33	0.26
	(0.147)	0.23	0.25	0.18
	(0.115)	0.17	0.18	0.1
	(0.091)	0.12	0.12	0.03
	(0.072)	0.09	0.08	0.02
	(0.059)	0.07	0.06	0.03
	(0.047)	0.05	0.03	0.03
	(0.037)	0.02	0.01	0.01
	(0.029)	0.01	0	(0.00)
	(0.023)	(0.00)	(0.00)	(0.00)

		24b	12b	6b
	P	Delta (0-6)	Delta (0-6)	Delta (0-6)
0-6 hr	(0.318)	2.43	2.97	3.24
	(0.244)	1.84	2.21	2.43
	(0.193)	1.36	1.6	1.78
	(0.172)	1	1.14	1.29
	(0.176)	0.73	0.81	0.93
	(0.267)	0.62	0.63	0.72
	(0.306)	0.52	0.57	0.65
	(0.314)	0.46	0.5	0.57
	(0.236)	0.34	0.39	0.44
	(0.195)	0.28	0.29	0.33
	(0.150)	0.21	0.22	0.26
	(0.116)	0.15	0.16	0.19
	(0.090)	0.11	0.11	0.13
	(0.070)	0.07	0.08	0.09
	(0.056)	0.06	0.06	0.07
	(0.044)	0.04	0.03	0.04
	(0.034)	0.02	0.02	0.02
	(0.027)	0.01	0.01	0.01
	(0.021)	(0.00)	0	0

	P	24c Delta (0-9)	12c Delta (0-9)
0-9 hr	(0.432)	2.83	2.89
	(0.327)	2.07	2.14
	(0.255)	1.46	1.53
	(0.225)	1.02	1.09
	(0.225)	0.71	0.77
	(0.334)	0.6	0.59
	(0.373)	0.51	0.54
	(0.373)	0.45	0.47
	(0.273)	0.33	0.36
	(0.220)	0.26	0.27
	(0.165)	0.19	0.21
	(0.124)	0.14	0.15
	(0.094)	0.1	0.1
	(0.071)	0.07	0.07
	(0.056)	0.05	0.05
	(0.043)	0.04	0.03
	(0.032)	0.02	0.01
	(0.024)	0.01	0
	(0.018)	0	(0.00)

	P	24d Delta (0-12)	12d Delta (0-12)			24e Delta (0-18)
0-12 hr	(0.437)	2.81	2.8	**0-18 hr**	(0.439)	2.72
	(0.330)	2.04	2.07		(0.330)	1.96
	(0.257)	1.44	1.49		(0.256)	1.36
	(0.226)	0.99	1.06		(0.225)	0.93
	(0.226)	0.69	0.75		(0.223)	0.64
	(0.334)	0.58	0.58		(0.328)	0.54
	(0.372)	0.49	0.53		(0.364)	0.46
	(0.371)	0.44	0.46		(0.360)	0.41
	(0.271)	0.32	0.36		(0.261)	0.3
	(0.217)	0.25	0.27		(0.208)	0.24
	(0.163)	0.19	0.21		(0.155)	0.17
	(0.122)	0.13	0.15		(0.115)	0.12
	(0.092)	0.09	0.1		(0.087)	0.09
	(0.070)	0.06	0.07		(0.065)	0.06
	(0.054)	0.05	0.05		(0.050)	0.05
	(0.041)	0.04	0.03		(0.038)	0.04
	(0.031)	0.02	0.01		(0.028)	0.02
	(0.023)	0.01	0.01		(0.021)	0.01
	(0.018)	0	0		(0.016)	0

APPENDIX O

Paired Test Results for P versus Lambda

APPENDIX O

Paired Test Results for P versus Lambda

DATA FOR STATISTICAL ANALYSIS
6, 12, & 24 hr column tests

Calculations

#1 6 hr vs 12 hr for lambda = 0.0 - 0.2
#2 6 hr vs 24 hr for lambda = 0.0 - 0.2
#3 12 hr vs 24 hr for lambda = 0.0 - 0.2

where: n = number of comparisons
D = difference btw values 1 and 2
Dm = mean difference = D/n
d = deviation = D - Dm
SD = std dev of D = Sq rt[d^2/(n-1)]
SDm = std dev of Dm = SD/(Sq rt[n])
test statistic = t = absolute value (Dm/SDm)
mean absolute difference = (total of absol. dif)/n

1 Paired Data
for a = 6 hr
versus b = 12
hr tests

Pair no.	P a	P b	Difference D=a-b	Absol. Dif. | a-b |	Deviation d=D-Dm	Sqrd. Dev. d^2
1	(0.760)	(0.780)	0.02	0.02	0	0
2	(0.509)	(0.556)	0.047	0.047	0.027	0.001
3	(0.338)	(0.409)	0.071	0.071	0.051	0.003
4	(0.222)	(0.310)	0.087	0.087	0.068	0.005
5	(0.157)	(0.242)	0.085	0.085	0.066	0.004
6	(0.158)	(0.214)	0.056	0.056	0.036	0.001
7	(0.175)	(0.197)	0.022	0.022	0.002	0
8	(0.219)	(0.237)	0.018	0.018	(0.002)	0
9	(0.273)	(0.316)	0.043	0.043	0.024	0.001
10	(0.314)	(0.317)	0.003	0.003	(0.017)	0
11	(0.240)	(0.244)	0.004	0.004	(0.016)	0
12	(0.196)	(0.185)	(0.011)	0.011	(0.030)	0.001
13	(0.150)	(0.143)	(0.007)	0.007	(0.027)	0.001
14	(0.107)	(0.107)	0	0	(0.019)	0
15	(0.076)	(0.080)	0.005	0.005	(0.015)	0
16	(0.062)	(0.061)	(0.001)	0.001	(0.021)	0

17	(0.054)	(0.047)	(0.007)	0.007	(0.026)	0.001
18	(0.044)	(0.035)	(0.008)	0.008	(0.028)	0.001
19	(0.033)	(0.027)	(0.007)	0.007	(0.026)	0.001
20	(0.026)	(0.021)	(0.005)	0.005	(0.025)	0.001
21	(0.020)	(0.016)	(0.004)	0.004	(0.024)	0.001
Total	(4.13)	(4.54)	0.41	0.51	0	0.02
Mean	(0.20)	(0.22)	0.02			

	TABLE VALUES	**Paired Data for a = 6 hr versus b = 12 hr tests**	
SD^2	0.001		
SD	0.032	**Dm**	0.02
SDm	0.007	**mean absolute difference**	0.024
Sq rt n	4.58	**t = test statistic**	2.79

2 **Paired Data for a = 6 hr versus b = 24 hr tests**

Pair no.	**P a**	**P b**	**Difference D=a-b**	**Absol. Dif. | a-b |**	**Deviation d=D-Dm**	**Sqrd. Dev. d^2**
1	(0.760)	(0.817)	0.057	0.057	0.027	0.001
2	(0.509)	(0.596)	0.087	0.087	0.057	0.003
3	(0.338)	(0.414)	0.076	0.076	0.046	0.002
4	(0.222)	(0.311)	0.089	0.089	0.059	0.003
5	(0.157)	(0.241)	0.084	0.084	0.054	0.003
6	(0.158)	(0.211)	0.053	0.053	0.023	0.001
7	(0.175)	(0.210)	0.035	0.035	0.005	0
8	(0.219)	(0.308)	0.089	0.089	0.059	0.003
9	(0.273)	(0.341)	0.069	0.069	0.039	0.001
10	(0.314)	(0.337)	0.024	0.024	(0.006)	0

11	(0.240)	(0.244)	0.005	0.005	(0.025)	0.001
12	(0.196)	(0.195)	(0.001)	0.001	(0.031)	0.001
13	(0.150)	(0.145)	(0.005)	0.005	(0.035)	0.001
14	(0.107)	(0.107)	0	0	(0.030)	0.001
15	(0.076)	(0.081)	0.005	0.005	(0.025)	0.001
16	(0.062)	(0.061)	(0.002)	0.002	(0.032)	0.001
17	(0.054)	(0.047)	(0.007)	0.007	(0.037)	0.001
18	(0.044)	(0.036)	(0.008)	0.008	(0.038)	0.001
19	(0.033)	(0.026)	(0.007)	0.007	(0.037)	0.001
20	(0.026)	(0.020)	(0.006)	0.006	(0.036)	0.001
21	(0.020)	(0.015)	(0.005)	0.005	(0.035)	0.001
Total	(4.13)	(4.76)	0.63	0.72	0	0.03
Mean	(0.20)	(0.23)	0.03			

	TABLE VALUES		**Paired Data for a = 6 hr versus b = 24 hr tests**	
SD^2	0.002			
SD	0.039		**Dm**	0.03
SDm	0.009		**mean absolute difference**	0.034
Sq rt n	4.58		**t = test statistic**	3.54

3 **Paired Data for a = 12 hr versus b = 24 hr tests**

Pair no.	**P a**	**P b**	**Difference D=a-b**	**Absol. Dif. | a-b |**	**Deviation d=D-Dm**	**Sqrd. Dev. d^2**
1	(0.780)	(0.817)	0.037	0.037	0.026	0.001
2	(0.556)	(0.596)	0.04	0.04	0.029	0.001
3	(0.409)	(0.414)	0.005	0.005	(0.005)	0
4	(0.310)	(0.311)	0.001	0.001	(0.009)	0

5	(0.242)	(0.241)	(0.001)	0.001	(0.011)	0
6	(0.214)	(0.211)	(0.003)	0.003	(0.013)	0
7	(0.197)	(0.210)	0.013	0.013	0.003	0
8	(0.237)	(0.308)	0.071	0.071	0.061	0.004
9	(0.316)	(0.341)	0.025	0.025	0.015	0
10	(0.317)	(0.337)	0.021	0.021	0.01	0
11	(0.244)	(0.244)	0.001	0.001	(0.010)	0
12	(0.185)	(0.195)	0.009	0.009	(0.001)	0
13	(0.143)	(0.145)	0.002	0.002	(0.009)	0
14	(0.107)	(0.107)	0	0	(0.010)	0
15	(0.080)	(0.081)	0	0	(0.010)	0
16	(0.061)	(0.061)	(0.001)	0.001	(0.011)	0
17	(0.047)	(0.047)	(0.000)	0	(0.011)	0
18	(0.035)	(0.036)	0	0	(0.010)	0
19	(0.027)	(0.026)	(0.000)	0	(0.011)	0
20	(0.021)	(0.020)	(0.001)	0.001	(0.011)	0
21	(0.016)	(0.015)	(0.001)	0.001	(0.012)	0
Total	(4.54)	(4.76)	0.22	0.23	(0.00)	0.01
Mean	(0.22)	(0.23)	0.01			

	TABLE VALUES		**Paired Data for a = 12 hr versus b = 24 hr tests**	
SD^2	0			
SD	0.019		**Dm**	0.01
SDm	0.004		**mean absolute difference**	0.011
Sq rt n	4.58		**t = test statistic**	2.55

APPENDIX P

Paired Test Results for Delta versus Lambda

APPENDIX P

Paired Test Results for Delta versus Lambda

DATA FOR STATISTICAL ANALYSIS
6, 12, & 24 hr column tests

Calculations

#1 6 hr vs 12 hr
#2 6 hr vs 24 hr
#3 12 hr vs 24 hr

where: n = number of comparisons
D = difference btw values 1 and 2
Dm = mean difference = D/n
d = deviation = D - Dm
SD = std dev of D = Sq rt[d^2/(n-1)]
SDm = std dev of Dm = SD/(Sq rt[n])
test statistic = t = absolute value (Dm/SDm)
mean absolute difference = (total of absol. dif)/n

1 **Paired Data for a = 6 hr versus b = 12 hr tests**

Pair no.	Delta a	Delta b	Difference D=a-b	Absol. Dif. | a-b |	Deviation d=D-Dm	Sqrd. Dev. d^2
1	3.24	2.8	0.438	0.438	0.324	0.105
2	2.43	2.07	0.357	0.357	0.243	0.059
3	1.78	1.49	0.284	0.284	0.17	0.029
4	1.29	1.06	0.223	0.223	0.11	0.012
5	0.93	0.75	0.174	0.174	0.061	0.004
6	0.72	0.58	0.141	0.141	0.028	0.001
7	0.65	0.53	0.123	0.123	0.009	0
8	0.57	0.46	0.105	0.105	(0.009)	0
9	0.44	0.36	0.083	0.083	(0.030)	0.001
10	0.33	0.27	0.065	0.065	(0.048)	0.002
11	0.26	0.21	0.051	0.051	(0.062)	0.004
12	0.19	0.15	0.039	0.039	(0.075)	0.006
13	0.13	0.1	0.028	0.028	(0.086)	0.007
14	0.09	0.07	0.02	0.02	(0.094)	0.009
15	0.07	0.05	0.014	0.014	(0.099)	0.01

16	0.04	0.03	0.008	0.008	(0.105)	0.011
17	0.02	0.01	0.004	0.004	(0.110)	0.012
18	0.01	0.01	0.001	0.001	(0.112)	0.013
19	0	0	(0.001)	0.001	(0.114)	0.013
Total	13.17	11.01	2.16	2.16	(0.00)	0.3
Mean	0.69	0.58	0.114			

	TABLE VALUES	**Paired Data for a = 6 hr versus b = 12 hr tests**	
SD^2	0.017		
SD	0.129	**Dm**	0.114
SDm	0.03	**mean absolute difference**	0.114
Sq rt n	4.36	**t = test statistic**	3.85

2 **Paired Data for a = 6 hr versus b = 24 hr tests**

Pair no.	**Delta a**	**Delta b**	**Difference D=a-b**	**Absol. Dif. | a-b |**	**Deviation d=D-Dm**	**Sqrd. Dev. d^2**
1	3.24	2.55	0.688	0.688	0.488	0.238
2	2.43	1.83	0.598	0.598	0.398	0.158
3	1.78	1.27	0.506	0.506	0.306	0.094
4	1.29	0.86	0.423	0.423	0.223	0.05
5	0.93	0.59	0.336	0.336	0.136	0.019
6	0.72	0.49	0.23	0.23	0.03	0.001
7	0.65	0.42	0.226	0.226	0.027	0.001
8	0.57	0.38	0.188	0.188	(0.012)	0
9	0.44	0.27	0.168	0.168	(0.032)	0.001
10	0.33	0.22	0.117	0.117	(0.083)	0.007
11	0.26	0.16	0.1	0.1	(0.100)	0.01

12	0.19	0.11	0.078	0.078	(0.122)	0.015
13	0.13	0.08	0.056	0.056	(0.144)	0.021
14	0.09	0.05	0.041	0.041	(0.158)	0.025
15	0.07	0.04	0.026	0.026	(0.174)	0.03
16	0.04	0.03	0.007	0.007	(0.193)	0.037
17	0.02	0.01	0.004	0.004	(0.196)	0.038
18	0.01	0.01	0.003	0.003	(0.197)	0.039
19	0	(0.00)	0.003	0.003	(0.197)	0.039
Total	13.17	9.37	3.8	3.8	(0.00)	0.82
Mean	0.69	0.49	0.2			

	TABLE VALUES	**Paired Data for a = 6 hr versus b = 24 hr tests**	
SD^2	0.046		
SD	0.214	**Dm**	0.2
SDm	0.049	**mean absolute difference**	0.2
Sq rt n	4.36	**t = test statistic**	4.08

3 **Paired Data for a = 12 hr versus b = 24 hr tests**

Pair no.	**Delta a**	**Delta b**	**Difference D=a-b**	**Absol. Dif. | a-b |**	**Deviation d=D-Dm**	**Sqrd. Dev. d^2**
1	2.8	2.55	0.25	0.25	0.164	0.027
2	2.07	1.83	0.241	0.241	0.154	0.024
3	1.49	1.27	0.222	0.222	0.136	0.018
4	1.06	0.86	0.2	0.2	0.114	0.013
5	0.75	0.59	0.162	0.162	0.075	0.006
6	0.58	0.49	0.089	0.089	0.003	0
7	0.53	0.42	0.104	0.104	0.018	0

8	0.46	0.38	0.084	0.084	(0.003)	0
9	0.36	0.27	0.084	0.084	(0.002)	0
10	0.27	0.22	0.051	0.051	(0.035)	0.001
11	0.21	0.16	0.049	0.049	(0.038)	0.001
12	0.15	0.11	0.04	0.04	(0.047)	0.002
13	0.1	0.08	0.028	0.028	(0.059)	0.003
14	0.07	0.05	0.021	0.021	(0.065)	0.004
15	0.05	0.04	0.012	0.012	(0.074)	0.006
16	0.03	0.03	(0.001)	0.001	(0.088)	0.008
17	0.01	0.01	(0.000)	0	(0.086)	0.007
18	0.01	0.01	0.002	0.002	(0.085)	0.007
19	0	(0.00)	0.004	0.004	(0.082)	0.007
Total	11.01	9.37	1.64	1.64	(0.00)	0.14
Mean	0.58	0.49	0.086			

	TABLE VALUES		**Paired Data for a = 12 hr versus b = 24 hr tests**	
SD^2	0.008			
SD	0.087		**Dm**	0.086
SDm	0.02		**mean absolute difference**	0.087
Sq rt n	4.36		**t = test statistic**	4.35

APPENDIX Q

Paired Test Results for Delta versus P

APPENDIX Q

Paired Test Results for Delta versus P

DATA FOR STATISTICAL ANALYSIS
6, 12, & 24 hr column tests

Calculations

#1 6 (0-3) hr vs 12 (0-3) hr
#2 6 (0-3) hr vs 24 (0-3) hr
#3 12 (0-3) hr vs 24 (0-3) hr
#4 6 (0-6) hr vs 12 (0-6) hr
#5 6 (0-6) hr vs 24 (0-6) hr
#6 12 (0-6) hr vs 24 (0-6) hr
#7 12 (0-9) hr vs 24 (0-9) hr
#8 12 (0-12) hr vs 24 (0-12) hr

where: n = number of comparisons
D = difference btw values 1 and 2
Dm = mean difference = D/n
d = deviation = D - Dm
SD = std dev of D = Sq rt[d^2/(n-1)]
SDm = std dev of Dm = SD/(Sq rt[n])
test statistic = t = absolute value (Dm/SDm)
mean absolute difference = (total of absol. dif)/n

1 **Paired Data for a = 6 (0-3) hr vs b = 12 (0-3) hr**

Pair no.	Delta a	Delta b	Difference D=a-b	Absol. Dif. | a-b |	Deviation d=D-Dm	Sqrd. Dev. d^2
1	3.02	3.4	(0.382)	0.382	(0.266)	0.071
2	2.19	2.52	(0.322)	0.322	(0.207)	0.043
3	1.55	1.82	(0.268)	0.268	(0.153)	0.023
4	1.1	1.3	(0.199)	0.199	(0.083)	0.007
5	0.79	0.92	(0.135)	0.135	(0.019)	0
6	0.6	0.71	(0.116)	0.116	(0.001)	0
7	0.5	0.64	(0.145)	0.145	(0.029)	0.001
8	0.46	0.57	(0.108)	0.108	0.008	0
9	0.33	0.43	(0.101)	0.101	0.015	0
10	0.26	0.33	(0.069)	0.069	0.046	0.002
11	0.18	0.25	(0.067)	0.067	0.049	0.002
12	0.1	0.18	(0.080)	0.08	0.036	0.001
13	0.03	0.12	(0.095)	0.095	0.021	0
14	0.02	0.08	(0.067)	0.067	0.048	0.002
15	0.03	0.06	(0.031)	0.031	0.085	0.007

16	0.03	0.03	(0.004)	0.004	0.112	0.013
17	0.01	0.01	(0.002)	0.002	0.114	0.013
18	(0.00)	0	(0.006)	0.006	0.109	0.012
19	(0.00)	(0.00)	(0.001)	0.001	0.115	0.013
Total	11.17	13.37	(2.20)	2.2	(0.00)	0.21
Mean	0.59	0.7	(0.116)			

	TABLE VALUES		**Paired Data for a = 6 (0-3) hr vs b = 12 (0-3) hr**	
SD^2	0.012			
SD	0.108	**Dm**		(0.116)
SDm	0.025	**mean absolute difference**		0.116
Sq rt n	4.36	**t = test statistic**		(4.66)

2 **Paired Data for a = 6 (0-3) hr vs b = 24 (0-3) hr**

Pair no.	**Delta a**	**Delta b**	**Difference D=a-b**	**Absol. Dif. | a-b |**	**Deviation d=D-Dm**	**Sqrd. Dev. d^2**
1	3.02	2.33	0.689	0.689	0.651	0.424
2	2.19	1.81	0.386	0.386	0.348	0.121
3	1.55	1.37	0.176	0.176	0.138	0.019
4	1.1	1.03	0.068	0.068	0.03	0.001
5	0.79	0.78	0.004	0.004	(0.034)	0.001
6	0.6	0.66	(0.061)	0.061	(0.099)	0.01
7	0.5	0.56	(0.060)	0.06	(0.098)	0.01
8	0.46	0.49	(0.030)	0.03	(0.068)	0.005
9	0.33	0.37	(0.041)	0.041	(0.079)	0.006
10	0.26	0.3	(0.046)	0.046	(0.083)	0.007
11	0.18	0.23	(0.049)	0.049	(0.086)	0.007
12	0.1	0.17	(0.072)	0.072	(0.110)	0.012
13	0.03	0.12	(0.097)	0.097	(0.134)	0.018
14	0.02	0.09	(0.072)	0.072	(0.109)	0.012
15	0.03	0.07	(0.037)	0.037	(0.075)	0.006
16	0.03	0.05	(0.019)	0.019	(0.057)	0.003
17	0.01	0.02	(0.013)	0.013	(0.050)	0.003
18	(0.00)	0.01	(0.010)	0.01	(0.048)	0.002
19	(0.00)	(0.00)	0.002	0.002	(0.035)	0.001

Total	11.17	10.46	0.72	1.93	0	0.67
Mean	0.59	0.55	0.038			

	TABLE VALUES		**Paired Data for a = 6 (0-3) hr vs b = 24 (0-3) hr**	
SD^2	0.037			
SD	0.193		**Dm**	0.038
SDm	0.044		**mean absolute difference**	0.102
Sq rt n	4.36		**t = test statistic**	0.86

3 **Paired Data for a = 12 (0-3) hr vs b = 24 (0-3) hr**

Pair no.	**Delta a**	**Delta b**	**Difference D=a-b**	**Absol. Dif. | a-b |**	**Deviation d=D-Dm**	**Sqrd. Dev. d^2**
1	3.4	2.33	1.071	1.071	0.917	0.841
2	2.52	1.81	0.708	0.708	0.555	0.308
3	1.82	1.37	0.444	0.444	0.291	0.085
4	1.3	1.03	0.267	0.267	0.113	0.013
5	0.92	0.78	0.138	0.138	(0.015)	0
6	0.71	0.66	0.055	0.055	(0.098)	0.01
7	0.64	0.56	0.084	0.084	(0.069)	0.005
8	0.57	0.49	0.077	0.077	(0.076)	0.006
9	0.43	0.37	0.06	0.06	(0.094)	0.009
10	0.33	0.3	0.024	0.024	(0.130)	0.017
11	0.25	0.23	0.019	0.019	(0.135)	0.018
12	0.18	0.17	0.008	0.008	(0.145)	0.021
13	0.12	0.12	(0.002)	0.002	(0.155)	0.024
14	0.08	0.09	(0.004)	0.004	(0.158)	0.025
15	0.06	0.07	(0.006)	0.006	(0.160)	0.026
16	0.03	0.05	(0.015)	0.015	(0.169)	0.028
17	0.01	0.02	(0.010)	0.01	(0.164)	0.027
18	0	0.01	(0.004)	0.004	(0.157)	0.025
19	(0.00)	(0.00)	0.004	0.004	(0.150)	0.022
Total	13.37	10.46	2.92	3	0	1.51
Mean	0.7	0.55	0.154			

	TABLE VALUES	Paired Data for a = 12 (0-3) hr vs b = 24 (0-3) hr	
SD^2	0.084		
SD	0.29	Dm	0.154
SDm	0.066	mean absolute difference	0.158
Sq rt n	4.36	t = test statistic	2.31

4 **Paired Data for a = 6 (0-6) hr vs b = 12 (0-6) hr**

Pair no.	Delta a	Delta b	Difference D=a-b	Absol. Dif. | a-b |	Deviation d=D-Dm	Sqrd. Dev. d^2
1	3.24	2.97	0.266	0.266	0.194	0.038
2	2.43	2.21	0.222	0.222	0.15	0.023
3	1.78	1.6	0.18	0.18	0.108	0.012
4	1.29	1.14	0.144	0.144	0.072	0.005
5	0.93	0.81	0.113	0.113	0.042	0.002
6	0.72	0.63	0.092	0.092	0.02	0
7	0.65	0.57	0.078	0.078	0.007	0
8	0.57	0.5	0.067	0.067	(0.005)	0
9	0.44	0.39	0.054	0.054	(0.018)	0
10	0.33	0.29	0.042	0.042	(0.029)	0.001
11	0.26	0.22	0.033	0.033	(0.039)	0.001
12	0.19	0.16	0.025	0.025	(0.047)	0.002
13	0.13	0.11	0.018	0.018	(0.053)	0.003
14	0.09	0.08	0.013	0.013	(0.059)	0.003
15	0.07	0.06	0.009	0.009	(0.063)	0.004
16	0.04	0.03	0.005	0.005	(0.067)	0.004
17	0.02	0.02	0.002	0.002	(0.069)	0.005
18	0.01	0.01	0	0	(0.071)	0.005
19	0	0	(0.001)	0.001	(0.073)	0.005
Total	13.17	11.81	1.36	1.37	0	0.11
Mean	0.69	0.62	0.072			

	TABLE VALUES	Paired Data for a = 6 (0-6) hr vs b = 12 (0-6) hr	
SD^2	0.006		
SD	0.08	Dm	0.072

SDm	0.018	**mean absolute difference**	0.072
Sq rt n	4.36	**t = test statistic**	3.93

5 **Paired Data for a = 6 (0-6) hr vs b = 24 (0-6) hr**

Pair no.	Delta a	Delta b	Difference D=a-b	Absol. Dif. | a-b |	Deviation d=D-Dm	Sqrd. Dev. d^2
1	3.24	2.43	0.805	0.805	0.651	0.424
2	2.43	1.84	0.583	0.583	0.429	0.184
3	1.78	1.36	0.413	0.413	0.258	0.067
4	1.29	1	0.291	0.291	0.137	0.019
5	0.93	0.73	0.193	0.193	0.039	0.002
6	0.72	0.62	0.109	0.109	(0.045)	0.002
7	0.65	0.52	0.127	0.127	(0.028)	0.001
8	0.57	0.46	0.11	0.11	(0.044)	0.002
9	0.44	0.34	0.096	0.096	(0.058)	0.003
10	0.33	0.28	0.058	0.058	(0.096)	0.009
11	0.26	0.21	0.051	0.051	(0.104)	0.011
12	0.19	0.15	0.038	0.038	(0.117)	0.014
13	0.13	0.11	0.024	0.024	(0.130)	0.017
14	0.09	0.07	0.018	0.018	(0.137)	0.019
15	0.07	0.06	0.011	0.011	(0.144)	0.021
16	0.04	0.04	(0.002)	0.002	(0.156)	0.024
17	0.02	0.02	(0.000)	0	(0.155)	0.024
18	0.01	0.01	0.003	0.003	(0.151)	0.023
19	0	(0.00)	0.007	0.007	(0.147)	0.022
Total	13.17	10.24	2.94	2.94	0	0.89
Mean	0.69	0.54	0.155			

TABLE VALUES

Paired Data for a = 6 (0-6) hr vs b = 24 (0-6) hr

SD^2	0.049		
SD	0.222	**Dm**	0.155
SDm	0.051	**mean absolute difference**	0.155
Sq rt n	4.36	**t = test statistic**	3.04

6 **Paired Data for a = 12 (0-6) hr vs b = 24 (0-6) hr**

Pair no.	Delta a	Delta b	Difference D=a-b	Absol. Dif. | a-b |	Deviation d=D-Dm	Sqrd. Dev. d^2
1	2.97	2.43	0.54	0.54	0.457	0.209
2	2.21	1.84	0.361	0.361	0.278	0.077
3	1.6	1.36	0.233	0.233	0.15	0.023
4	1.14	1	0.148	0.148	0.065	0.004
5	0.81	0.73	0.08	0.08	(0.003)	0
6	0.63	0.62	0.017	0.017	(0.066)	0.004
7	0.57	0.52	0.048	0.048	(0.035)	0.001
8	0.5	0.46	0.044	0.044	(0.039)	0.002
9	0.39	0.34	0.043	0.043	(0.040)	0.002
10	0.29	0.28	0.016	0.016	(0.067)	0.004
11	0.22	0.21	0.017	0.017	(0.065)	0.004
12	0.16	0.15	0.013	0.013	(0.070)	0.005
13	0.11	0.11	0.006	0.006	(0.077)	0.006
14	0.08	0.07	0.005	0.005	(0.078)	0.006
15	0.06	0.06	0.002	0.002	(0.081)	0.007
16	0.03	0.04	(0.007)	0.007	(0.090)	0.008
17	0.02	0.02	(0.002)	0.002	(0.085)	0.007
18	0.01	0.01	0.003	0.003	(0.080)	0.006
19	0	(0.00)	0.009	0.009	(0.074)	0.006
Total	11.81	10.24	1.57	1.59	0	0.38
Mean	0.62	0.54	0.083			

	TABLE VALUES		Paired Data for a = 12 (0-6) hr vs b = 24 (0-6) hr	
SD^2	0.021			
SD	0.146		**Dm**	0.083
SDm	0.033		**mean absolute difference**	0.084
Sq rt n	4.36		**t = test statistic**	2.48

7 **Paired Data for a = 12 (0-9) hr vs b = 24 (0-9) hr**

Pair no.	Delta a	Delta b	Difference D=a-b	Absol. Dif. | a-b |	Deviation d=D-Dm	Sqrd. Dev. d^2
1	2.89	2.83	0.061	0.061	0.04	0.002
2	2.14	2.07	0.068	0.068	0.048	0.002
3	1.53	1.46	0.072	0.072	0.051	0.003
4	1.09	1.02	0.072	0.072	0.051	0.003
5	0.77	0.71	0.054	0.054	0.033	0.001
6	0.59	0.6	(0.004)	0.004	(0.025)	0.001
7	0.54	0.51	0.027	0.027	0.006	0
8	0.47	0.45	0.018	0.018	(0.003)	0
9	0.36	0.33	0.031	0.031	0.01	0
10	0.27	0.26	0.006	0.006	(0.015)	0
11	0.21	0.19	0.012	0.012	(0.009)	0
12	0.15	0.14	0.01	0.01	(0.011)	0
13	0.1	0.1	0.004	0.004	(0.017)	0
14	0.07	0.07	0.002	0.002	(0.019)	0
15	0.05	0.05	(0.004)	0.004	(0.025)	0.001
16	0.03	0.04	(0.015)	0.015	(0.035)	0.001
17	0.01	0.02	(0.011)	0.011	(0.031)	0.001
18	0	0.01	(0.006)	0.006	(0.027)	0.001
19	(0.00)	0	(0.002)	0.002	(0.023)	0.001
Total	11.27	10.87	0.4	0.48	(0.00)	0.02
Mean	0.59	0.57	0.021			

	TABLE VALUES	**Paired Data for a = 12 (0-9) hr vs b = 24 (0-9) hr**	
SD^2	0.001		
SD	0.03	**Dm**	0.021
SDm	0.007	**mean absolute difference**	0.025
Sq rt n	4.36	**t = test statistic**	3.03

8 **Paired Data for a = 12 (0-12) hr vs b = 24 (0-12) hr**

Pair no.	Delta a	Delta b	Difference D=a-b	Absol. Dif. | a-b |	Deviation d=D-Dm	Sqrd. Dev. d^2
1	2.8	2.81	(0.012)	0.012	(0.032)	0.001

2	2.07	2.04	0.029	0.029	0.009	0
3	1.49	1.44	0.056	0.056	0.036	0.001
4	1.06	0.99	0.071	0.071	0.051	0.003
5	0.75	0.69	0.061	0.061	0.041	0.002
6	0.58	0.58	0.005	0.005	(0.015)	0
7	0.53	0.49	0.034	0.034	0.014	0
8	0.46	0.44	0.024	0.024	0.004	0
9	0.36	0.32	0.038	0.038	0.018	0
10	0.27	0.25	0.014	0.014	(0.006)	0
11	0.21	0.19	0.02	0.02	0	0
12	0.15	0.13	0.018	0.018	(0.002)	0
13	0.1	0.09	0.012	0.012	(0.008)	0
14	0.07	0.06	0.01	0.01	(0.010)	0
15	0.05	0.05	0.003	0.003	(0.016)	0
16	0.03	0.04	(0.007)	0.007	(0.027)	0.001
17	0.01	0.02	(0.004)	0.004	(0.023)	0.001
18	0.01	0.01	0	0	(0.020)	0
19	0	0	0.004	0.004	(0.016)	0
Total	11.01	10.64	0.37	0.42	0	0.01
Mean	0.58	0.56	0.02			

	TABLE VALUES		**Paired Data for a = 12 (0-12) hr vs b = 24 (0-12) hr**	
SD^2	0.001			
SD	0.023		**Dm**	0.02
SDm	0.005		**mean absolute difference**	0.022
Sq rt n	4.36		**t = test statistic**	3.68

APPENDIX R

Paired Test Statistics Compilation for Delta and P

APPENDIX R

Paired Test Statistics Compilation for Delta and P

Pairs	n	Dm	Test Stat	t-statistic	Ho Accept.	TTEST Prob.
P vs Lambda for values of Lambda from 0.0 to .20						
6b vs 12d	21	0.02	2.79	2.08		0.011
6b vs 24f	21	0.03	3.54	2.08		0.002
12d vs 24f	21	0.01	2.55	2.08		0.019
12b vs 24b	21	(0.033)	(2.62)	2.08		0.016
12b vs 24c	21	0.017	3.8	2.08		0.001
12b vs 24d	21	0.017	3.73	2.08		0.001
12b vs 24e	21	0.014	2.92	2.08		0.008
12b vs 24f	21	(0.000)	(0.07)	2.08	yes	0.945
12c vs 24c	21	0.019	4.19	2.08		0
12c vs 24d	21	0.02	4.18	2.08		0
12c vs 24e	21	0.017	3.44	2.08		0.002
12c vs 24f	21	0.002	0.06	2.08	yes	0.954
12d vs 24d	21	0.028	4.83	2.08		0
12d vs 24e	21	0.025	4.06	2.08		0.001
P vs Lambda of each individual test						
6a vs 6b	21	0.01	8.41	2.08		0
12a vs 12b	21	(0.031)	(5.04)	2.08		0
12a vs 12c	21	(0.033)	(5.59)	2.08		0
12a vs 12d	21	(0.042)	(5.37)	2.08		0
12b vs 12c	21	(0.002)	(4.41)	2.08		0
12b vs 12d	21	(0.011)	(6.50)	2.08		0
12c vs 12d	21	(0.008)	(4.57)	2.08		0
24a vs 24b	21	0.019	3.33	2.08		0.003
24b vs 24c	21	0.05	3.64	2.08		0.002
24c vs 24d	21	0.001	0.58	2.08	yes	0.568
24c vs 24e	21	(0.003)	(1.29)	2.08	yes	0.211

24c vs 24f	21	(0.017)	(8.69)	2.08		0
24d vs 24e	21	(0.003)	(2.60)	2.08		0.017
24d vs 24f	21	(0.018)	(7.94)	2.08		0
24e vs 24f	21	(0.014)	(5.53)	2.08		0
Delta vs Lambda for values of Lambda from 0.02 to .20						
6b vs 12d	19	0.114	3.85	2.09		0.001
6b vs 24f	19	0.2	4.08	2.09		0.001
12d vs 24f	19	0.086	4.35	2.09		0
12b vs 24b	19	0.083	2.48	2.09		0.023
12b vs 24c	19	0.049	4.15	2.09		0.001
12b vs 24d	19	0.062	4.45	2.09		0
12b vs 24e	19	0.089	4.33	2.09		0
12b vs 24f	19	0.128	4.16	2.09		0.001
12c vs 24c	19	0.021	3.03	2.09		0.007
12c vs 24d	19	0.033	3.78	2.09		0.001
12c vs 24e	19	0.061	3.95	2.09		0.001
12c vs 24f	19	0.1	3.9	2.09		0.001
12d vs 24d	19	0.02	3.68	2.09		0.002
12d vs 24e	19	0.047	4.49	2.09		0
12d vs 24f	19	0.086	4.35	2.09		0
Delta vs Lambda of each individual test						
6a vs 6b	19	(0.105)	(6.16)	2.09		0
12a vs 12b	19	0.082	3.02	2.09		0.007
12a vs 12c	19	0.111	3.42	2.09		0.003
12a vs 12d	19	0.124	3.23	2.09		0.004
12b vs 12c	19	0.028	5.36	2.09		0
12b vs 12d	19	0.042	3.72	2.09		0.001
12c vs 12d	19	0.013	2.18	2.09		0.042
24a vs 24b	19	0.012	1.49	2.09	yes	0.153
24a vs 24c	19	(0.022)	(0.70)	2.09	yes	0.492
24a vs 24d	19	(0.010)	(0.31)	2.09	yes	0.76
24a vs 24e	19	0.018	0.66	2.09	yes	0.517

24a vs 24f	19	0.057	2.7	2.09		0.014
24b vs 24c	19	(0.034)	(1.38)	2.09	yes	0.184
24b vs 24d	19	(0.021)	(0.91)	2.09	yes	0.374
24b vs 24e	19	0.007	0.33	2.09	yes	0.745
24b vs 24f	19	0.045	3.25	2.09		0.004
24c vs 24d	19	0.012	5.98	2.09		0
24c vs 24e	19	0.04	4.51	2.09		0
24c vs 24f	19	0.079	4.09	2.09		0.001
24d vs 24e	19	0.028	4.02	2.09		0.001
24d vs 24f	19	0.067	3.81	2.09		0.001
24e vs 24f	19	0.039	3.58	2.09		0.002
Delta vs P for comparative time frames						
6a vs 12a	19	(0.116)	(4.66)	2.09		0
6a vs 24a	19	0.038	0.86	2.09	yes	0.401
12a vs 24a	19	0.154	2.31	2.09		0.032
6b vs 12b	19	0.072	3.93	2.09		0.001
6b vs 24b	19	0.155	3.04	2.09		0.007
12b vs 24b	19	0.083	2.48	2.09		0.023
12c vs 24c	19	0.021	3.03	2.09		0.007
12d vs 24d	19	0.02	3.68	2.09		0.002

2

VITA

John Linden Roll

Candidate for the Degree of

Doctor of Philosophy

Dissertation: MULTI-PHASE TRANSPORT OF TOLUENE IN UNSATURATED SOIL UNDER TRANSIENT FLOW CONDITIONS

Major Field: Biosystems Engineering

Biographical:

Education: Graduated from Carrollton Community High School, Carrollton, Illinois in June, 1966; received Bachelor of Science degree in Agricultural Engineering and a Master of Science degree in Agricultural Engineering from the University of Illinois, Urbana, Illinois in June 1971 and June 1973, respectively. Completed the requirements for the Doctor of Philosophy degree with a major in Biosystems Engineering at Oklahoma State University in December 1995.

Experience: Employed as an agricultural engineer with the Metropolitan Sanitary District of Greater Chicago for three and one half years. Employed as manager of reclamation and environmental permits for Freeman United Coal Mining Company for fourteen years. USDA National Needs Research Fellow in the Department of Biosystems and Agricultural Engineering at Oklahoma State University, 1990 to present.

Professional Memberships: Registered Professional Engineer in the State of Illinois since 1976; Member of the Society for Engineering in Agricultural, Food, and Biological Systems since 1973.